ON-LINE DIGITAL COMPUTER CONTROL OF THE NERVA NUCLEAR ROCKET ENGINE

NASA 03-002-006

ANNUAL REPORT

June 1971

ENGINEERING EXPERIMENT STATION
COLLEGE OF ENGINEERING
THE UNIVERSITY OF ARIZONA
TUCSON, ARIZONA 85721

ON-LINE DIGITAL COMPUTER CONTROL OF THE NERVA NUCLEAR ROCKET ENGINE

by

Larry Ellis Kendrick

NASA 03-002-006

ANNUAL REPORT

June 1971

Donald G. Schultz
Principal Investigator

TABLE OF CONTENTS

TABLE OF CONTENTS--Continued

LIST OF ILLUSTRATIONS

LIST OF ILLUSTRATIONS--Continued

LIST OF ILLUSTRATIONS--Continued

LIST OF ILLUSTRATIONS--Continued

LIST OF ILLUSTRATIONS--Continued

ABSTRACT

This study considers the problem of on-line digital computer control of the NERVA nuclear rocket engine. NERVA operates in the following manner. Liquid hydrogen is removed from a storage tank by a turbopump and pumped into a nuclear reactor. The hydrogen is heated in the reactor and exhausted from the engine nozzle to provide thrust. Energy to drive the turbopump is also derived from the reactor. Design objectives call for a thrust of 75,000 pounds. The physical complexity of the system is reflected in the differential equations description of the engine dynamics in that the describing equations are high order, nonlinear, and tightly coupled. This study proposes the method of State Dependent State Variable Feedback (SDSVF) as a practical approach to the control of NERVA and other complex nonlinear and/or time-varying systems. The difficulties inherent in other design methods are avoided by defining the optimal closed loop system in terms of a desired transfer function, rather than a performance index to maximize or minimize.

Selection of a desired closed loop transfer function in the nonlinear and/or time-varying case is made possible by treating the system as a sequence of state and/or time

dependent linear constant coefficient systems. These linear models are computed on-line by a digital computer. Each linear model has its own set of constant state variable feedback coefficients (also computed on-line) necessary to realize the desired closed loop transfer function. Thus, a sequence of state variable feedback coefficients is calculated to provide state dependent state variable control. A linearization method is developed and a control design method is chosen. It is shown that these procedures are easily programmed on a digital computer and that they are suitable for on-line computation.

The method is first illustrated by a simple example involving the control of a system described by Van der Pol's Equation. Although only second order the example is nontrivial since the plant to be controlled is inherently unstable. The SDSVF method of control is then applied to the problem of controlling NERVA. NERVA has not been constructed at this time, so that on-line control experiments were performed on the Common Analog Model (CAM) of NERVA. The CAM is a 52nd order hybrid simulation of NERVA and is not suitable for control analysis because of its high order and complexity. Models of nuclear rocket engines available from the literature do not adequately represent NERVA, and hence the Simplified Nonlinear Model (SNM) of NERVA is developed. This model is then used to design an on-line digital computer control system for the

Common Analog Model of NERVA. A series of control experiments show that SDSVF control provides adequate control of the NERVA engine over a wide operating range for various types of input demands.

The contributions of this study are the development of the concept of State Dependent State Variable Feedback control and the development of the Simplified Nonlinear Model of NERVA. The SDSVF control method provides a practical design method for the control of complex, high order, nonlinear and/or time-varying systems. The SNM provides a model of the NERVA engine which is significantly better for control system design and analysis than those currently available.

CHAPTER 1

INTRODUCTION AND OUTLINE

This study is concerned with the problem of the on-line digital computer control of the NERVA nuclear rocket engine. The NERVA rocket engine system represents the final step in the United States nuclear rocket program to develop a man rated nuclear rocket engine. The program has been in existence for more than fifteen years at a cost in excess of one billion dollars. Until last year, all attempts at the control of NERVA have been through analogue methods. The State Dependent State Variable Feedback approach presented in this dissertation represents one of the earliest attempts at on-line digital control.

The primary advantage of nuclear rocket engines is their inherent operating efficiency compared to chemical rocket engines. The efficiency of a rocket engine is defined as the thrust of the engine divided by the propellant flow rate and is called the specific impulse, I_{sp}, where

$$I_{sp} = \frac{F}{\dot{W}} \tag{1-1}$$

Here F is thrust in pounds and $\dot{W}$ is propellant flow rate in pounds-per-second. This expression can also be written as

$$I_{sp} = C_s\left(\frac{T}{MW}\right)^{1/2} \qquad (1\text{-}2)$$

where C_s is a nozzle constant, T is the temperature of the exiting propellant, and MW is the molecular weight of the propellant. The nuclear rocket engine gains its advantage over the chemical rocket engine because of the substantially lower molecular weight of its propellant. A nuclear rocket engine utilizes hydrogen with a molecular weight of two, whereas chemical rocket propellants have molecular weights of approximately twenty. The best chemical rocket engines provide a specific impulse of about four hundred and fifty seconds, while the NERVA engine (the first of its kind) is designed to have a specific impulse of eight hundred and twenty-five seconds.

The basic operating principle of the nuclear rocket engine is relatively simple. As is indicated in the simplified schematic of Figure 1-1, liquid hydrogen is removed from a storage tank by a turbopump and pumped into the core of the reactor. Here it is heated to high temperatures and exhausted from a nozzle similar to the type used with chemical rockets. The exhausting high temperature gas provides the thrust.

A program to develop the hardware necessary to implement the schematic of Figure 1-1 was begun in 1955 (Spence and Durham, 1965), when the Atomic Energy Commission (AEC) and the Air Force provided support for initial

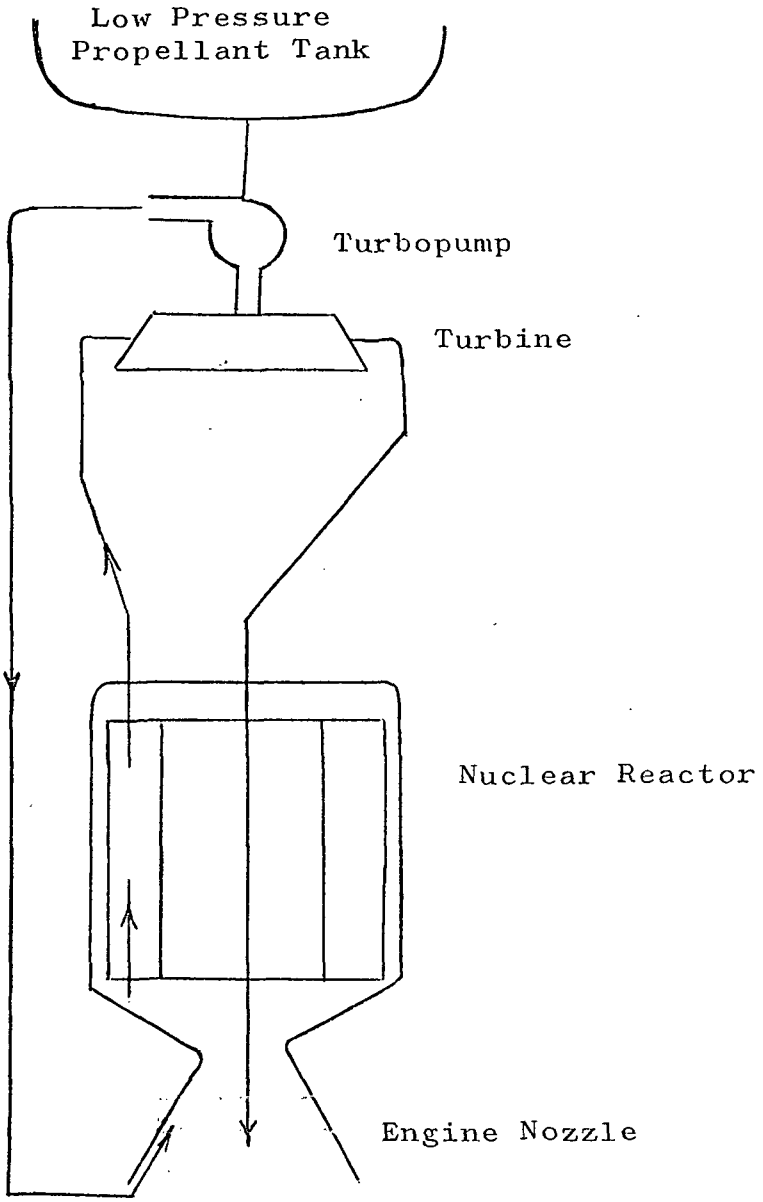

Figure 1-1. Simplified Schematic of a Nuclear Rocket Engine

studies at Los Alamos Scientific Laboratory (LASL) into the development of high-temperature, high-power-density reactors. This work resulted in reactor tests in July 1959 that demonstrated the feasibility of developing the required reactor technology. In 1960 the joint AEC/NASA Space Nuclear Propulsion Office (SNPO) was established to pursue development of nuclear-rocket-technology based on concepts developed at LASL. An industrial-contractor team consisting of Aerojet General Corporation and the Astro-nuclear Laboratory of Westinghouse Electric Corporation was selected in 1961. Additional reactor tests were conducted in 1965 (NRX-A2 and NRX-A3) and the first tests of both nuclear and non-nuclear systems were conducted in 1966 (XE-1 and XE-2). By the conclusion of the XE tests in 1967, it had been demonstrated that the engine system could operate at power levels of one thousand megawatts with temperatures of four thousand degrees Rankine (Schroeder, 1968).

Although the actual NERVA engine has not been assembled at this time, the extensive research and development program mentioned above has produced a vast amount of knowledge relative to the engine. Since this research is concerned with the control of NERVA, of particular interest is the description of the dynamic behavior of the NERVA engine system in terms of differential equations. The Aerojet Nuclear Systems Company and the Westinghouse

Astronuclear Laboratory have developed such a mathematical model, called the Common Analog Model (CAM). The CAM has been developed to perform detailed systems studies, and is therefore, an extremely complex, high order and accurate model. The model contains the fifty-two differential equations, plus an even larger number of nonlinear algebraic equations and numerous functions defined by experimental data. This study assumes that the CAM is an adequate representation of NERVA, and thus the goal of this research is to control the CAM with an on-line digital computer.

It is further assumed that an exact solution to any control problem associated with the CAM model is out of the question. Fifty-two coupled nonlinear differential equations simply cannot be handled analytically. Digital simulation requires roughly 60 seconds of computation time for each second of real-time solution, and hence becomes prohibitively expensive for a typical 30 second real-time run. However, the CAM has been implemented as a hybrid computer simulation at the Aerojet facility in Sacramento, California, and the hybrid simulation runs in real-time. The simulation includes a SIGMA 5 Digital Computer, a COMCOR 1500 Interface, two COMCOR 5000 Analog Computers, and two EAI 231R Analog Computers having a total of eight hundred analog amplifiers.

The difficulties encountered in attempting to solve the optimal control problem for complex, nonlinear systems such as NERVA are circumscribed in this study by proposing the method of State Dependent State Variable Feedback (SDSVF). The method is simple in concept. It is based on the realization of a desired transfer function using state variable feedback. This method of design was developed by Schultz and Melsa (1969) for the synthesis of linear control systems. In order to adapt the design method for use in controlling nonlinear systems, an on-line digital computer is utilized. The computer defines a sequence of linear constant coefficient models, each valid over a small portion of state space. The computer then calculates a set of feedback gains necessary to realize the desired transfer function for each of the linear models, and it computes control.

Chapter 2 contains a review of the most important work by previous investigators into the problem of nuclear rocket control. This review includes both design methods and mathematical models. The review is followed by development of the concept of State Dependent State Variable Feedback and the application of the control method to a system described by Van der Pol's Equation (Minorski, 1963).

Following this demonstration of the concept, State Dependent State Variable Feedback is used to control

a simple model of a nuclear rocket. This effort is successful and the results of these experiments are discussed briefly in Chapter 2. The purpose of this work was to develop familiarity with simple nuclear rocket engine models and provide experience in using State Dependent State Variable Feedback. This concludes the work performed at The University of Arizona. In order that the CAM Simulation be available, it was necessary that subsequent work be performed at the Aerojet Nuclear Systems Company's facility in Sacramento, California.

Initial attempts to apply SDSVF to control of the CAM were stymied by the lack of an adequate mathematical model on which to base control analysis. It was not possible to apply SDSVF directly to the CAM model equations because of the high order of the system (52nd order). The nuclear rocket models available from the literature are so simple that they cannot adequately represent CAM. The problem of inadequate nuclear rocket models is solved in Chapter 3 by developing a model based on the Common Analog Model of NERVA which, while simpler than CAM, does represent those characteristics of NERVA which are important in control system design. The development of this Simplified Nonlinear Model (SNM) required approximately six months of effort and is considered to be one of the major contributions of this study.

Up to this point all of the control experiments that had been conducted using SDSVF involved all digital simulation. Chapter 4 describes the first experiments in which an analog model is controlled in real-time by a digital computer using SDSVF. The model controlled is the SNM developed in Chapter 3. These experiments, in addition to verifying that SDSVF can be used to control as complex a system as the SNM, are used to investigate the possibility of reducing the order of the control models. It was important to reduce the order of the control model because the computation time required rises quickly with the order of the control model. When CAM is controlled, the computer is time-shared with the CAM Simulation which uses the digital computer more than half the time. It is shown that the control model can be reduced in order without affecting the system response adversely. To improve the response of the system to ramp inputs, the use of series compensation is tested and shown to be of value.

The control scheme developed in Chapter 4 to control the SNM is applied to the control of the CAM simulation in Chapter 5. Control is in real-time and, as mentioned previously, the digital computer is time-shared with the CAM Simulation. It is shown that the control scheme provides effective control of CAM over a wide operating range for both ramp and step inputs. The control system is shown to be relatively insensitive to errors in

the control model by varying the dominant system time constants $\pm$ 25 per cent and executing normal start-ups and shut-downs.

In this study a Simplified Nonlinear Model of the NERVA nuclear rocket engine is developed and the concept of State Dependent State Variable Feedback introduced. The model and the concept are used to design an on-line digital computer control system for the NERVA engine. The resulting control system is tested on the CAM and shown to provide effective control under a wide range of operating conditions. The results of the control experiments substantiate the validity of the Simplified Nonlinear Model and the effectiveness of State Dependent State Variable Feedback as a practical method of controlling complex, high order, nonlinear systems.

CHAPTER 2

STATE DEPENDENT STATE VARIABLE FEEDBACK

2.1 Introduction and Outline of Chapter

The literature contains numerous articles dealing with the design, testing, and control of nuclear rockets. In this chapter articles which deal specifically with simplified mathematical models of nuclear rocket engines and with the design of control systems for nuclear rocket engines are reviewed briefly. These models provide insight into the structure of a nuclear rocket engine but are not complex enough to represent the NERVA engine. In particular, the hydrogen flow is considered to be incompressible when in fact NERVA has both compressible and incompressible flow, and the description of the turbine/turbopump assembly is grossly simplified. The control design methods proposed in the papers reviewed are also discussed. These design methods are difficult to apply to the simplified models and would be useless on the more complex models required to represent NERVA accurately. To overcome this problem the State Dependent State Variable Feedback (SDSVF) method of control using an on-line digital computer is proposed as a practical method of controlling complex, high order, non-linear systems. The details involved in implementing the

control method are developed and the method is demonstrated by applying the method to the problem of controlling a system described by Van der Pol's Equation. Following this example SDSVF is applied to the control of the Smith-Stenning model of a nuclear rocket engine and the results of this effort are described briefly. The primary purpose of this effort is to provide the author with insight into the response of nuclear rocket engine models and additional experience in applying the SDSVF control method.

2.2 Review of the Literature

The simplified flow schematic in Figure 1-1 contains the basic components of a nuclear rocket engine. The literature contains a number of mathematical models based on this configuration (Smith and Stenning, 1961; Perry and Mohler, 1961; Wheatley and Mohler, 1960). These models contain four differential equations, two to describe the nuclear properties of the reactor, one to describe the properties of the reactor as a heat exchanger, and one for the speed of the turbopump. The equation for the pump speed is usually rewritten in terms of the propellant pressure as it exits the reactor. A representative model of this type is the Smith-Stenning Model (Smith and Stenning, 1961), the equations of which are shown below.

$$\frac{dS}{dt} = \frac{\delta - \beta}{\ell} S + \lambda C \qquad (2\text{-}1)$$

$$\frac{dC}{dt} = \frac{\beta}{\ell} S - \lambda C \tag{2-2}$$

$$\frac{dT}{dt} = C_p WT + A_1 S \tag{2-3}$$

$$\frac{dP}{dt} = A_2 \theta_v \sqrt{T} - A_3 \frac{P^2}{\sqrt{T}} \tag{2-4}$$

$$\delta = f_1(P,T) + A_4 \theta_D = f_2(P,T,\theta_D) \tag{2-5}$$

$$W = f_3(P,T) \tag{2-6}$$

where S = nuclear power

C = concentration of delayed neutrons

T = propellant temperature at core exit

P = propellant pressure at core exit

W = propellant flow rate

δ = total reactivity

θ_D = control drum angle

θ_v = turbine valve angle

β = delayed neutron yield fraction

ℓ = mean generation time of neutrons

λ = decay constant of the delayed neutrons

C_p = reactor-core heat transfer coefficient

A_1, A_2, A_3, A_4 = constants

It is significant to note that even this simple nuclear rocket engine model contains nonlinear differential and

algebraic equations, is multiple input-multiple output, and is tightly coupled.

Smith (1962) has shown that models of the Smith-Stenning type are open loop stable for very wide ranges in system parameters and has also investigated the closed loop stability of these simple models when controlled using classical controllers (Smith, 1962). Mohler (1965) discusses the use of Pontryagin's Maximum Principle (Pontryagin et al., 1962) to determine the optimal control for a nuclear rocket when minimum fuel consumption is the performance index. He shows that minimum fuel consumption requires a maximum effort process. This type of control is not permissible for a nuclear rocket engine because of the constraints on maximum rate of temperature and pressure change necessary to prevent structural damage to the reactor and stalling in the turbopump. In addition the resulting control is time dependent rather than state dependent. State dependent control is much preferred in situations such as this one, where significant model errors are possible. These problems led Mohler to the conclusion that some type of sub-optimal control scheme should be used. Weaver and Secker (1965) investigate the problem of noisy measurements and model inaccuracies in applying optimal control to a nuclear rocket engine. The solution proposed involves the use of a model following technique,

employing feedback to correct deviations from a desired trajectory.

The papers described above investigate and propose solutions to many of the problems encountered in the design of a control system for a nuclear rocket engine. However, the results of these studies are not directly applicable to the problem of controlling NERVA for the following reasons: First, the mathematical models used do not adequately represent the NERVA engine. They assume incompressible fluid flow when in fact NERVA has both compressible and incompressible flow. The description of the turbopump/turbine is grossly simplified, and the reactivity of the reactor is not represented accurately. Secondly, the analytic control design methods used are not practical tools for attacking the more complicated models necessary to represent NERVA.

Consideration of the problem of inadequate mathematical models is deferred until a later chapter, but the problem of inadequate control design methods is attacked in the next section by proposing the State Dependent State Variable Feedback method of control.

2.3 Development of State Dependent State Variable Feedback Control Method

The solution to the optimal control problem for a large class of linear or nonlinear systems is theoretically available from the Maximum Principle of Pontryagin

(Pontryagin et al., 1962) or Bellman's Dynamic Programming (Bellman, 1957). Unfortunately the practical utilization of both these methods suffers from a number of frequently described disadvantages. In particular, the solution of the optimal control problem for an n^{th} order system using the maximum principle requires solving a two point boundary problem of order 2n. Then, even if this difficult computational problem is solved, the solution is open loop; that is, the optimal control u is normally found as a function of time, $u(t)$, rather than the desired closed loop dependence on state, $u(\underset{\sim}{x})$. Solution of the optimal control problem using dynamic programming produces a solution that is a function of state, $u(\underset{\sim}{x})$. However, the computational problem is still difficult. For a system of order greater than two or three, with wide dynamic range in the state variables, the computation time and storage requirements make the method impractical.

This study proposes the method of State Dependent State Variable Feedback as a practical approach to the control of complex nonlinear and/or time-varying systems with large dynamic range in the state variables. The difficulties inherent in the maximum principle and dynamic programming are avoided by defining the optimal closed loop system in terms of a desired closed loop transfer function, rather than a performance index to be maximized or minimized.

Selection of a desired closed loop transfer function in the nonlinear and/or time-varying case is made possible by treating the system as a sequence of state and/or time dependent linear constant coefficient systems. These linear models are computed on-line by a digital computer. Each linear constant coefficient model has its own set of constant state variable feedback coefficients (also computed on-line) necessary to realize the desired closed loop transfer function. Thus, a sequence of state variable feedback coefficients is calculated to provide state and/or time dependent, state variable feedback control.

The procedure described requires periodic sampling of the system state and repeated linearization about the operating point to determine the state and/or time dependent linear constant coefficient model. After each new linear model is defined, a new set of feedback coefficients must be calculated to realize the desired closed loop transfer function. This procedure must be repeated often enough to insure that the sequence of linear models is an adequate representation of the nonlinear and/or time-varying system.

The state dependent control, $u(\underset{\sim}{x})$, is found as a linear combination of the state variables defined by the feedback coefficients. Since a digital computer is used to calculate the control, the control can only be computed

at discrete instants of time. The method of design used assumes continuous control, thus control must be calculated frequently enough to insure that errors generated by the discrete nature of the control signal are small.

2.3a Linearization Method

The types of nonlinear and/or time-varying systems of interest in this paper can be represented in state variable notation as shown below

$$\underset{\sim}{\dot{x}} = \underset{\sim}{F}(\underset{\sim}{x},\underset{\sim}{u},t) \tag{2-7}$$

$$\underset{\sim}{y} = \underset{\sim}{G}(\underset{\sim}{x},t) \tag{2-8}$$

It is assumed the system equations can be written in the following form:

$$\begin{bmatrix} \dot{x}_1 \\ \dot{x}_2 \\ \cdot \\ \cdot \\ \cdot \\ \dot{x}_n \end{bmatrix} = \begin{bmatrix} a_{11}(\underset{\sim}{x},\underset{\sim}{u},t) & \cdots & a_{1n}(\underset{\sim}{x},\underset{\sim}{u},t) \\ a_{21}(\underset{\sim}{x},\underset{\sim}{u},t) & \cdots & a_{2n}(\underset{\sim}{x},\underset{\sim}{u},t) \\ \cdot & \cdots & \cdot \\ \cdot & \cdots & \cdot \\ \cdot & \cdots & \cdot \\ a_{n1}(\underset{\sim}{x},\underset{\sim}{u},t) & \cdots & a_{nn}(\underset{\sim}{x},\underset{\sim}{u},t) \end{bmatrix} \begin{bmatrix} x_1 \\ x_2 \\ \cdot \\ \cdot \\ \cdot \\ x_n \end{bmatrix}$$

$$+ \begin{bmatrix} b_{11}(\underset{\sim}{x},\underset{\sim}{u},t) & \cdots & b_{1m}(\underset{\sim}{x},\underset{\sim}{u},t) \\ b_{21}(\underset{\sim}{x},\underset{\sim}{u},t) & \cdots & b_{2m}(\underset{\sim}{x},\underset{\sim}{u},t) \\ \cdot & \cdots & \cdot \\ \cdot & \cdots & \cdot \\ \cdot & \cdots & \cdot \\ b_{n1}(\underset{\sim}{x},\underset{\sim}{u},t) & \cdots & b_{nm}(\underset{\sim}{x},\underset{\sim}{u},t) \end{bmatrix} \begin{bmatrix} u_1 \\ u_2 \\ \cdot \\ \cdot \\ \cdot \\ u_m \end{bmatrix}$$

$$\begin{bmatrix} y_1 \\ y_2 \\ \vdots \\ y_m \end{bmatrix} = \begin{bmatrix} c_{11}(\underset{\sim}{x},t) & \cdots & c_{1n}(\underset{\sim}{x},t) \\ c_{21}(\underset{\sim}{x},t) & \cdots & c_{2n}(\underset{\sim}{x},t) \\ \vdots & & \vdots \\ c_{m1}(\underset{\sim}{x},t) & \cdots & c_{mn}(\underset{\sim}{x},t) \end{bmatrix} \begin{bmatrix} x_1 \\ x_2 \\ \vdots \\ x_n \end{bmatrix}$$

or

$$\dot{\underset{\sim}{x}} = \underset{\sim}{A}(\underset{\sim}{x},\underset{\sim}{u},t)\underset{\sim}{x} + \underset{\sim}{B}(\underset{\sim}{x},\underset{\sim}{u},t)\underset{\sim}{u}$$

$$\underset{\sim}{y} = \underset{\sim}{C}^T(\underset{\sim}{x},t)\underset{\sim}{x}$$

where a_{ij}, b_i, c_{ij} are bounded and continuous.

This latter set of equations is in the same form as the usual linear set of equations, except that the elements of $\underset{\sim}{A}$, $\underset{\sim}{B}$, and $\underset{\sim}{C}$ are functions of state, control, and time rather than constants. If the elements of these matrices are evaluated at some point in state space, $(\underset{\sim}{x}^o,\underset{\sim}{u}^o,t^o)$ and then treated as constants, they define a linear model valid for a short interval of time in some neighborhood of the operating point, $(\underset{\sim}{x}^o,\underset{\sim}{u}^o,t^o)$. This procedure must be repeated often enough so that the system state $(\underset{\sim}{x},\underset{\sim}{u},t)$ always remains in the vicinity of the current operating point, $(\underset{\sim}{x}^o,\underset{\sim}{u}^o,t^o)$.

The problem is to define a design procedure which can be implemented fast enough to insure that the above conditions are satisfied. This problem is simplified by the fact that for all systems analyzed using this method

which have the same number of inputs and outputs, m, it has been possible to linearize in such a manner as to result in "m" single input-single output systems.

2.3b Linear Design Method

The linear design technique used in this paper involves the use of state variable feedback to realize a desired closed loop transfer function. The method of design was developed by Schultz and Melsa (1967) who show that for the linear case selecting a desired transfer function is equivalent to choosing an integral quadratic performance index. The approach is only applicable to single input-single output systems; however, this is not a restriction because, as was stated previously, a system with an equal number of inputs and outputs, m, can always be linearized in such a manner as to result in "m" single input-single output systems. In dealing with physical systems it is often much easier to specify a desired transfer function than to specify an adequate quadratic performance index. The basic design method involves:

1. Representation of the linear model in the usual state variable feedback form, i.e.,

$$\dot{\underset{\sim}{x}} = \underset{\sim\sim}{A}\underset{\sim}{x} + \underset{\sim}{b}u$$

$$u = K[r - \underset{\sim}{k}^T\underset{\sim}{x}]$$

$$y = \underset{\sim}{c}^T\underset{\sim}{x}$$

where r is the input, K the adjustable forward gain, and k^T the feedback gains.

2. Determination of the transfer function of the closed loop system in terms of the forward gain and the feedback gains.
3. Choice of a desired closed loop transfer function.
4. Solution of the equations, resulting from equating the transfer functions from 2 and 3, for feedback gains and forward gain.

For linear systems the steps above need only be performed one time. However, when dealing with nonlinear systems, steps 2 and 4 must be repeated each time an updated linear model is calculated. The technique used in this paper to perform steps 2 and 4 on-line is based on a program developed by Melsa (1967) to aid in the design of linear control systems using state variable feedback. The technique makes use of the fact that solving for the feedback gains to realize a desired transfer function is trivial if the system is represented in terms of phase variables. Phase variable representation implies that the state variables are chosen to be the output and its n-1 derivatives. The system equations are transformed into phase variable form and the feedback gains for phase variables are calculated. The result is then transformed

back into the original state variables. The method is described below:

Assume that the system under study has a transfer function given by

$$G_1(s) = \frac{n_1 + n_2 s + \ldots n_m s^{m-1}}{d_1 + d_2 s + \ldots d_n s^{n-1} + s^n} \qquad (2\text{-}9)$$

and the desired transfer function is given by

$$G_2(s) = \frac{K(n_1 + n_2 s + \ldots + n_m s^{m+1})}{e_1 + e_2 s + \ldots e_n s^{n-1} + s^n} \qquad (2\text{-}10)$$

If the state variables chosen for this system are phase variables, the state variable representation is given by

$$\dot{\underset{\sim}{x}}^P = \underset{\sim}{A}^P \underset{\sim}{x}^P + \underset{\sim}{b}^P u \qquad (2\text{-}11)$$

$$y = (\underset{\sim}{C}^P)^T \underset{\sim}{x}^P \qquad (2\text{-}12)$$

$$A^P = \begin{bmatrix} 0 & 1 & 0 & \ldots & 0 \\ 0 & 0 & 1 & 0 \ldots & 0 \\ \cdot & \cdot & \cdot & \ldots & \cdot \\ \cdot & \cdot & \cdot & \ldots & \cdot \\ \cdot & \cdot & \cdot & \ldots & \cdot \\ \cdot & \cdot & \cdot & \ldots & \cdot \\ -d_1 & -d_2 & -d_3 & \ldots & -d_n \end{bmatrix} \quad b^P = \begin{bmatrix} 0 \\ 0 \\ \cdot \\ \cdot \\ \cdot \\ 0 \\ 1 \end{bmatrix}$$

$$[\underset{\sim}{C}^P]^T = [n_1, n_2, \ldots, n_m, 0 \ldots, 0]$$

A comparison of the phase variable representation and the transfer function representation reveals that the transfer function can be determined by inspection from the phase variable representation. If the closed loop expression for the control is given by,

$$u(t) = K[r(t) - (\underset{\sim}{k}^P)^T \underset{\sim}{x}^P(t)] \tag{2-13}$$

then the phase variable representation becomes

$$\underset{\sim}{x}^P = \begin{bmatrix} 0 & 1 & 0 & \cdots & 0 & 0 \\ 0 & 0 & 0 & \cdots & 0 & 0 \\ \vdots & \vdots & \vdots & & \vdots & \vdots \\ -(d_1+Kk_1^P) & -(d_2+Kk_2^P) & \cdots & & -(d_n+Kk_n^P) & \end{bmatrix} \underset{\sim}{x}^P + \begin{bmatrix} 0 \\ 0 \\ \vdots \\ 1 \end{bmatrix} r(t)$$

$$y(t) = K[n_1, n_2 \cdots n_m, 0 \ 0 \ . \ . \ 0] \underset{\sim}{x}^P(t)$$

Thus, the closed loop transfer function is given by

$$\frac{y(s)}{r(s)} = \frac{K(n_m s^{m-1}+n_{m-1}s^{m-2}+ \cdots n_1)}{s^n+s^{n-1}(d_n+Kk_n^P)+s^{n-2}(d_{n-1}+Kk_{n-1}^P)+ \cdots +(d_1+Kk_1^P)} \tag{2-14}$$

From Equation (2-14), it can be seen that the coefficients of the closed loop transfer function can be determined from the equation

$$e_i = d_i + Kk_i^P$$

and K is defined by the equation

$$K = \frac{e_1}{n_1}$$

assuming zero steady-state error is desired. It is also clear that state variable feedback affects only the gain of the numerator, not the location of the zeros.

As shown above, it is trivial to solve for the gain and feedback coefficients to achieve a desired transfer function when the system under study is represented in phase variables. However, most systems are not normally described using this set of state variables. Kalman (1963) has shown that it is possible to transform any controllable plant to phase variables by means of a non-singular linear transformation of variables of the form

$$\underset{\sim}{x} = \underset{\sim}{Q}\ \underset{\sim}{x}^P \tag{2-15}$$

or

$$\underset{\sim}{x}^P = \underset{\sim}{Q}^{-1}\ \underset{\sim}{x} \tag{2-16}$$

One method of obtaining this matrix is by use of the recursive relation shown below (Tuel, 1966)

$$\underset{\sim}{Q}^n = \underset{\sim}{b} \tag{2-17}$$

$$\underset{\sim}{Q}^{n-i} = \underset{\sim}{A}\ \underset{\sim}{Q}^{n-i+1} + d_{n-1+1}\ \underset{\sim}{b} \tag{2-18}$$

$$\underset{\sim}{Q} = \underset{\sim}{Q}^1/\underset{\sim}{Q}^2/\ \ldots\ /\underset{\sim}{Q}^n \tag{2-19}$$

where $\underset{\sim}{Q}^i$ indicates the i^{th} column of the $\underset{\sim}{Q}$ matrix and the d_i are the coefficients of the characteristic equation. The coefficients of the characteristic equation can be found by using the principal minor method (Korn and Korn, 1961). Using this method the coefficients of the characteristic equation are given by

$$d_i = (-1)^{n-1} \sum \left[\text{of the } \binom{n}{n-i+1} \begin{matrix} (n-1+1) \text{ order} \\ \text{principle minors} \\ \text{of A} \end{matrix} \right] \quad (2\text{-}20)$$

Once the feedback phase variable coefficients have been determined, they must be transformed back in terms of the actual system state variables. The defining equation for this transformation is

$$\underset{\sim}{k} = [\underset{\sim}{Q}^T]^{-1} \underset{\sim}{k}^P \quad (2\text{-}21)$$

Thus, the steps in solving for the required feedback coefficients are given by

1. Determine characteristic equation
2. Define matrix $\underset{\sim}{Q}$
3. Determine $[\underset{\sim}{Q}^T]^{-1}$
4. Calculate phase-variable feedbacks and gain

   a. $K = \dfrac{e_1}{n_1}$

   b. $k_i^P = \dfrac{e_i - d_i}{k}$

5. Determine state variable feedback and gain

$$\underset{\sim}{k} = [\underset{\sim}{Q}^T]^{-1} \underset{\sim}{k}^P$$

or $$\underset{\sim}{k}^T = [\underset{\sim}{k}^P]^T \underset{\sim}{Q}^{-1}$$

These steps are easily programmed, and the most time consuming calculation is the inversion of a matrix ($\underset{\sim}{Q}$) which is the same order as the linear system model.

2.3c Digital Computer Program Flow Chart

The State Dependent State Variable Feedback method of control is implemented by an on-line digital computer. The computer is required to update both the system and the control. The factors controlling the timing of these updates are discussed and a flow chart of a program to implement state dependent state variable control is developed.

State Dependent State Variable Feedback control involves essentially two types of computations, system update and control update. Control update involves measuring the system state, multiplying by the current set of feedback coefficients and transmitting the value of control to the system. The allowable interval between control updates is based on the necessity of keeping small the error generated because the control is discrete rather than continuous.

System update involves measurement of system state, linearization about a dynamic operating point, and computation of the required feedback gains and forward gain. The interval between system updates is controlled by the requirement that the linear model always be an adequate representation of the nonlinear system. Thus, the system update interval depends on the structure of the nonlinear system and the rate at which the system moves through state space. Normally the control must be updated much more frequently than the system.

Because of the different factors controlling the system update and the control update, it is convenient to divide the control program into two subprograms, one for each type of update. Shown in Figure 2-1 are flow charts for each of the update subprograms.

The validity of State Dependent State Variable Feedback is based on the ability of the digital computer to update the system and the control frequently enough to insure that the linear model is valid and that the assumption of continuous control is valid. An examination of the flow chart of the control update indicates that only state measurement and multiplication by feedback gains are involved. These tasks require almost no computer time. The system update flow chart, on the other hand, indicates that a matrix inversion must be performed for each update. The matrix is of the same order as the system. This

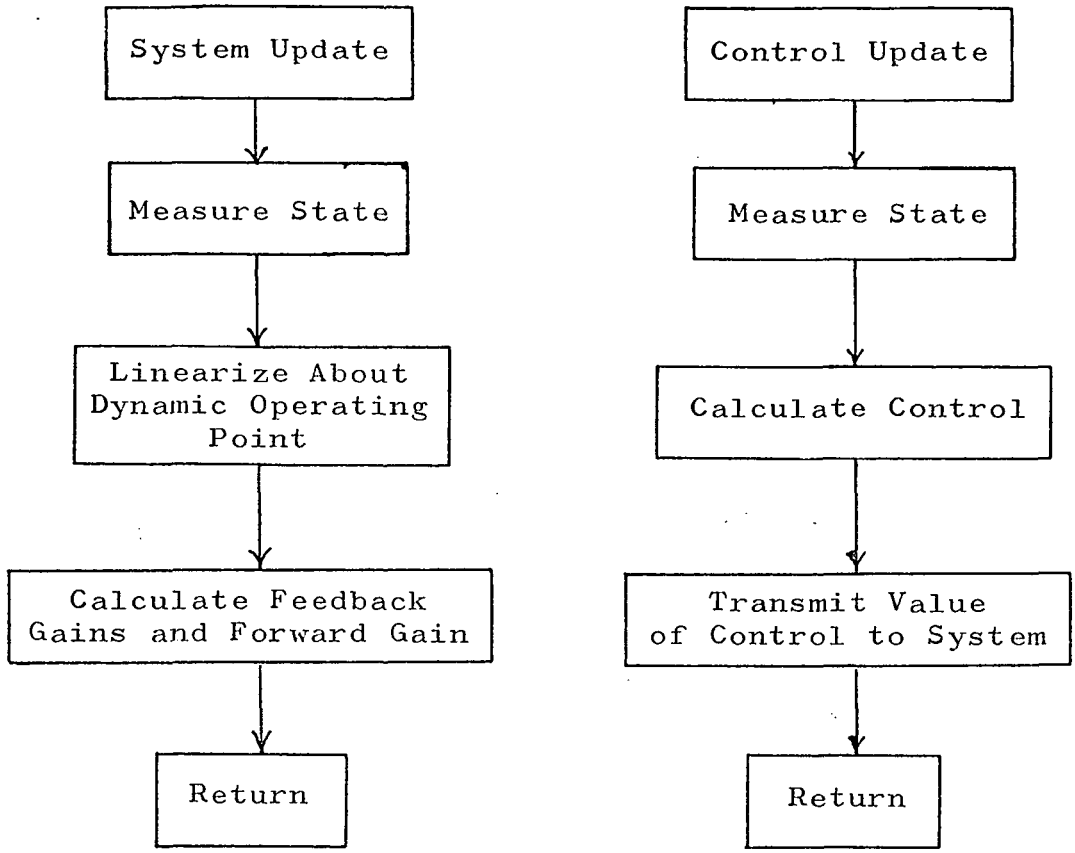

Figure 2-1. Flow Charts of System and Control Update

requirement is significant and must be considered before applying SDSVF control to a system.

2.4 Examples of the Use of State Dependent State Variable Feedback Control

State Dependent State Variable Feedback control is illustrated by the use of two examples. The first example involves the control of a system described by Van der Pol's Equation. Although Van der Pol's Equation is only second order, the example is nontrivial since the plant to be controlled is inherently unstable. The effect of different choices of the closed loop transfer function and model update interval are illustrated. In the second example, the procedure required to apply SDSVF to the Smith-Stenning model is described and the results of control experiments on the Smith-Stenning model are discussed.

2.4a Example #1 Van der Pol's Equation

Van der Pol's Equation is shown below

$$\frac{d^2y}{dt^2} + \alpha(y^2 - 1)\frac{dy}{dt} + y = 0 \qquad (2\text{-}22)$$

The system to be controlled is described by

$$\frac{d^2y}{dt^2} = \alpha(y^2 - 1)\frac{dy}{dt} + y = u(t) \qquad (2\text{-}23)$$

This may be rewritten as state equations in phase variables as

$$\begin{bmatrix}\dot{x}_1\\ \dot{x}_2\end{bmatrix} = \begin{bmatrix}0 & 1\\ -1 & -\alpha(x_1^2 - 1)\end{bmatrix}\begin{bmatrix}x_1\\ x_2\end{bmatrix}\begin{bmatrix}0\\ 1\end{bmatrix} u(t) \qquad (2\text{-}24)$$

Now let $\alpha(x_1^2 - 1) = a$, and apply the step by step design procedure outlined above. Note, since the initial state variables chosen here are phase variables, $\underset{\sim}{Q} = I = \underset{\sim}{Q}^{-1} = I$ and $\underset{\sim}{c}^T = [1,0]$. Because the system to be controlled is so simple the control design process is carried out by hand.

Step 1 of the linear design procedure requires that the system be put into the usual state variable feedback form

$$\dot{\underset{\sim}{x}} = [\underset{\sim}{A} - \underset{\sim}{K}\underset{\sim}{b}\underset{\sim}{k}^T]\underset{\sim}{x} + \underset{\sim}{K}\underset{\sim}{b}r \qquad (2\text{-}25)$$

$$y = \underset{\sim}{c}^T\underset{\sim}{x} \qquad (2\text{-}26)$$

or

$$\dot{x} = \underset{\sim}{A}_K\underset{\sim}{x} + \underset{\sim}{K}\underset{\sim}{b}r \qquad (2\text{-}27)$$

$$y = \underset{\sim}{c}^T\underset{\sim}{x} \qquad (2\text{-}28)$$

For Van der Pol's Equation the corresponding expressions are

$$\begin{bmatrix}\dot{x}_1\\ \dot{x}_2\end{bmatrix} = \begin{bmatrix}0 & 1\\ (-1 - Kk_1) & (-a - Kk_2)\end{bmatrix}\begin{bmatrix}x_1\\ x_2\end{bmatrix} + K\begin{bmatrix}0\\ 1\end{bmatrix} r \qquad (2\text{-}29)$$

$$y = [1,0] \begin{bmatrix} x_1 \\ x_2 \end{bmatrix} \qquad (2\text{-}30)$$

A block diagram of this set of equations is shown in Figure 2-2.

Step 2 of the design procedure requires finding the transfer function of the closed loop system $\frac{y(s)}{r(s)}$. Taking the Laplace Transform of Equations (2-27) and (2-28) and manipulating yields:

$$\frac{y(s)}{r(s)} = K \underset{\sim}{c}^T [s\underset{\sim}{I} - \underset{\sim}{A}_K]^{-1} \underset{\sim}{b} \qquad (2\text{-}31)$$

Performing these same operations on Equations (2-29) and (2-30) yields:

$$\frac{y(s)}{r(s)} = \frac{K}{s^2 + s[a + Kk_2] + [1 + Kk_1]} \qquad (2\text{-}32)$$

Step 3 requires the choice of a desired closed loop transfer function. The transfer function chosen here is

$$\frac{y(s)}{r(s)} = \frac{2}{(s + 1)(s + 2)} = \frac{2}{s^2 + 3s + 2}.$$

This transfer function yields an overdamped step response with zero steady state error. Equating the two transfer functions as required in Step 4 yields

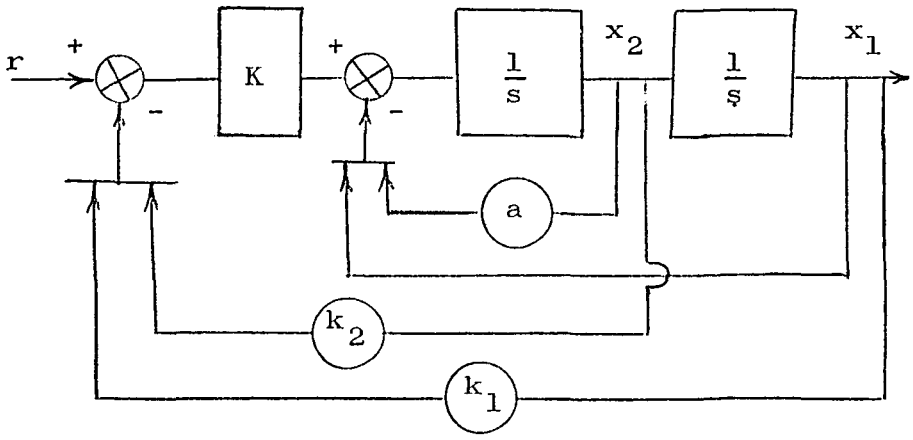

Figure 2-2. Linear Block Diagram of Van der Pol's Equation in Normal State Variable Feedback Form

$$K = 2$$

$$k_2 = (3 - a)/K = (3 - a)/2$$

$$k_1 = (2 - 1)/K = 1/2$$

The steps outlined above are those required for a normal linear system. In this nonlinear problem an on-line digital computer must perform this process periodically, since "a" is dependent on the system state.

The system update and control update intervals must now be chosen. The time constant of the desired transfer function is greater than 1 second. A control update interval of .02 second assures that errors resulting from the discrete nature of the control signal are small. The system update interval must be chosen so that the linear model is accurate. The only nonlinear term in the model is

$$a = \alpha(x_{1_o}^{\ 2} - 1)$$

Assume the system is known to operate near the origin of state space and that the types of inputs expected are step inputs of magnitude ≤ 3. The time constant of the closed loop system is greater than 1 second. Thus, as a worst case the value of "a" might change from $-\alpha$ to 8α in 1 second. If $\alpha = .25$, this implies

$$-1/4 \leq a \leq 2$$

The maximum value of the rate of change of "a" would be 2.25/1. sec = 2.25/sec. Thus, an update interval of .2 second insures that "a" changes not more than .2 sec x 2.25/sec = .45.

The coefficient of the characteristic equation in which "a" is involved is

$$a + Kk_2 = 3$$

Thus, a change in "a" of .45 between updates should not adversely affect the system performance. On this basis the system update interval is chosen to be .2 second.

Figure 2-3 shows the uncontrolled response of Van der Pol's Equation where $\alpha = .25$. Figure 2-4 compares the response of the controlled system when the desired transfer function is $\frac{2}{s^2 + 3s + 2}$ to that of a linear system with the same transfer function. The initial condition in each case is ($x_1 = -1$, $x_2 = 0$) and the demand input is $x_1 = 3$. The two responses are identical. Figure 2-5 shows the uncontrolled response of Van der Pol's Equation where $\alpha = 3.0$. Figure 2-6 again compares the response of the controlled system to a linear system with the same transfer function. Again the two responses are very similar. Figures 2-7 and 2-8 compare the response of the controlled system to the linear response when the system update time is changed to .4 second and .8 second. It can be seen that as the update time is increased, the response of the controlled nonlinear

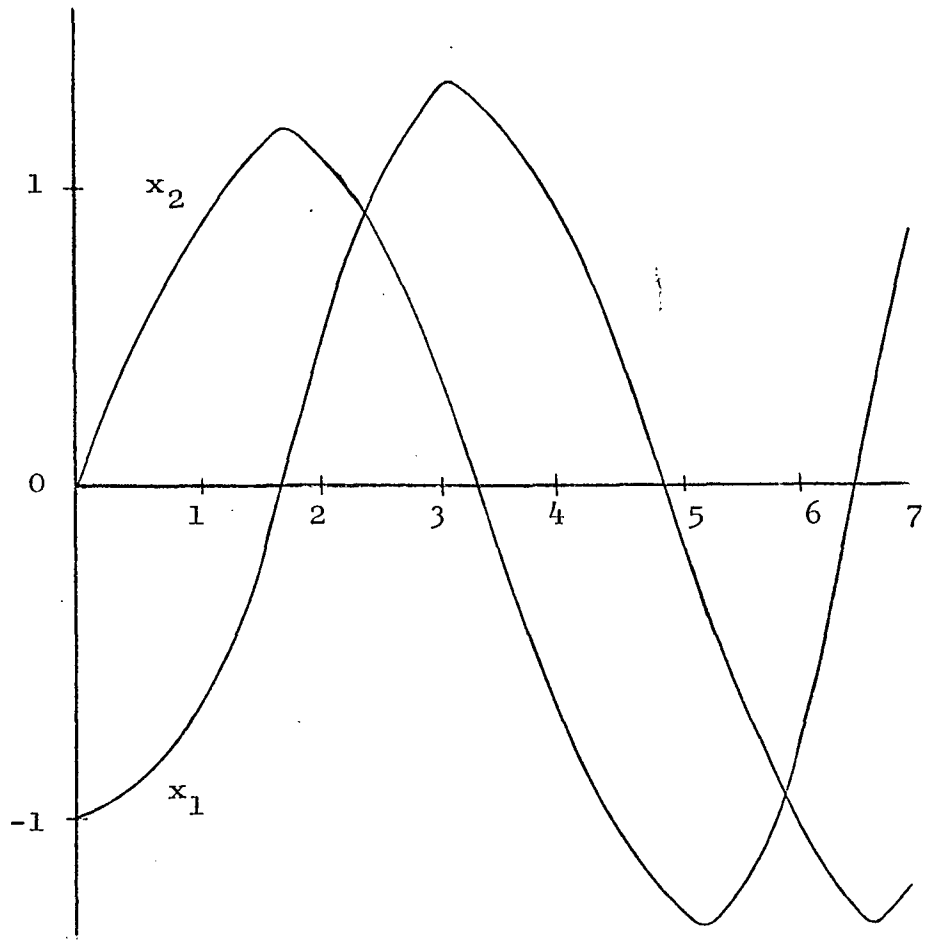

Figure 2-3. Uncontrolled Response of Van der Pol's Equation (α = .25)

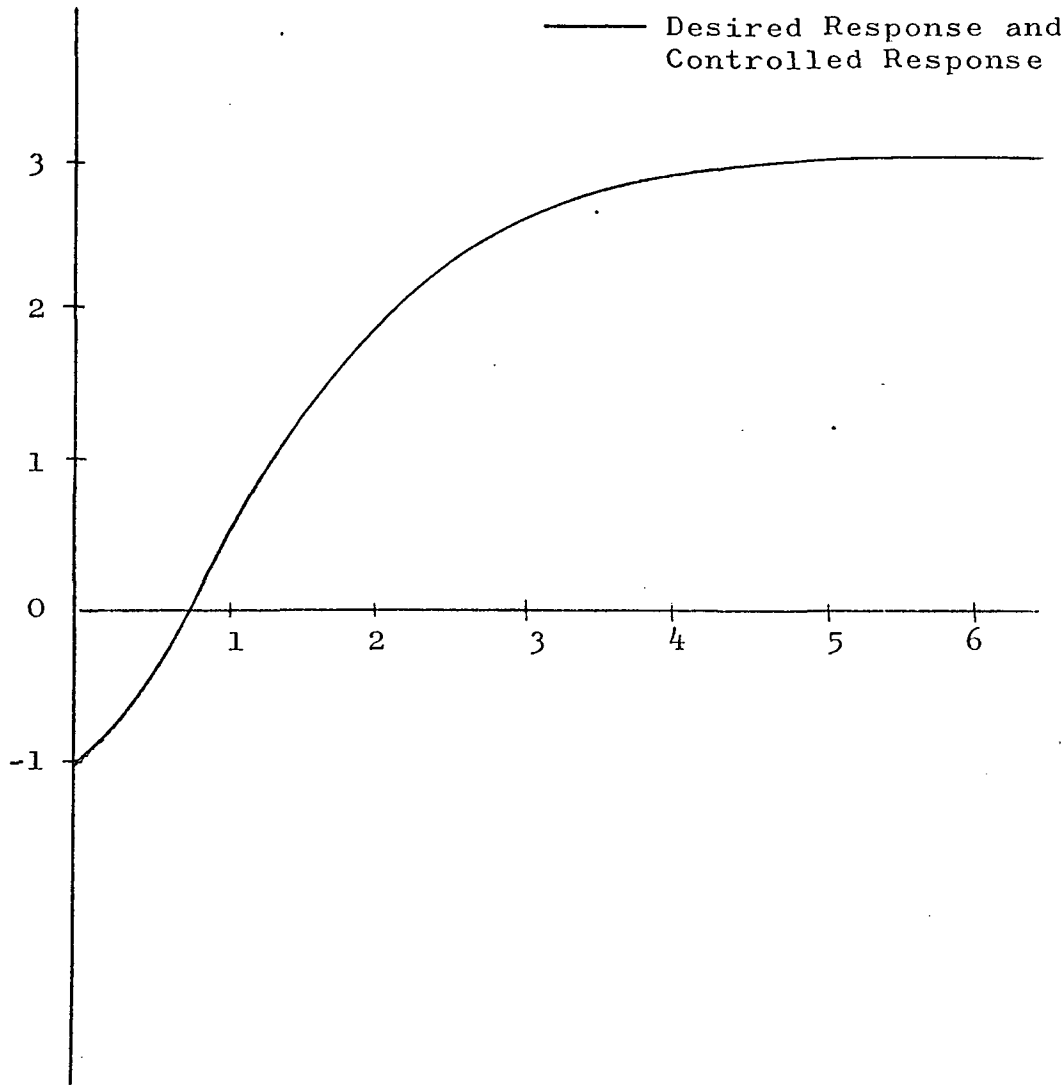

Figure 2-4. Response of Controlled Plant Compared to Desired Response (Update = .2 seconds)

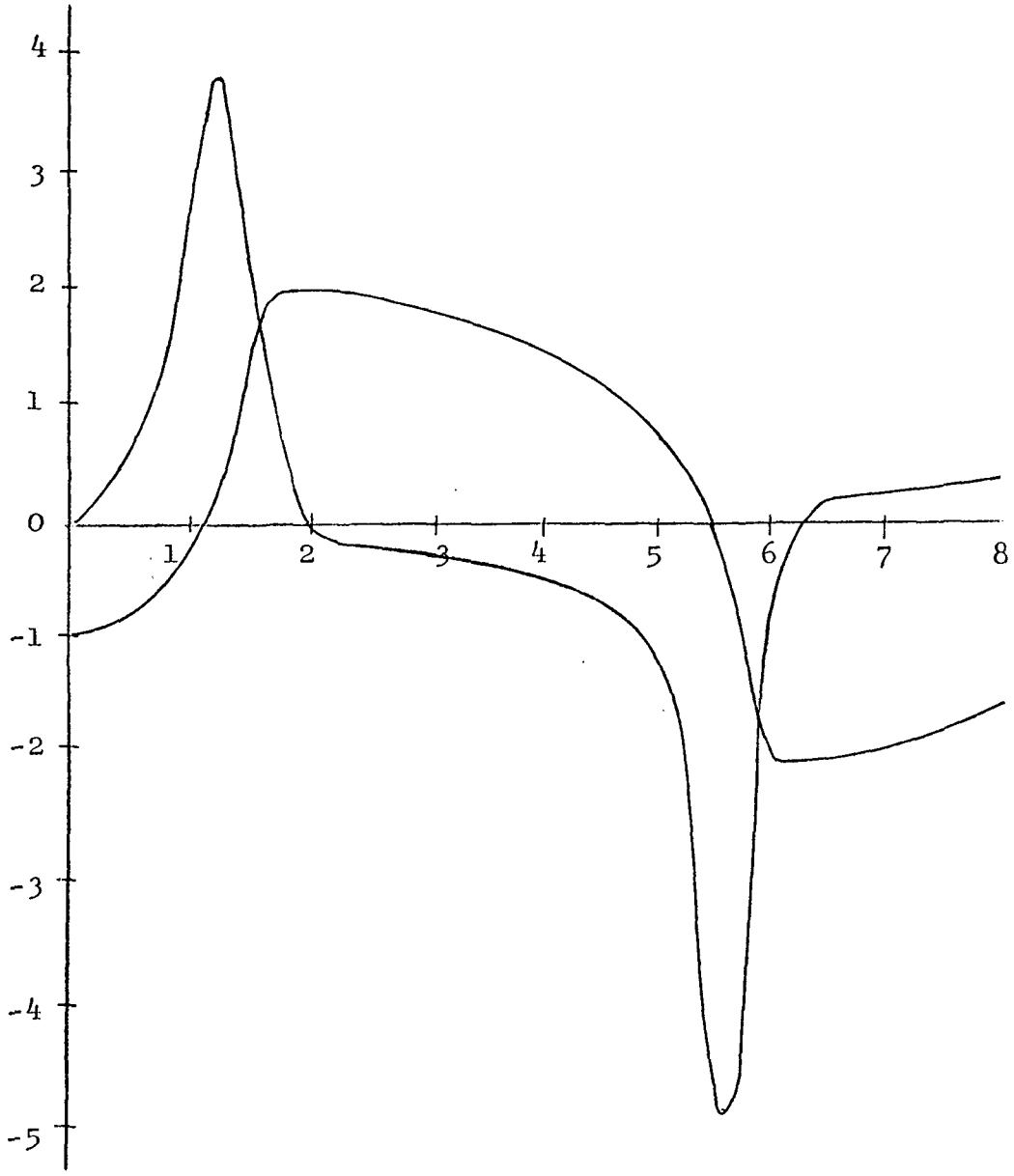

Figure 2-5. Uncontrolled Response of Van der Pol's Equation (α = 3.0)

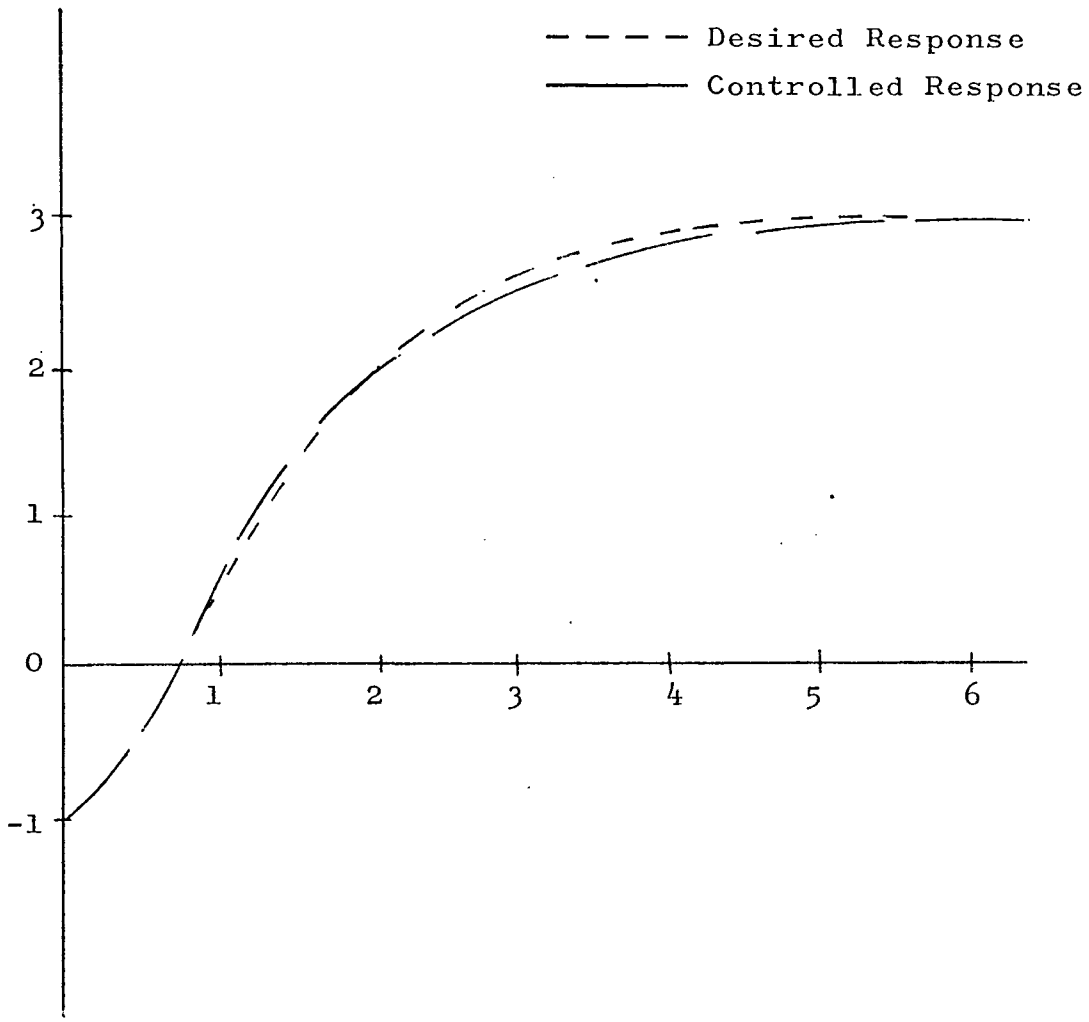

Figure 2-6. Comparison of Controlled Response to Desired Response (Update = .2, α = 3.0)

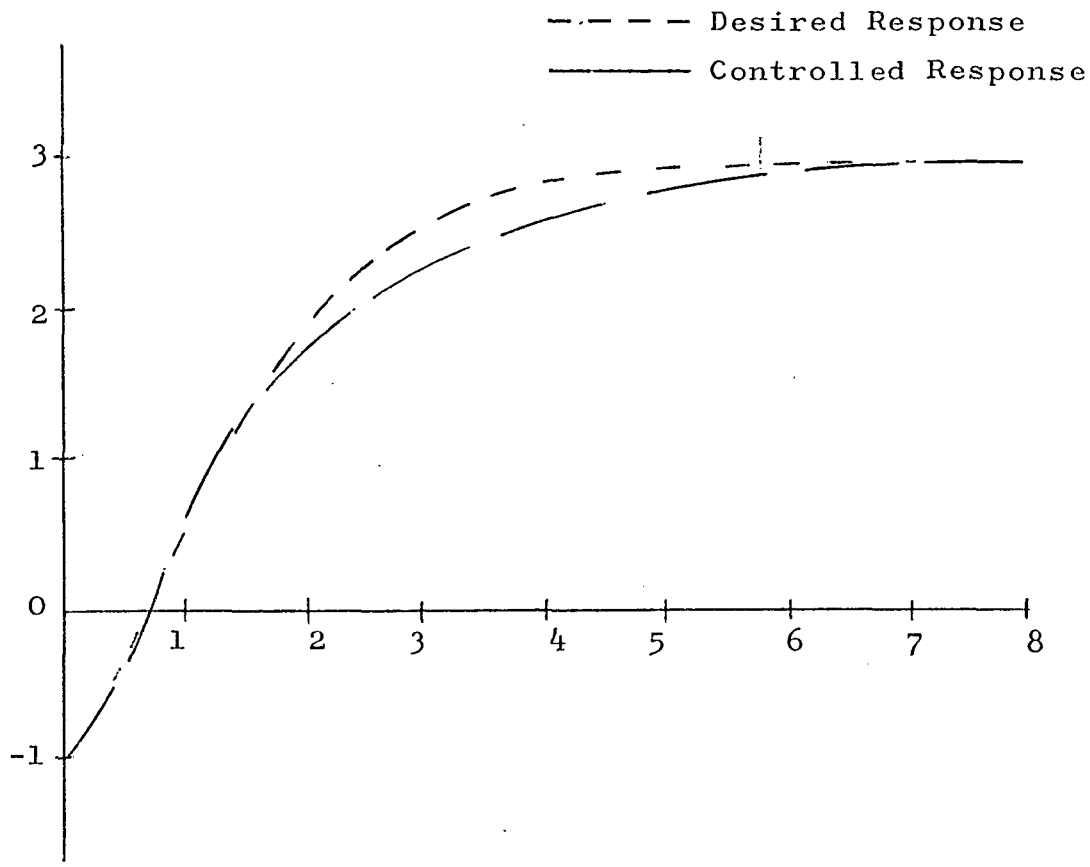

Figure 2-7. Comparison of Controlled Response to Desired Response (Update = .4 seconds, α = 3.0)

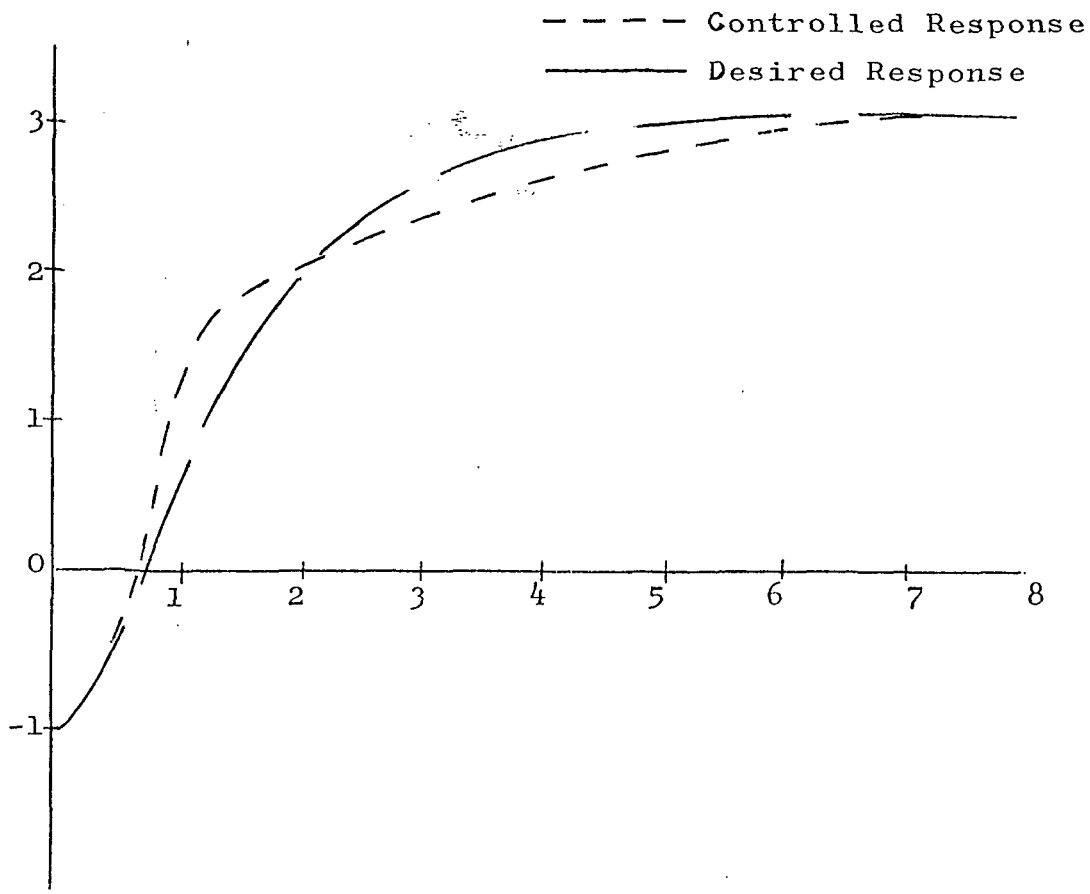

Figure 2-8. Comparison of Controlled Response to Desired Response (Update = .8 seconds, α = 3.0)

system differs more and more from the desired linear response. Figures 2-9 and 2-10 compare the response of the controlled nonlinear system to that of linear systems with transfer functions of $\frac{2}{s^2 + 1.5s + 2}$ and $\frac{2}{s^2 + .5s + 2}$. The system update time is .2 second in both cases.

These responses show that State Dependent State Variable Feedback can be used to control an extremely nonlinear system with reasonable update intervals. The control method works best when the desired transfer function is overdamped but by decreasing the update interval underdamped responses can be obtained. It is also apparent that the system update interval affects the performance significantly. In order for the control method to work properly, sufficient on-line computation capacity must be available to insure that the linear control model is accurate.

2.4b Example of Use of SDSVF to Control Smith-Stenning Model

The variable which must be controlled for any rocket engine is the engine thrust. When controlling a nuclear rocket engine there are additional considerations. First, the thrust buildup must occur in such a manner as to insure that the engine operates efficiently, i.e., high I_{sp}. In addition the rate of change of temperature and pressure during thrust buildup must not be so large as to cause damage to the reactor or other portions of the engine

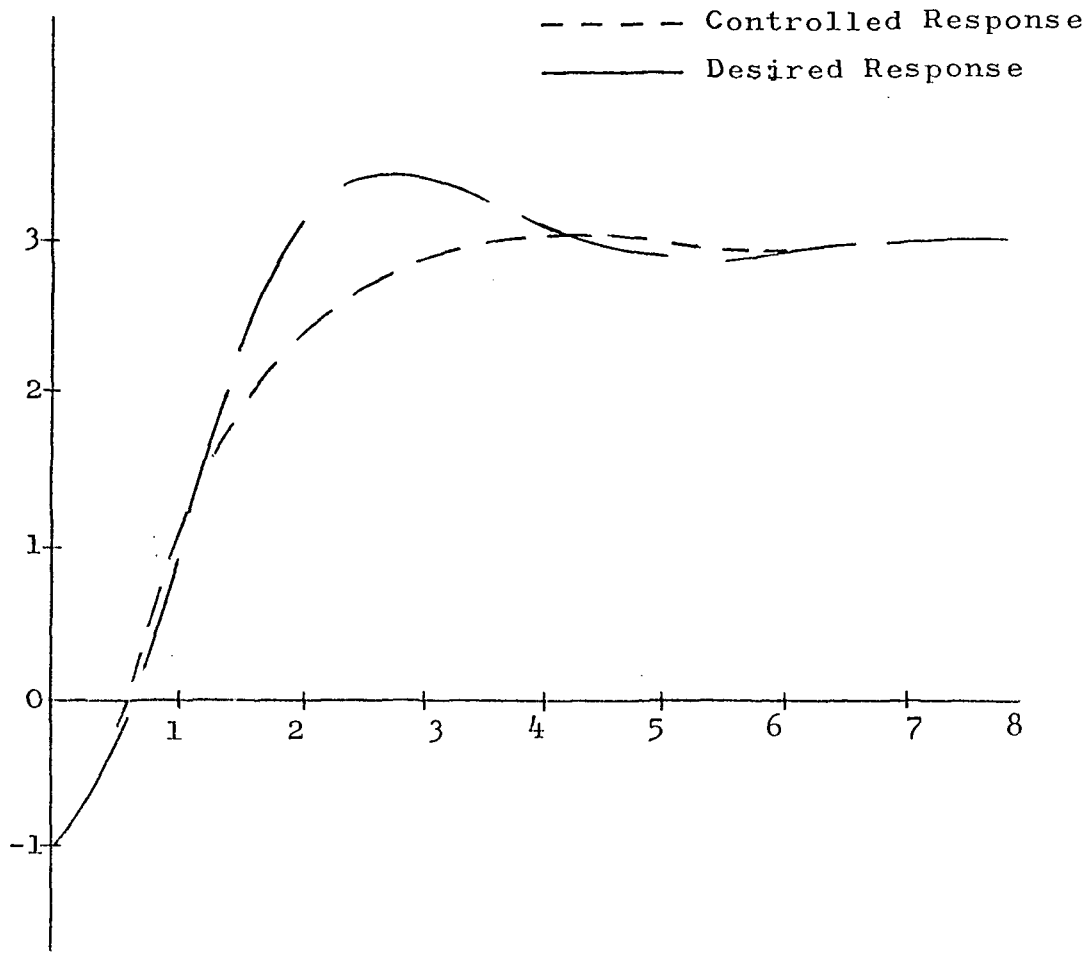

Figure 2-9. Comparison of Controlled Response to Desired Response (Update = .2 seconds, α = 3.0)

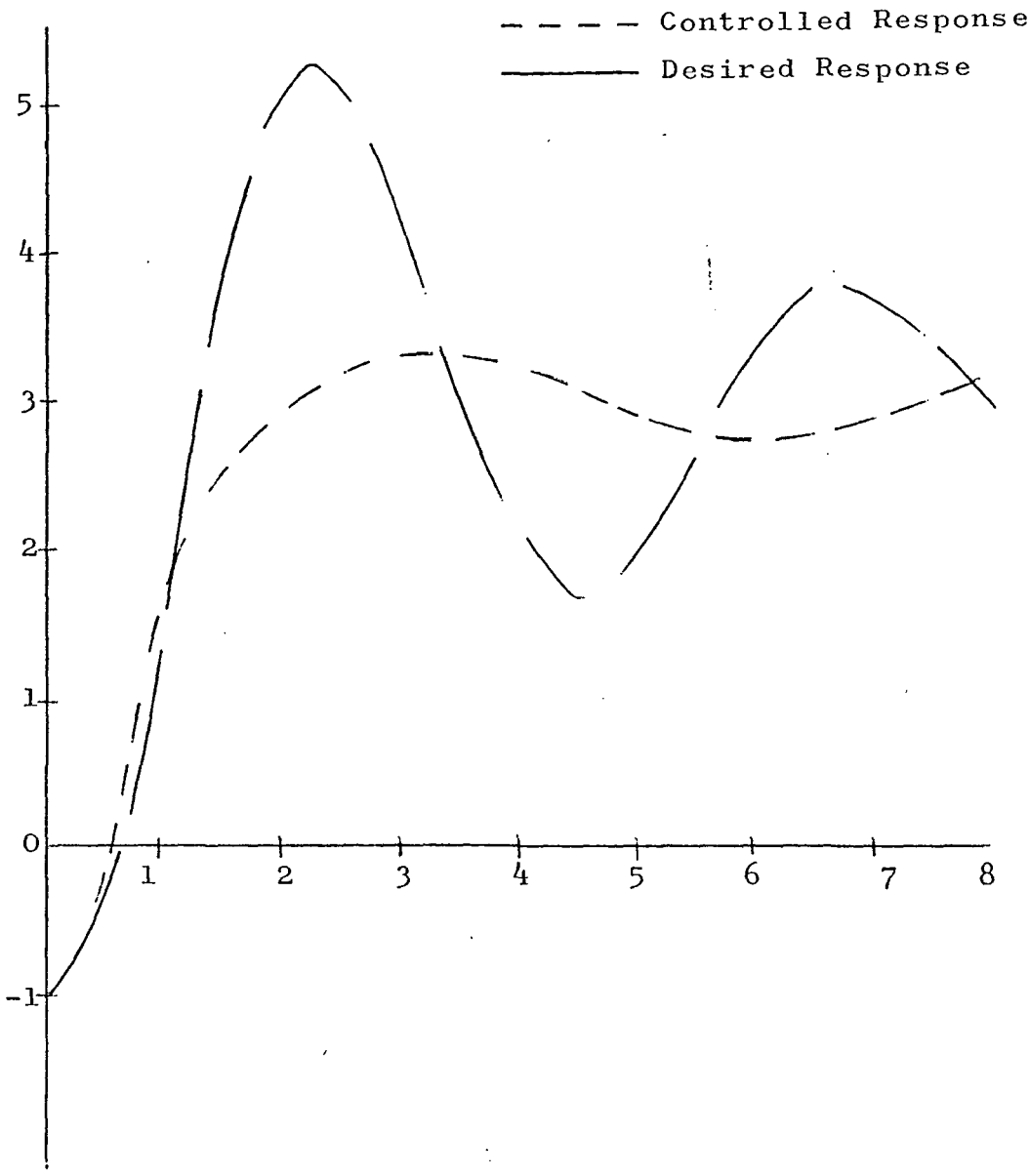

Figure 2-10. Comparison of Controlled Response to Desired Response (Update = .2 seconds, α = 3.0)

system. Because of these requirements, a nuclear rocket engine control system directly controls the temperature and pressure of the propellant at the reactor exit. The two control inputs available are control drum angle and turbine valve angle. In applying SDSVF control to the Smith-Stenning Model, the control drum angle is used to control temperature and the turbine valve angle is used to control pressure. Using this convention and applying the linearization method to the Smith-Stenning Model yields the following equations at the operating point (P^o, T^o, C^o, S^o, $\theta_D{}^o$, $\theta_v{}^o$)

$$\frac{dS}{dt} = -\left[\frac{\beta}{\ell} - \frac{f_2(P^o, T^o, \theta_D{}^o)}{\ell}\right] S + \lambda C + A_4 S^o \Delta\theta_D \qquad (2\text{-}33)$$

$$\frac{dC}{dt} = \frac{\beta}{\ell} S - \lambda C \qquad (2\text{-}34)$$

$$\frac{dT}{dt} = -C_p F_3(P^o, T^o)T + A_1 S \qquad (2\text{-}35)$$

$$\frac{dP}{dt} = -A_3 \frac{P^o}{\sqrt{T^o}} P + A_2 \sqrt{T^o}\ \theta_v \qquad (2\text{-}36)$$

When the time constants of these linear equations are evaluated, the nuclear power level (S) time constant is much faster than the other system time constants. For this reason this differential equation is approximated by an algebraic equation as shown below

$$\text{let } \frac{\beta}{\ell} - \frac{f_2\ (P^o,\ T^o,\ \theta_D{}^o)}{\ell} = DKTO$$

then assuming $\frac{dS}{dt} = 0$ implies

$$S = \frac{\lambda C}{DKTO} + A_4 S^o \Delta\theta_D \tag{2-37}$$

substituting (2-37) into (2-34), (2-35), and (2-36)

$$\frac{dC}{dt} = \left[\frac{\beta}{\ell}\left(\frac{\lambda}{DKTO}\right) - \lambda\right] C + \frac{\beta}{\ell} A_4 S^o \Delta\theta_D \tag{2-38}$$

$$\frac{dT}{dt} = + \frac{A_1 \lambda}{DKTO} C - C_p f_3(P^o,\ T^o)T + A_1 A_4 S^o \Delta\dot{\theta}_D \tag{2-39}$$

$$\frac{dP}{dt} = - \frac{A_3 P^o}{\sqrt{T^o}} P + A_2 \sqrt{T^o}\ \theta_v \tag{2-40}$$

Examining the equation above it is seen that the original set of nonlinear coupled equations has been reduced to two single input-single output linear systems as shown below

Temperature Loop

$$\begin{bmatrix} \dot{C} \\ \dot{T} \end{bmatrix} = \begin{bmatrix} \left(\frac{\beta}{\ell}\ \frac{\lambda}{DKTO} - \lambda\right) & 0.0 \\ \frac{A_1 \lambda}{DKTO} & -C_p f_3(P^o, T^o) \end{bmatrix} \begin{bmatrix} C \\ T \end{bmatrix} + \begin{bmatrix} \frac{\beta}{\ell} A_1 S^o \\ A_1 A_4 S^o \end{bmatrix} \Delta\theta_D \tag{2-41}$$

Pressure Loop

$$\dot{P} = \left[\frac{-A_3 P^o}{\sqrt{T^o}}\right] P + \left[A_2 \sqrt{T^o}\right] \theta_v \qquad (2\text{-}42)$$

It is now possible to apply the SDSVF design procedure in exactly the same manner as in the Van der Pol example except that now two desired transfer functions must be specified, two sets of feedback coefficients must be calculated, and two control signals must be calculated at the update times.

The details involved in the control experiments conducted on the Smith-Stenning Model are not discussed further in this study, other than to state that SDSVF did prove to be effective in obtaining the desired system response. A more detailed description of these experiments is not included because the control of this system illustrates only two capabilities of SDSVF not included in the Van der Pol example, the replacement of a differential equation by an algebraic equation and decoupling the system during the linearization process. Both of these capabilities are better demonstrated by control experiments described later in this study.

The two examples contained in this chapter demonstrated the capabilities of SDSVF in the control of reasonably complex nonlinear systems. The next chapter

considers the problems encountered in applying SDSVF to control of the NERVA engine.

CHAPTER 3

DEVELOPMENT OF SIMPLIFIED NONLINEAR MODEL

3.1 Introduction and Outline of the Chapter

In Chapter 2 the concept of State Dependent State Variable Feedback was introduced, the techniques required to implement SDSVF developed, and the control method illustrated by controlling two nonlinear systems. One of these was a simple model of a nuclear rocket engine. The next logical step is to apply the control method to the best available model of the NERVA engine, since the NERVA engine itself has not been constructed.

The best existing model of NERVA is the Common Analog Model (CAM) developed by Aerojet Nuclear Systems Company and Westinghouse Astronuclear Laboratory. The CAM was developed to be used for detailed systems studies and is extremely complex. Appendix A contains those portions of the CAM equations which are not classified. The model contains 52 first order differential equations, an even larger number of nonlinear algebraic equations and numerous functions defined by experimental data. When run as a digital computer simulation on an IBM 360/70 digital computer, the computer time to problem time ratio is greater than 60 to 1. Thus for a typical problem time run

of 30 to 60 seconds, digital simulation becomes prohibitively expensive. The CAM is, however, implemented as a hybrid simulation at the Aerojet Nuclear Systems Company facility in Sacramento, California. The simulation utilizes a SIGMA 5 Digital Computer, a COMCOR 5000 Interface, 2 COMCOR 1500 Analog Computers, and 2 EAI 231R Analog Computers. This hybrid simulation of CAM runs in real-time. In order to have access to the hybrid simulation, all further work presented in this study was conducted at the Aerojet facility in Sacramento, California. Appendix B contains a more complete description of the Aerojet Nuclear Systems Company's hybrid computer facility.

It is not possible to apply SDSVF to the CAM equations directly because of the requirement to invert a matrix, of the same order as the control model of CAM, each time the system is updated. Inversion of a 52nd order matrix during any reasonable update interval is impossible. The only way to solve this problem is to use a lower order control model. Examination of the frequency response data from the CAM simulation, shown in Figures 3-1 and 3-2, indicates that a much lower order control model may be adequate. However, the only simplified models available are of the Smith-Stenning type, and these do not adequately represent NERVA. For this reason a Simplified Nonlinear Model (SNM) is developed based on CAM. This model is to be

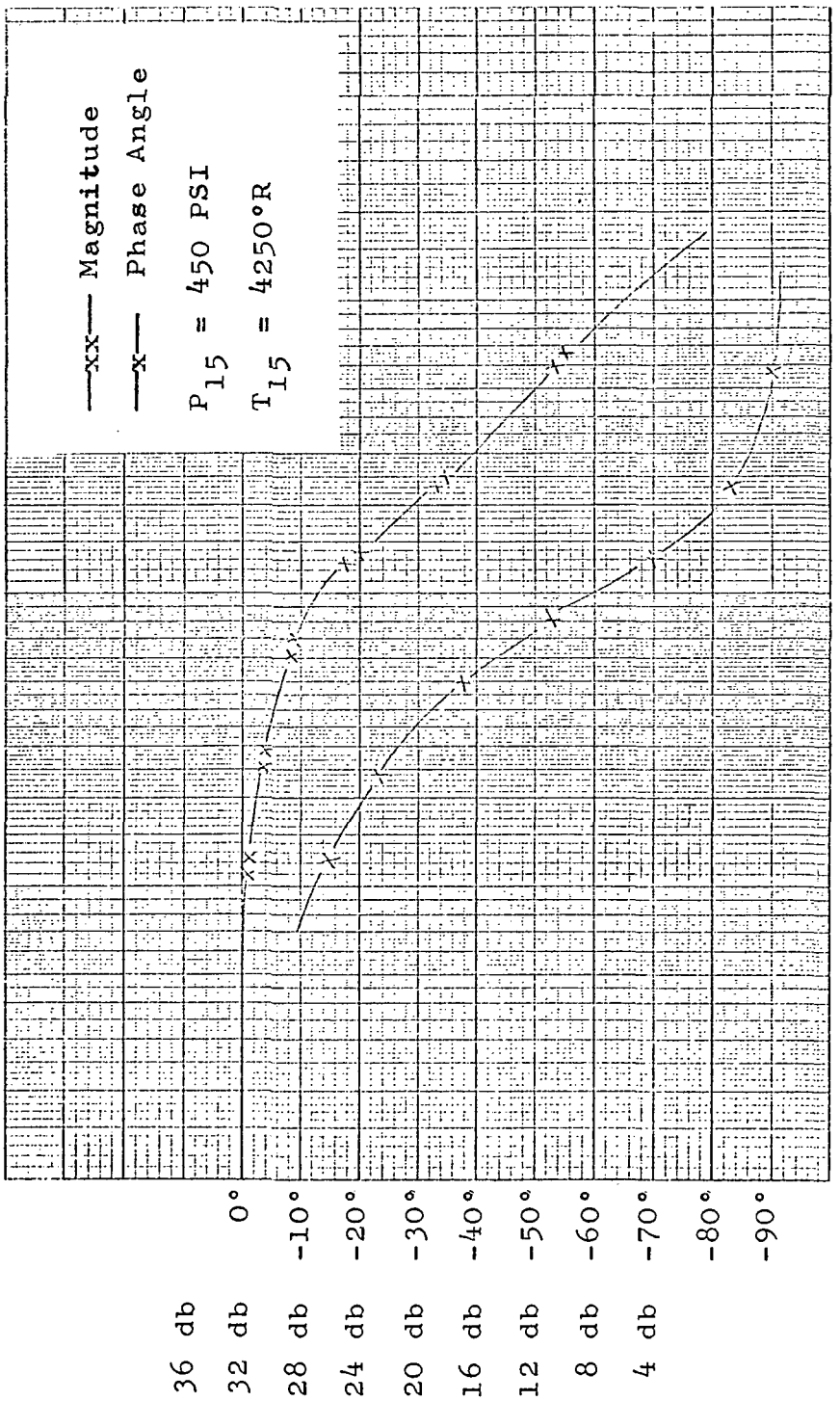

Figure 3-1. CAM Frequency Response at Design (T_{15}/θ_D)

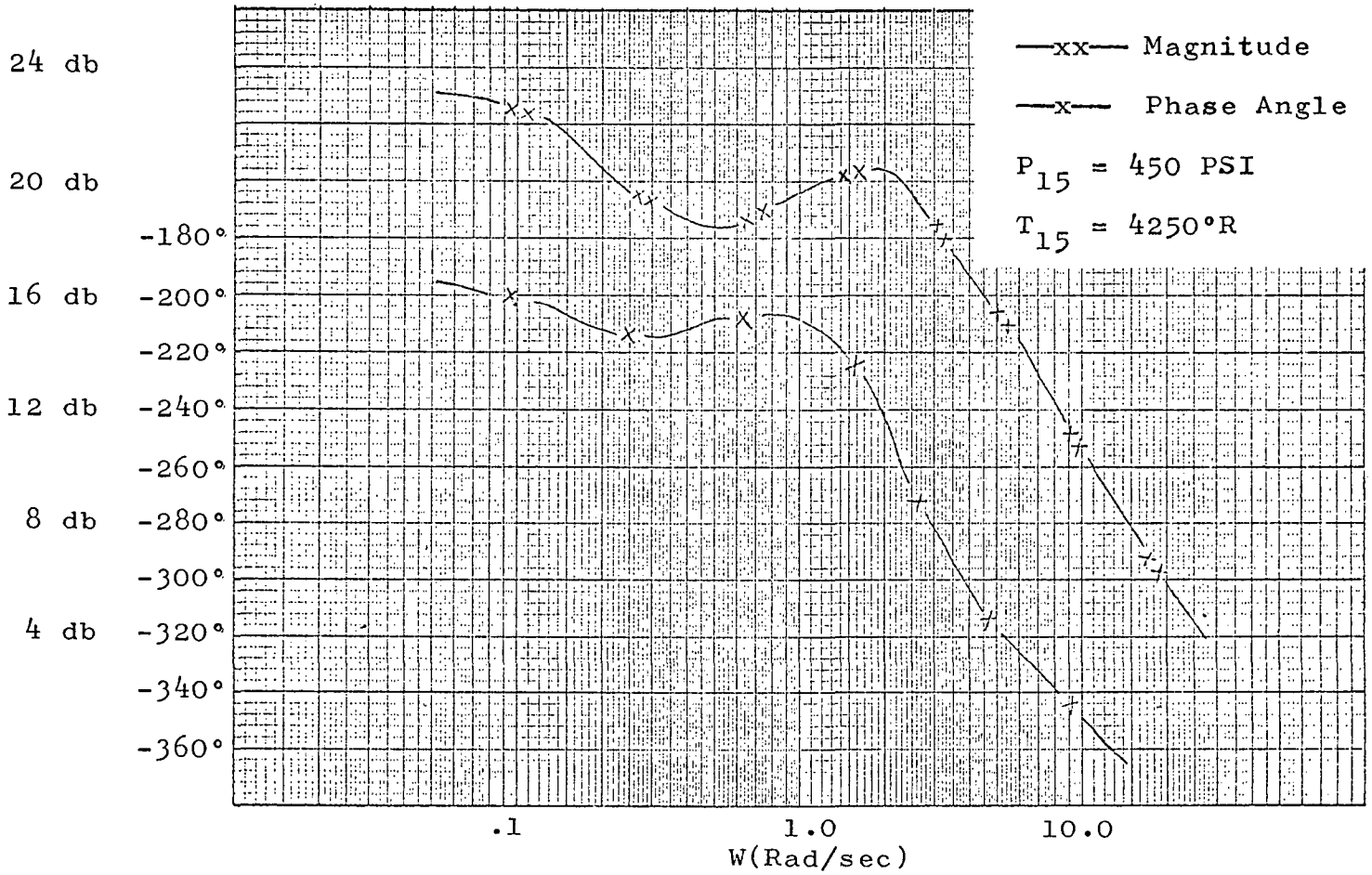

Figure 3-2. CAM Frequency Response at Design (P_{15}/θ_{BCV})

used to design a control system for the CAM simulation using SDSVF in a later chapter.

There is no completely algorithmic method of developing a mathematical model of a system. The method used to develop the SNM starts with the CAM equations and reduces the order and complexity of the model while at the same time maintaining the validity of the model from a control systems design point of view. The objective is to generate a system description, in the form of Equations 2-7 and 2-8, that represents the NERVA engine over the controlled thrust buildup region of operation. This region covers roughly the region of operation from (T_{15} = 1000° R, P_{15} = 50 PSI) up to (T_{15} = 5000° R, P_{15} = 500 PSI).

This is accomplished in three steps. The first step involves an initial selection of the CAM variables to be included in the SNM. The selection of these variables is based on the concept that a control system is a device for power amplification and transmission. On this basis, the only variables important to a control model are those involved in the power transmission and amplification between the system inputs and the system outputs. Following this initial selection of variables, the number of variables represented by differential equations is reduced by linearizing the defining differential equation of each variable and comparing the time constant of the variable to the dominant system time constant. If the time constant of

a variable is less than one-tenth the dominant system tine constant, then the differential equation is replaced by an algebraic equation. This procedure reduces the number of differential equations to eight, with a corresponding increase in the number of nonlinear algebraic equations. The final step in the modeling procedure forces a reduction of the number of nonlinear algebraic equations by curve fitting static data from CAM with a reduced number of nonlinear algebraic equations.

There is no completely satisfactory method of determining the validity of the SNM. The model is tentatively accepted as valid on the basis of comparison of data from CAM with similar data from an analog simulation of the SNM. The data include small signal frequency responses at various operating points and static operating maps. The conclusive test of the model's validity is the design of a control system for the CAM Simulation in Chapter 5.

3.2 Initial Selection of Variables Included in Simplified Nonlinear Model

The NERVA engine system is composed of two subsystems, the nuclear reactor subsystem and the propellant flow subsystem. To determine all of the variables to be initially included in the SNM, the power flow must be traced through both subsystems. In addition the power flow between the two subsystems must be traced. To illustrate

the procedure, the power flow is traced through the propellant flow subsystem, between the turbine by-pass control valve and the propellant exit pressure. Figure A-1 in Appendix A is a flow schematic of the NERVA engine. Reference to this figure is recommended in order to determine the portions of the flow structure being considered. Table A-1 in Appendix A defines the variable names used. NERVA contains dual turbines, turbopumps, and valves for reliability purposes; however, only one of each is considered in the following analysis.

The process of tracing the power flow begins by putting the output variable, P_{15}, on the list of variables to be included in the SNM. Then the defining equation for P_{15} is examined

$$P_{15} = 5.32\ T_{15}\ R_{15} \tag{3-1}$$

There are two variables in this equation that are undefined thus far, T_{15} and R_{15}. One of the variables, T_{15}, is a variable from the nuclear reactor subsystem. The power flow is now being traced through the propellant flow subsystem. Therefore, T_{15} is treated as a parameter to be defined when the power flow is traced through the nuclear reactor. It is not added to the list of variables for the SNM at this time. The other undefined variable, R_{15}, is a propellant flow subsystem variable. It is added to the

variable list for the SNM and its defining equation examined.

$$\frac{dR_{15}}{dt} = .063\ (W_c - W_n) \tag{3-2}$$

Both of the new variables introduced in this equation are variables in the propellant flow subsystem. They are added to the variable list for the SNM and their defining equations examined.

$$W_n = 13.3\ P_{15}/\sqrt{T_{15}} \tag{3-3}$$

$$W_c = \sqrt{P_{14.5} - P_{15}}/\sqrt{.0023/R_{14.5}} \tag{3-4}$$

The new variables introduced by these equations are $P_{14.5}$ and $R_{14.5}$. They are added to the SNM variable list and their defining equations examined.

Continuing this process yields the following set of equations:

$$P_{14.5} = 5.32\ T_{14.5}\ R_{14.5} \tag{3-5}$$

$$\frac{dR_{14.5}}{dt} = .173\ (W_{cs} - W_c) \tag{3-6}$$

$$W_{cs} = 19.5\ \sqrt{R_{14}(P_{14} - P_{14.5})} \tag{3-7}$$

$$P_{14} = 5.32/(1 - .186\ R_{14}) - 214\ R_{14} \tag{3-8}$$

$$\frac{dR_{14}}{dt} = .107\ (W_{14} - W_{cs}) \tag{3-9}$$

$$W_{14} = 26.1 \sqrt{R_{13}(P_{13} - P_{14})} \tag{3-10}$$

$$P_{13} = 5.32\ T_{13}\ R_{13} \tag{3-11}$$

$$\frac{dR_{13}}{dt} = .13\ (W_{scv} + W_{Bcv} - W_{14}) \tag{3-12}$$

$$W_{scv} = .23\ \theta_{scv} \sqrt{R_{12}(P_{12} - P_{13})} \tag{3-13}$$

$$W_{Bcv} = .042\ \theta_{Bcv} \sqrt{R_{11}(P_{11} - P_{13})} \tag{3-14}$$

$$P_{12} = 5.32\ T_{12}\ R_{12} \tag{3-15}$$

$$\frac{dR_{12}}{dt} = 1.85\ (W_T - W_{scv}) \tag{3-16}$$

$$W_T = 16.58\ f_1\ (\frac{P_{11}}{P_{12}}) / \sqrt{T_{11}} \tag{3-17}$$

$$P_{11} = 5.32\ T_{11}\ R_{11} \tag{3-18}$$

$$\frac{dR_{11}}{dt} = .166\ (W_{11} - W_{Bcv} - W_T) \tag{3-19}$$

$$W_{11} = 17.8 \sqrt{R_{10}(P_{10} - P_{11})} \tag{3-20}$$

$$P_{10} = 5.32\ T_{10}/(1 - .186\ R_{10}) - 214\ R_{10} \tag{3-21}$$

$$\frac{dR_{10}}{dt} = .12\ (W_{ps} - W_{11}) \tag{3-22}$$

$$W_{ps} = 36 \sqrt{R_9(P_9 - P_{10})} \tag{3-23}$$

$$P_9 = 5.32\ T_9/(1 - .186\ R_9) - 214\ R_9 \tag{3-24}$$

$$\frac{dR_9}{dt} = .188\ (W_R + W_{ss} + W_{ssb} - W_{ps}) \tag{3-25}$$

$$W_R = 10\ \sqrt{R_7(P_7 - P_{10})} \tag{3-26}$$

$$P_7 = f_3(R_7) \tag{3-27}$$

$$\frac{dR_7}{dt} = .368\ (W_{Nc} - W_R) \tag{3-28}$$

$$\frac{dW_{Nc}}{dt} = 117\ (P_5 - P_7 - \frac{.0314}{R_7}\ W_{Nc}^{\ 2}) \tag{3-29}$$

$$\frac{dP_5}{dt} = \frac{1810 + 1.4\ P_5}{4.44}\ (W_5 - W_{Nc} - W_{ssB}) \tag{3-30}$$

$$\frac{dW_5}{dt} = 34.2\ (P_4 - P_5) - 109\ W_5^{\ 2} \tag{3-31}$$

$$\frac{dP_4}{dt} = \frac{1810 + 1.4\ P_4}{1.23}\ (W_P - W_5 - W_{ssv}) \tag{3-32}$$

$$\frac{dW_P}{dt} = 127.5\ (P_2 - P_4) - .783\ W_P^{\ 2} \tag{3-33}$$

$$P_2 = P_1 + N^2\ f_1\ (\frac{W_P}{N}) \tag{3-34}$$

$$\frac{dN}{dt} = 88.1\ (M_T - M_P) \tag{3-35}$$

$$M_P = N^2\ f_2\ (\frac{W_P}{N}) \tag{3-36}$$

$$M_T = 7430\ \frac{W_T}{N}\ E_T\ \Delta E_s \tag{3-37}$$

Examination of the variables in Equation (3-36) shows that no new variables are added to the variable list since N is defined by Equation (3-35) and W_P is defined by Equation (3-33). The same is true in Equation (3-37). The only new variables here are E_T and ΔE_s and these are variables from the nuclear reactor subsystem. When this situation occurs, i.e., all variables are defined by some other equation in the set, the procedure is complete.

The equations are now examined to determine if any parallel paths of power flow exist. Where parallel paths do exist, a check is made to determine if any of the paths can be neglected without significantly affecting the power level.

The only parallel path in the portion of the system just examined is the parallel propellant flows W_{ss}, W_{ssb}, and W_R and none of these flows can be neglected. If any one could have been neglected it would have been removed from the variable list.

This procedure is repeated for the power flow through the nuclear reactor subsystem and the power flow between subsystems. This determines all of the variables initially included in the SNM.

3.3 Reducing the Number of Differential Equations

The next step in the reduction procedure is reduction of the number of variables described by differential

equations. The rationale for doing this is based on the fact that in designing control systems only the low frequency response of the system is of interest. The high frequency performance of the system is of little importance since the portion of the system with low frequency response will attenuate any high frequency response. Therefore, it is unnecessary to include dynamic variables in the model which affect only the high frequency performance of a system. If it is determined that a variable described by a differential equation contributes only to the high frequency performance of a system, the differential equation can be replaced by an algebraic equation that defines the steady-state value of the variable. This is equivalent to assuming that the time constant of the variable is zero. The necessary algebraic equation can often be obtained by realizing that steady-state occurs when the variable's derivative goes to zero. Thus the differential equation can be set equal to zero and an expression for the variable of interest determined. On other occasions, it may be necessary to consider the physical laws governing the situation in order to determine the required algebraic equation.

The frequency responses in Figures 3-1 and 3-2 indicate that the dominant system time constants are approximately one second. Therefore any variable having a

time constant of less than one-tenth second is represented by an algebraic equation.

The variables of this system form many interlocking loops, making it difficult to isolate an individual variable and determine its time constant. To aid in this process the equations are linearized, a block diagram is drawn, and block diagram manipulation is used. Figure 3-3 shows a block diagram of the portion of the engine system being considered.

The procedure is to use block diagram manipulations to isolate a variable and determine its time constant. If it has a time constant of less than one-tenth second, then that portion of the block diagram is replaced by a gain rather than a dynamic block. It is possible by this procedure to reduce the block diagram to that shown in Figure 3-4. The corresponding set of describing equations is

$$\frac{dN}{dt} = -(A_{11} - \alpha_1\alpha_2)\ N - (\alpha_2\alpha_3 + \alpha_4)\ \Delta\theta_{Bcv} \qquad (3\text{-}38)$$

$$P_{15} = (\alpha_5 - \alpha_2\alpha_6)\ \Delta\theta_{Bcv} + \alpha_1\alpha_6\ N \qquad (3\text{-}39)$$

Thus only one variable in this portion of the system must be described by a differential equation. The procedure is repeated for the other portions of the system and results in a decision to include eight state variables in the SNM.

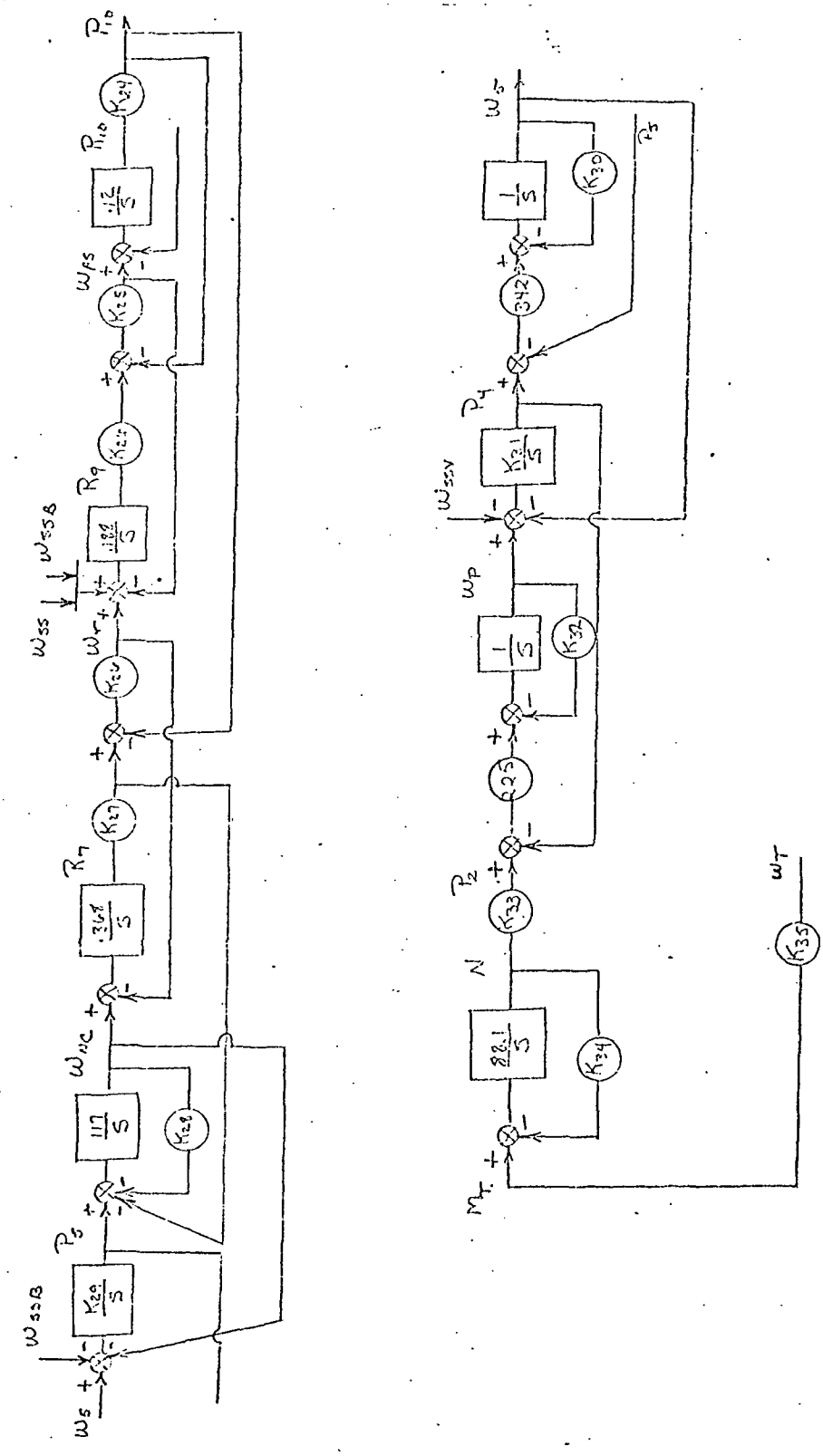

Figure 3-3. Block Diagram of Linearized CAM Flow Subsystem

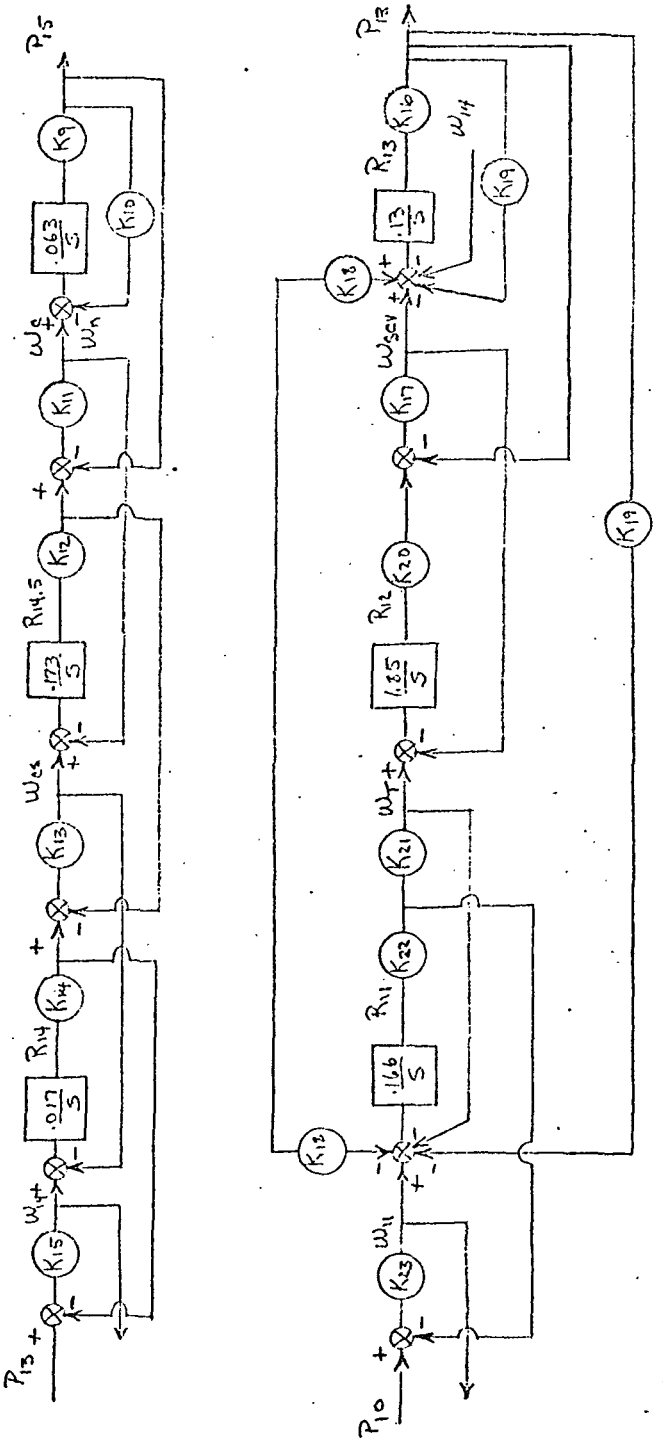

Figure 3-3.--Continued

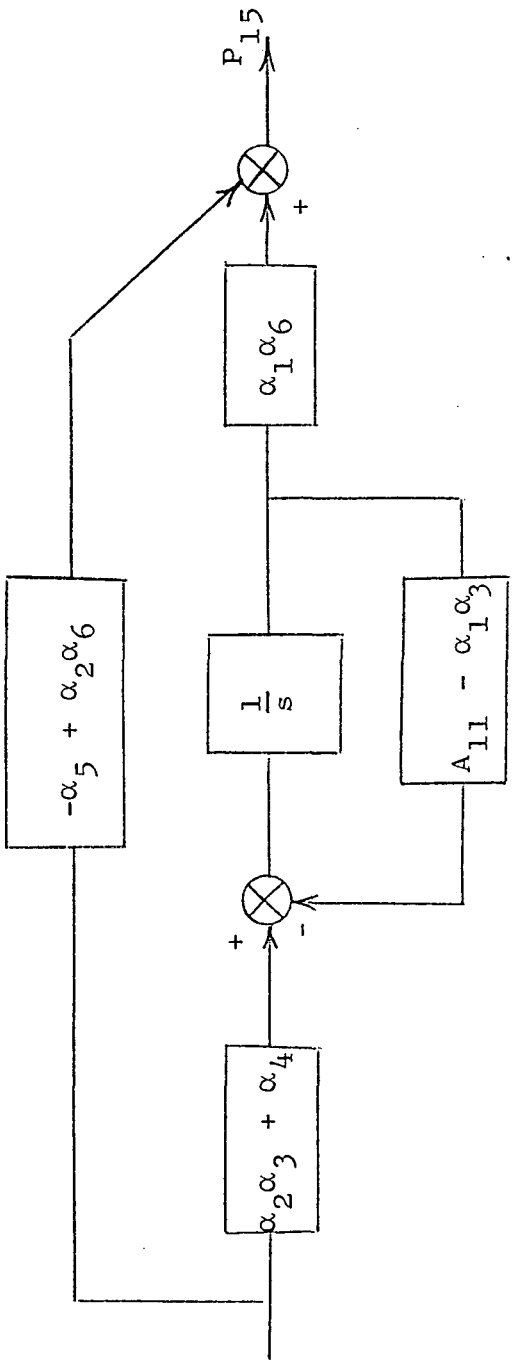

Figure 3-4. Final Reduced Block Diagram of Flow Subsystem

3.4 Reduction of Number of Algebraic Variables

Although the procedure described in the previous section reduced the number of dynamic variables included in the SNM, it did not eliminate any of the algebraic variables. In fact it generated additional algebraic variables. To reduce the number of algebraic variables, it is necessary to curve fit the nonlinear algebraic equations with a reduced number of equations. The procedure used is again illustrated using the propellant flow structure. The problem is to choose a set of algebraic variables which, along with the dynamic variables already chosen, are adequate to describe the features of the propellant flow structure. The selection of variables is made based on the assumption that the major components of the engine must be described in the SNM. The major system components in the propellant flow structure and the variables chosen are:

1. Engine nozzle and reactor core
   - P_{15} propellant exit pressure
   - W_n propellant flow through nozzle
   - P_{13} propellant pressure entering core
2. Turbine
   - P_{13} propellant pressure exiting turbine
   - W_T propellant flow through turbine
   - W_{Bcv} propellant by-passing turbine
   - P_{11} propellant pressure entering turbine

3. Turbopump

   N speed of turbopump

   P_2 propellant pressure at pump exit

4. Piping between turbopump and turbine

   P_2 propellant pressure at pump exit

   W_{11} propellant flow through pump

   W_{ss} propellant flow through support structure

   W_{nO} propellant flow through engine nozzle

   P_{11} propellant pressure at turbine entrance

The only dynamic variable included in this list is N. The relationships between these variables are determined in various ways. Some of the relationships are defined in the CAM equations. For example the relationship between the turbopump pressure, P_2, the turbopump speed, N, and the flow through the turbopump, W_{11}, is given by Equation (3-34), i.e.,

$$P_2 = P_1 + N^2 f_1 \left(\frac{W_{11}}{N}\right) \qquad (3\text{-}34)$$

Other relationships are defined by using the known physical laws governing the process and adjusting coefficients to match static data from the CAM Simulation. For example, the flow through the turbine by-pass value, W_{Bcv}, is known to be compressible, with an in-line valve. The general form of an equation describing this type of situation is

$$W = k\theta_{Bcv}\sqrt{\rho \Delta P} \qquad (3\text{-}40)$$

where k is a constant, θ_{Bcv} is the valve angle, ρ is the density of the fluid, and ΔP the drop across the valve. Curve fitting to CAM static data produced the following equation

$$W_{Bcv} = .0182\ \theta_{Bcv} \sqrt{\frac{P_{11}}{T_{11}} (P_{11} - P_{13})} \qquad (3\text{-}41)$$

where T_{11} is the temperature of the propellant on entering the by-pass valve.

A third method of defining the algebraic relations between variables is to curve fit static data using the variables involved, but ignoring the normal form of exact physical equations. For example, consider the determination of the value of the pressure at the entrance to the reactor core, P_{13}, as a function of the exit pressure, P_{15}, and the propellant flow rate, W_N. It is known that P_{13} is larger than P_{15} thus

$$P_{13} = P_{15} + \Delta P \qquad (3\text{-}42)$$

It is also known that ΔP will be a function of the propellant flow rate, thus

$$P_{13} = P_{15} + f(W_n) \qquad (3\text{-}43)$$

From the Equation (3-3)

$$W_n = \frac{13.3}{\sqrt{T_{15}}} P_{15} \qquad (3\text{-}3)$$

Thus

$$P_{13} = P_{15} + f\left(\frac{P_{15}}{\sqrt{T_{15}}}\right) \tag{3-44}$$

Curve fitting this expression using static data from the CAM Simulation yields the following equation

$$P_{13} = P_{15}\left(1 + \frac{33.3}{\sqrt{T_{15}}}\right). \tag{3-45}$$

The remaining relationships in the propellant flow structure and the remainder of the system are established using a combination of these methods. The equations for the resulting SNM of the NERVA engine are shown below:

Nuclear Reactor Equations:

$$\frac{dT_{15}}{dt} = .005[3.88\ |W_n|\ (T_2 - T_{15}) + 3300\ S] \tag{3-46}$$

$$\frac{dT_2}{dt} = .005[3.94\ |W_n|\ (T_1 - T_2) + 6260\ S] \tag{3-47}$$

$$\frac{dT_1}{dt} = .0039[-2.82\ |W_n|\ T_1 + 4260\ S] \tag{3-48}$$

$$\frac{dS}{dt} = .0276CI_1 + .235CI_2 + 1.65CI_3 - (1 - DKT)\ 660\ S \tag{3-49}$$

$$DKT = .55\sqrt{W_{ss}} + .325\ \frac{P_{13} + P_{15}}{T_c} + .0244\ \frac{(P_2 + P_{11})}{T_7}$$

$$- .77 \times 10^{-3}\ (T_c - 500) + DKD \tag{3-50}$$

$$T_c = .13\ (3T_1 + 2T_2 + 3T_{15}) \tag{3-51}$$

$$\frac{dCI_1}{dt} = 181\ S - .0276\ CI_1 \tag{3-52}$$

$$\frac{dCI_2}{dt} = 369\ S - .235\ CI_1 \tag{3-53}$$

$$\frac{dCI_3}{dt} = 110\ S - 1.65\ CI_1 \tag{3-54}$$

T_{15} exit temperature of propellant (°R)

T_2 temperature of propellant station 2 (°R)

T_1 temperature of propellant station 1 (°R)

DKT total reactivity (dollars)

DKD reactivity of drums (dollars)

S nuclear power level (% full power)

$CI_{1,2,3}$ precursor densities

Propellant Flow Equations:

$$P_{15} = .076\ T_{15}\ W_n \tag{3-55}$$

$$W_n = W_T + W_{Bcv} \tag{3-56}$$

$$W_{Bcv} = .0182\ \theta_{Bcv} \sqrt{\frac{P_{11}}{T_{11}}\ (P_{11} - P_{13})} \tag{3-57}$$

$$P_{13} = P_{15}[1 + 33.3/\sqrt{T_{15}}] \tag{3-58}$$

$$W_T = W_{11} - W_{Bcv} \tag{3-59}$$

$$W_{11} = W_{no} + W_{ss} \tag{3-60}$$

$$W_{no} = 1.5 \sqrt{\frac{P_2 + P_{11}}{2T_7} (P_2 - P_{11})} \tag{3-61}$$

$$W_{ss} = .0184\ \theta_{ssv} \sqrt{\frac{P_2 + P_{11}}{2T_7} (P_2 - P_{11})} \tag{3-62}$$

$$P11 = .354\ W_T \sqrt{T_{11}} + .79\ P13 \tag{3-63}$$

$$P2 = 3.434\ X10^{-6} N^2 - .2967\ X10^{-3}\ W11\ N + P1 \tag{3-64}$$

$$\frac{dN}{dt} = 88.1\ \ 1.02\ X10^{4}\ \frac{W_t T11}{N}\ \ 1 - \left(\frac{P13}{P11}\right)\ .25$$

$$- .96\ X10^{-6} N^2 - .2385\ X10^{-3}\ W11\ N \tag{3-65}$$

$$\frac{dT_7}{dt} = -.011\ W_{11}\ (T_7 - 95) + 1.59\ S \tag{3-66}$$

$$T_{11} = 1.6\ T_7 \tag{3-67}$$

P15 = Exit pressure (#/in^2)

W_N = Hydrogen flow through core (#/sec)

W_{BCV} = Flow through turbine by-pass valve (#/sec)

P13 = Pressure at turbine exit (#/in^2)

P11 = Pressure at turbine entrance (#/in^2)

W_T = Turbine flow (#/sec)

W_{No} = Flow through skirt (#/sec)

W_{ss} = Flow through support structure (#/sec)

T_7 = Average temperature of hydrogen in skirt (°R)

T_{11} = Temperature of hydrogen at turbine inlet (°R)

P19 = Pressure at support structure valve (#/in^2)

P2 = Pressure at pump outlet (#/in^2)

N = Speed of turbopump (RPM)

3.5 Tentative Check of Validity of SNM

The method used to provide an initial check of the validity of the SNM is to compare its response statically and dynamically to the CAM. In order to do this conveniently, it is necessary to implement the SNM on an analog computer. Figures 3-5 and 3-6 show the analog computer diagrams for the analog implementation of the SNM. The dynamic performance of the SNM and the CAM are compared using the small signal frequency responses of the two models at two different operating points. Two frequency responses are taken at each operating point, the response between the control drum and the propellant exit temperature, T_{15}/θ_D, and the response between the turbine by-pass control valve and the propellant exit pressure, P_{15}/θ_{Bcv}. Figures 3-7, 3-8, 3-9, and 3-10 compare the responses. In each case the SNM agrees well with CAM in both phase and gain. The static performances of the two models are compared on the basis of static maps on which the output variables (T_{15}, P_{15}) are plotted as functions of the input

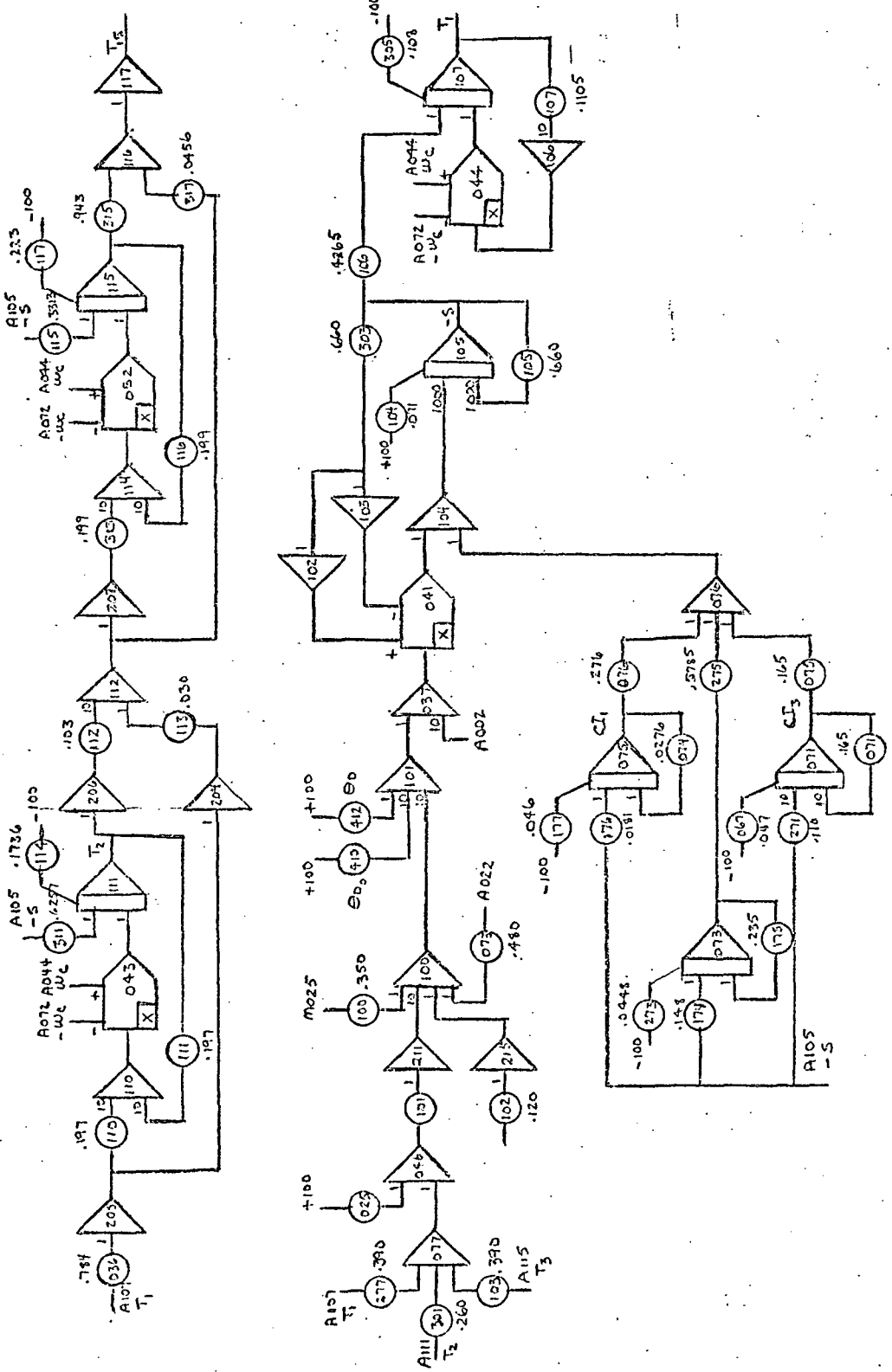

Figure 3-5. Analog Diagram of Nuclear Reactor Subsystem

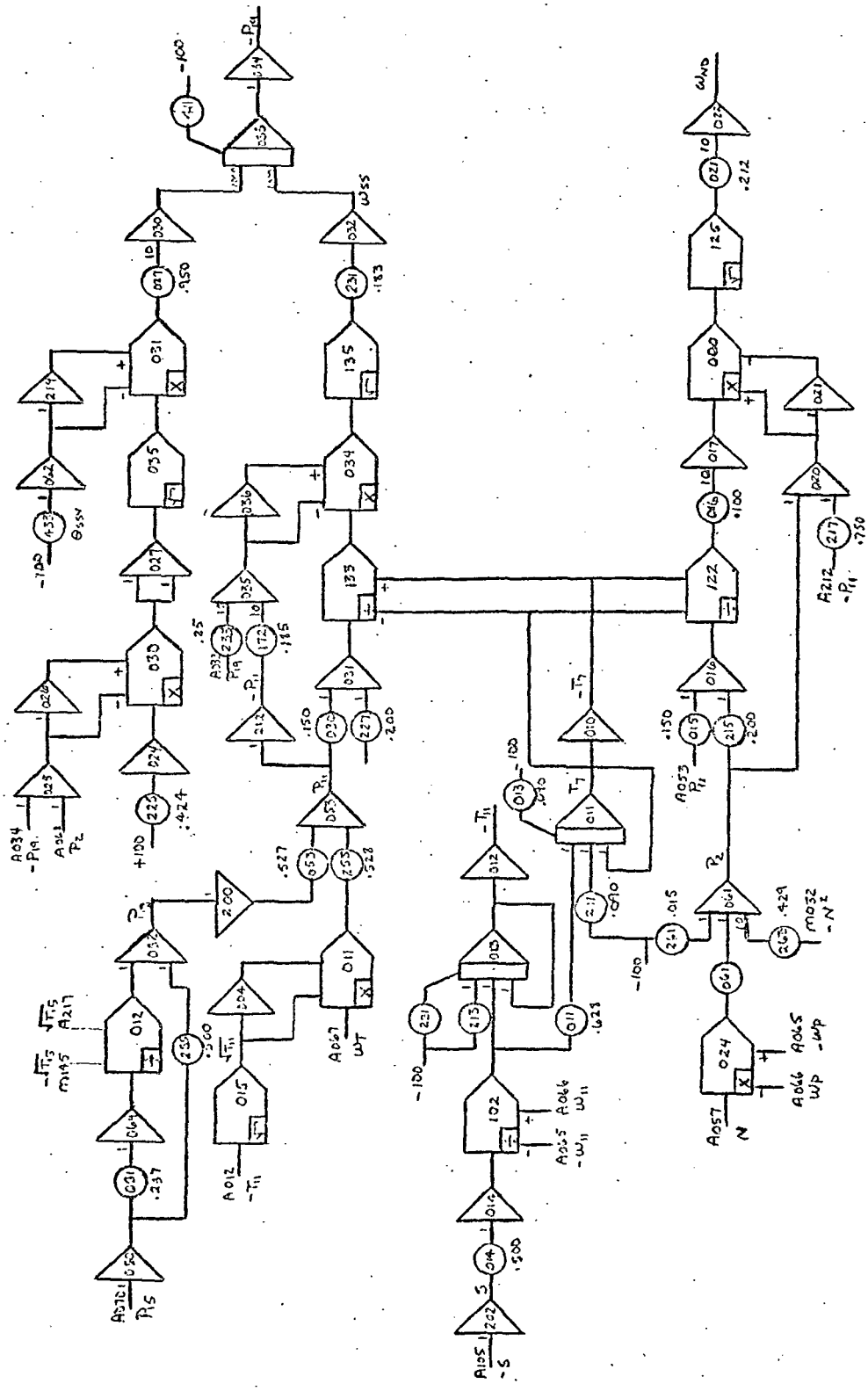

Figure 3-6. Analog Diagram of Flow Subsystem

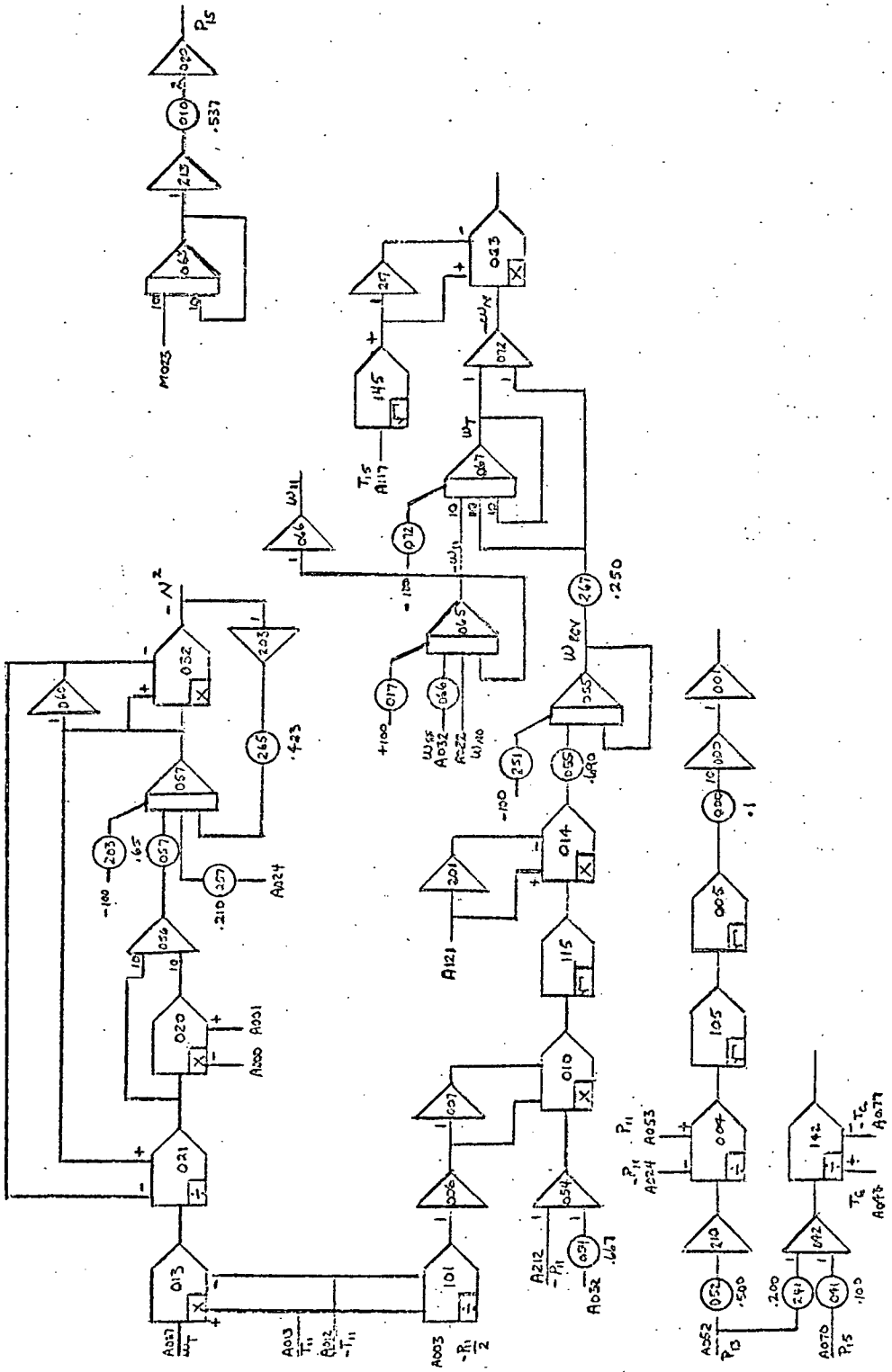

Figure 3-6.--Continued

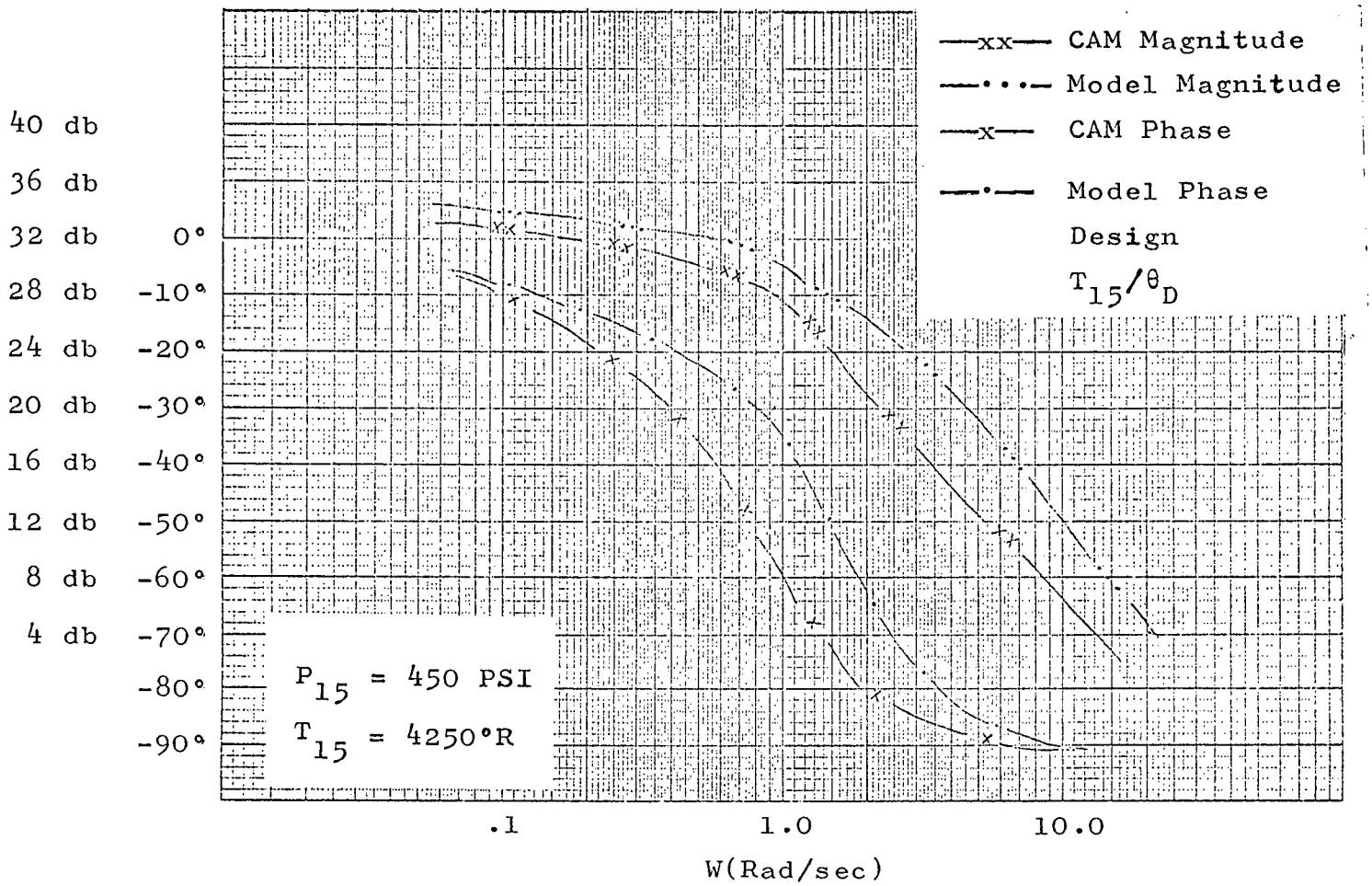

Figure 3-7. Comparison of CAM and SNM Frequency Responses (T_{15}/θ_D)

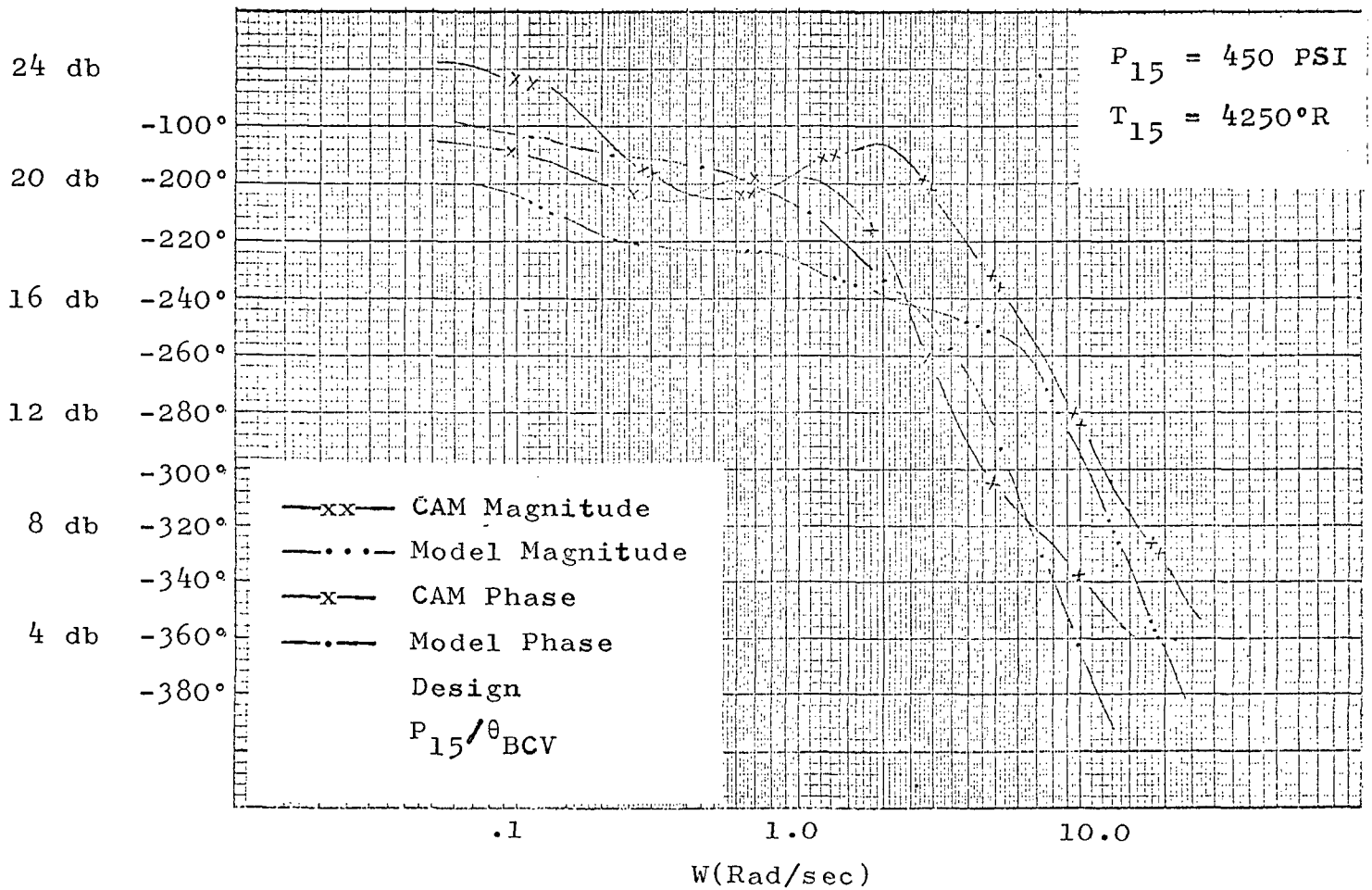

Figure 3-8. Comparison of CAM and SNM Frequency Responses (P_{15}/θ_{BCV})

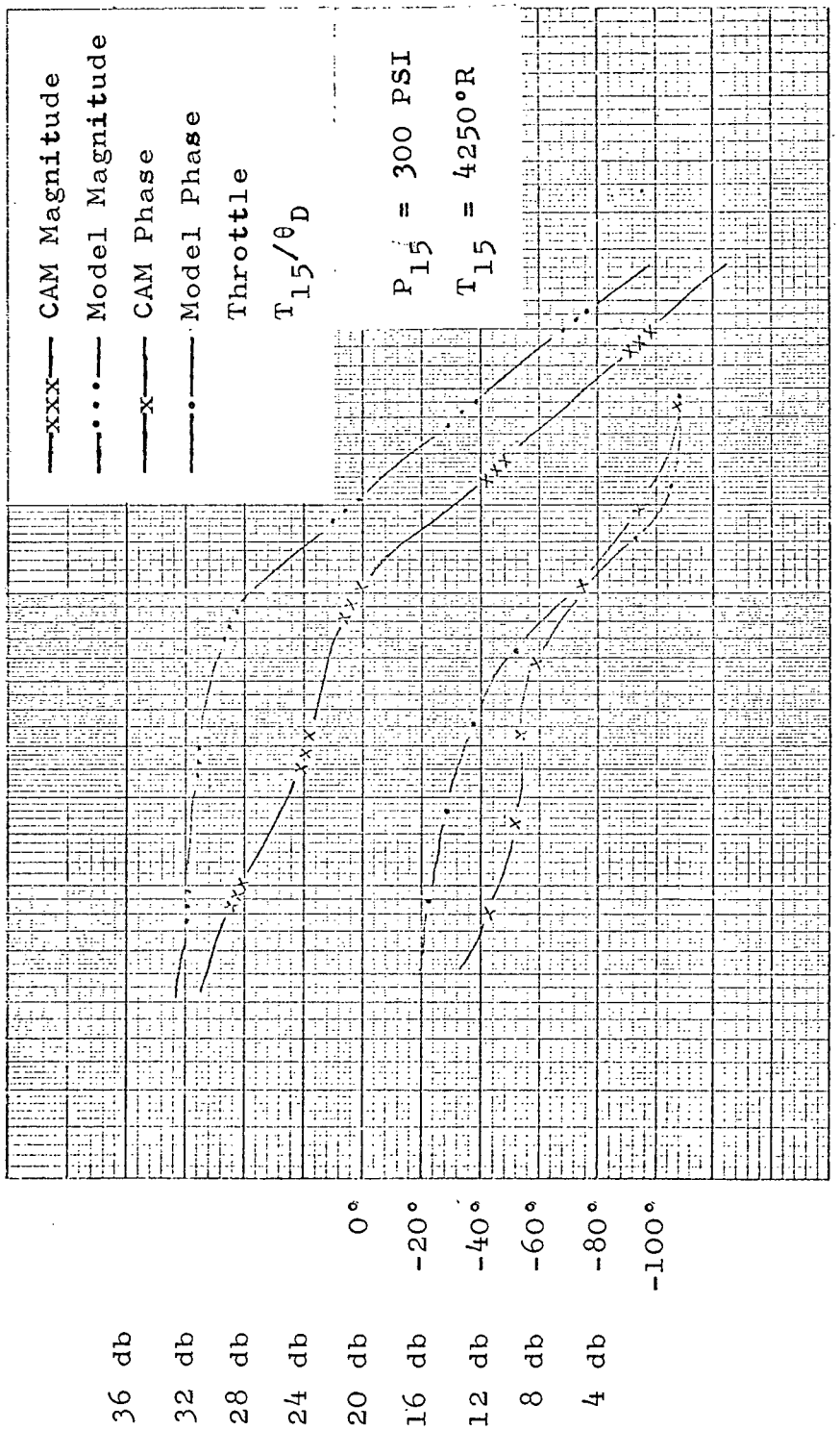

Figure 3-9. Comparison of CAM and SNM Frequency Responses (T_{15}/θ_D)

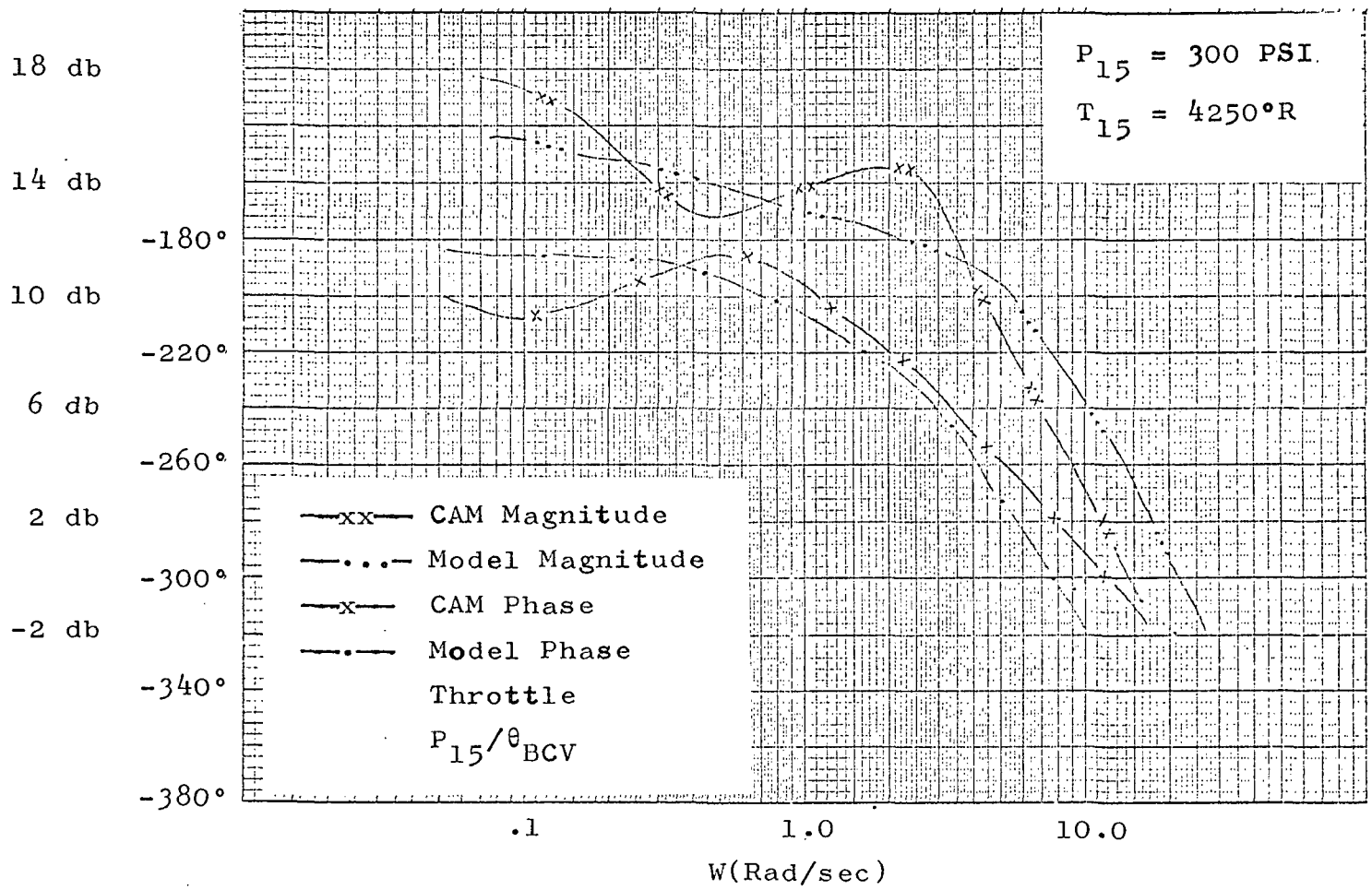

Figure 3-10. Comparison of CAM and SNM Frequency Responses (P_{15}/θ_{BCV})

variables (θ_D, θ_{Bcv}) over the entire operating range of the systems. The comparisons are given in Figures 3-11 and 3-12. The SNM again agrees closely with CAM.

3.6 Summary of the Chapter

In this chapter the Simplified Nonlinear Model of the NERVA engine system was developed. It was developed to provide a reasonably low order control model for the design of a SDSVF control system for the CAM Simulation. The SNM was developed by starting from the CAM equations and reducing the order and complexity of the model while maintaining the validity of the model from a control system design point of view. The validity of the model was checked by comparing the static and dynamic responses of the CAM and the SNM. On the basis of these comparisons, the SNM is tentatively accepted as an adequate model of NERVA.

In the following chapter SDSVF is used to develop a control system for the SNM. The final test of the model is postponed until Chapter 5 when a control system for the CAM Simulation is developed using the SNM as the control model.

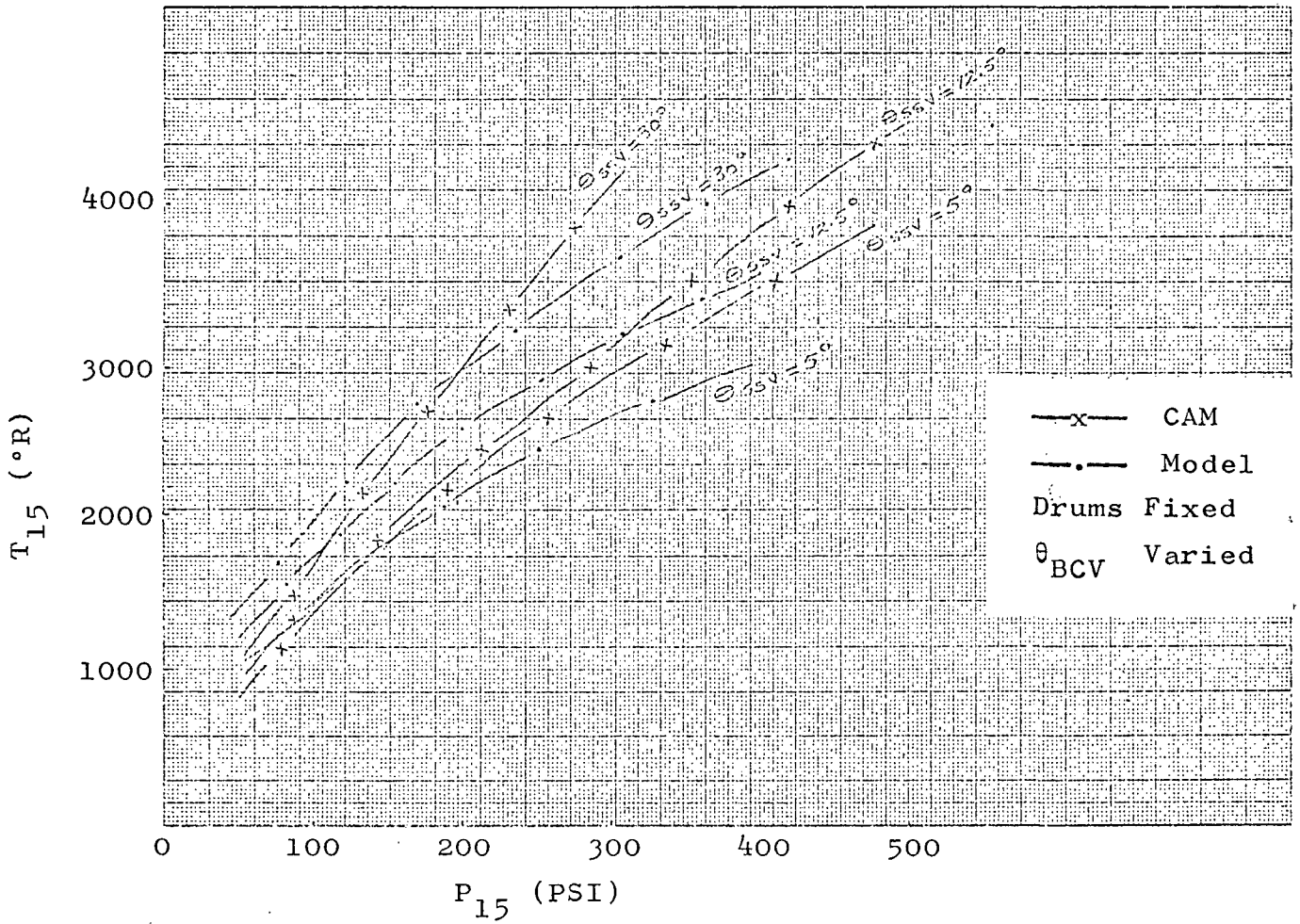

Figure 3-11. Comparison of CAM and SNM Static Maps (θ_{BCV} Input)

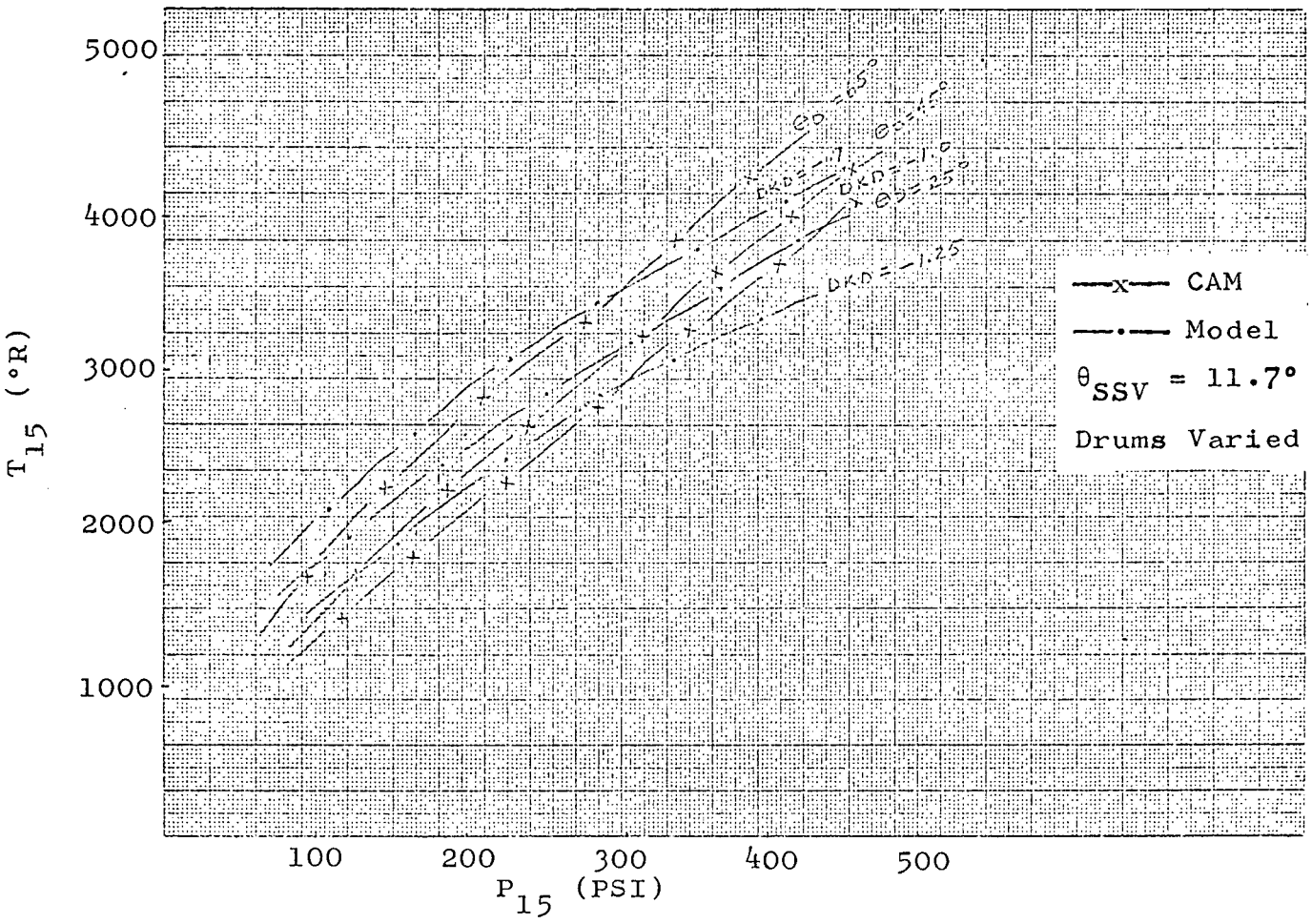

Figure 3-12. Comparison of CAM and SNM Static Maps (θ_D Input)

CHAPTER 4

CONTROL EXPERIMENTS ON THE SIMPLIFIED NONLINEAR MODEL

4.1 Introduction and Outline of Chapter

All of the control experiments reported thus far involve only digital simulation. That is, both the mathematical model and the controller are simulated as separate portions of a single digital computer program. The feedback coefficients are calculated in one section of the program and then used in the system simulation portion of the program. Therefore the time involved in performing the on-line control design calculations is not critical since the system simulation does not run while these calculations are in progress. This chapter describes experiments in which a mathematical model implemented on an analog computer is controlled in real-time by a digital computer using SDSVF. The model controlled is the Simplified Nonlinear Model of NERVA developed in Chapter 3.

The linearization technique developed in Chapter 2 is applied to the SNM and results in two single input-single output linear systems. These linear models are analyzed to provide a basis for choosing desired transfer functions and to provide a better understanding of the characteristics of the NERVA engine. A computer program to

implement SDSVF control in real-time is developed and SDSVF is used to control the SNM. This demonstration of the control method is followed by experiments which show that it is possible to reduce the order of the control model of the temperature loop without degrading performance significantly. This reduction of order of the control model is important because computation time rises quickly with the order of the control model, and when CAM is controlled the digital computer is time-shared with the CAM Simulation. The CAM Simulation itself uses the computer more than half the time. The chapter is concluded with experiments in which the system response to ramp inputs is improved by the use of series compensation and state variable feedback of the new state so introduced.

4.2 Linearization of SNM and Analysis of Linear Models

The final form of the SNM is given in Equations (3-46) through (3-62). The next step required in order to use SDSVF is to define the linear control model. Application of the linearization technique described in Chapter 2 results in two single input-single output linear models. Consider first the control model relating changes in control drum angle, θ_D, to changes in propellant exit temperature, T_{15}. The linearized equations are shown below

$$\frac{dT_{15}}{dt} = K_1(T_2 - T_{15}) - K_2S \tag{4-1}$$

$$\frac{dT_2}{dt} = K_3(T_3 - T_2) + K_4S \tag{4-2}$$

$$\frac{dT_1}{dt} = -K_5(T_1) + K_6S \tag{4-3}$$

$$\frac{dS}{dt} = .0276CI_1 + .235CI_2 + 1.65CI_3 - K_7S + K_8\Delta DKD \tag{4-4}$$

$$\frac{dCI_1}{dt} = 181S - .0276CI_1 \tag{4-5}$$

$$\frac{dCI_2}{dt} = 369S - .235CI_2 \tag{4-6}$$

$$\frac{dCI_3}{dt} = 110S - 1.65CI_3 \tag{4-7}$$

where $K_1 = (.005)(3.88)|W_c^o|$ $\quad K_2 = (.005)(3300)$

$K_3 = (.005)(3.94)|W_c^o|$ $\quad K_4 = (.005)(6260)$

$K_5 = (.00387)(2.82)|W_c^o|$ $\quad K_6 = (.005)(4260)$

$K_7 = (1 - DKT^o + DKD^o)660$ $\quad K_8 = (S^o)660$

ΔDKD = incremental reactivity of control drums

The time constant of Equation (4-4) is very fast. Therefore, the differential equation for nuclear power, S, can be replaced by an algebraic equation. Thus

$$0 = .0276CI_1 + .235CI_2 + 1.65CI_3 - K_7S + K_8\Delta DKD \qquad (4\text{-}8)$$

or

$$\dot{S} = \frac{.0276}{K_7} CI_1 + \frac{.235}{K_7} CI_2 + \frac{1.65}{K_7} CI_3 + \frac{K_8}{K_7} \Delta DKD \qquad (4\text{-}9)$$

Substituting this expression for nuclear power (S) into the remaining equation and putting the system equations into matrix form yields

$$\dot{\underset{\sim}{x}} = \underset{\sim\sim}{A}\underset{\sim}{x} + \underset{\sim}{b}u \qquad (4\text{-}10)$$

where

$$\underset{\sim}{A} = \begin{bmatrix} -K_1 & K_1 & 0.0 & .0276\frac{K_2}{K_7} & .235\frac{K_2}{K_7} & 1.65\frac{K_2}{K_7} \\ 0.0 & -K_3 & K_3 & .0276\frac{K_4}{K_7} & .235\frac{K_4}{K_7} & 1.65\frac{K_4}{K_7} \\ 0.0 & 0.0 & -K_5 & .0276\frac{K_6}{K_7} & .235\frac{K_6}{K_7} & 1.65\frac{K_6}{K_7} \\ 0.0 & 0.0 & 0.0 & (-1 + \frac{181}{K_7})\lambda_1 & \frac{181}{K_7}\lambda_2 & \frac{181}{K_7}\lambda_3 \\ 0.0 & 0.0 & 0.0 & \frac{369}{K_7}\lambda_1 & (-1 + \frac{369}{K_7})\lambda_2 & \frac{369}{K_7}\lambda_3 \\ 0.0 & 0.0 & 0.0 & \frac{110}{K_7}\lambda_1 & \frac{110}{K_7}\lambda_2 & (-1 + \frac{110}{K_7})\lambda_3 \end{bmatrix}$$

$$\underset{\sim}{b}^T = \begin{bmatrix} K_2 & K_4 & K_6 & 181\frac{K_8}{K_7} & 369\frac{K_8}{K_7} & 110\frac{K_8}{K_7} \end{bmatrix}$$

Figure 4-1 shows a block diagram of the temperature loop control model. The model is sixth order; however, because

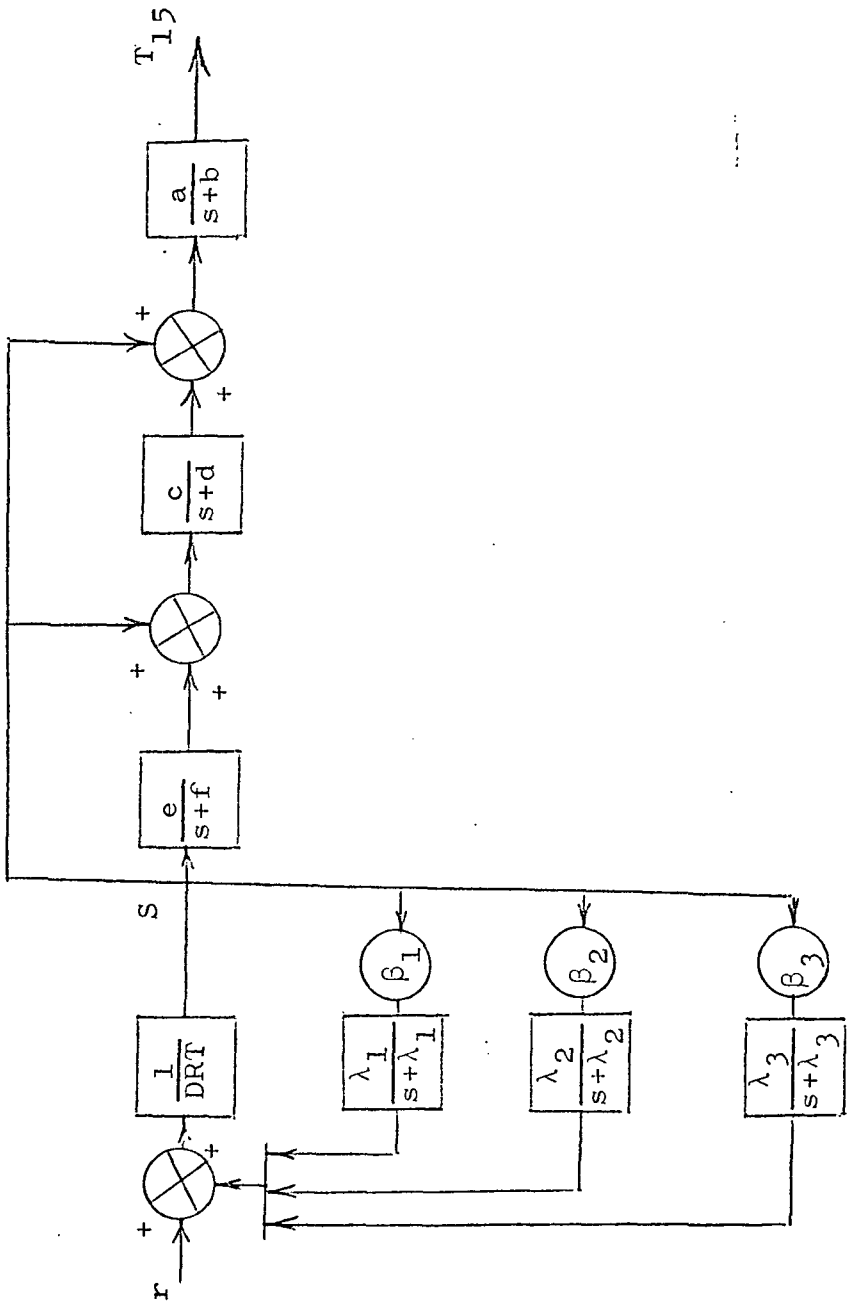

Figure 4-1. Linear Block Diagram of Nuclear Reactor Subsystem

of the manner in which the nuclear power feeds forward and the unusual feedback configuration involving the delayed neutrons, the system has five zeroes. This causes the system to behave somewhat like a first order system. Reference to the frequency response from the CAM Simulation in Figure 3-1 verifies that NERVA does have a frequency response similar to that of a first order system between T_{15} and θ_D.

In order to illustrate how the system changes as a function of state, shown below are the linear system equations and transfer functions with coefficients evaluated at full power (T_{15} = 4250 ^{o}R, P_{15} = 450 PSI) and at low power (T_{15} = 2000 ^{o}R, P_{15} = 100 PSI).

Full Power

$$\begin{bmatrix} \dot{T}_{15} \\ \dot{T}_2 \\ \dot{T}_1 \\ \dot{CI}_1 \\ \dot{CI}_2 \\ \dot{CI}_3 \end{bmatrix} = \begin{bmatrix} -1.84 & 1.89 & -.043 & .001 & .006 & .042 \\ 0.0 & -1.82 & 1.43 & .001 & .011 & .080 \\ 0.0 & 0.0 & -1.02 & .001 & .008 & .054 \\ 0.0 & 0.0 & 0.0 & -.020 & .065 & .460 \\ 0.0 & 0.0 & 0.0 & .016 & -.102 & .930 \\ 0.0 & 0.0 & 0.0 & .005 & .040 & -1.37 \end{bmatrix} \begin{bmatrix} T_{15} \\ T_2 \\ T_1 \\ CI_1 \\ CI_2 \\ CI_3 \end{bmatrix}$$

$$+\begin{bmatrix} 1670.0 \\ 3150.0 \\ 2140.0 \\ 18200.0 \\ 37100.0 \\ 11100.0 \end{bmatrix} \Delta DKD$$

$$\frac{T_{15}}{\theta_D} = \frac{(1670.0)(S+.027)(S+.235)(S+1.65)(S+2.1)(S+4.3)}{(S+1.84)(S+1.82)(S+1.4)(S+1.0)(S+.01)(S-.002)}$$

Low Power

$$\begin{bmatrix} \dot{T}_{15} \\ \dot{T}_2 \\ \dot{T}_1 \\ \dot{CI}_1 \\ \dot{CI}_2 \\ \dot{CI}_3 \end{bmatrix} = \begin{bmatrix} -.570 & .590 & .014 & .001 & .006 & .042 \\ 0.0 & -.570 & .445 & .001 & .110 & .079 \\ 0.0 & 0.0 & -.320 & .001 & .080 & .054 \\ 0.0 & 0.0 & 0.0 & -.020 & .065 & .450 \\ 0.0 & 0.0 & 0.0 & .160 & -.103 & .930 \\ 0.0 & 0.0 & 0.0 & .005 & .039 & -1.37 \end{bmatrix} \begin{bmatrix} T_{15} \\ T_2 \\ T_1 \\ CI_1 \\ CI_2 \\ CI_3 \end{bmatrix}$$

$$+\begin{bmatrix} 231.0 \\ 438.0 \\ 298.0 \\ 2530.0 \\ 5160.0 \\ 1538.0 \end{bmatrix} \Delta DKD$$

$$\frac{T_{15}}{\theta_D} = \frac{(231.0)(S+.027)(S+.235)(S+1.65)(S+.78+j.97)(S+.78-j.97)}{(S+.57)(S+.57)(S+.32)(S+1.3)(S+.16)(S-.07)}$$

These transfer functions have six poles and five zeroes as previously stated. It is apparent that both the static gain of the system and the dynamics of the system change significantly over the normal range of operation.

Now consider the linear model relating propellant exit pressure, P_{15}, to turbine by-pass valve angle, θ_{Bcv}:

$$P_{15} = H_1 W_n \tag{4-11}$$

$$W_n = W_T + W_{Bcv} \tag{4-12}$$

$$W_{Bcv} = H_2(P_2 - P_{13}) + H_3 \Delta\theta_{Bcv} \tag{4-13}$$

$$P_{13} = H_4 P_{15} \tag{4-14}$$

$$W_T = W_{11} - W_{Bcv} \tag{4-15}$$

$$W_{11} = (H_5 + H_6)(P_2 - P_{11}) \tag{4-16}$$

$$P_{11} = .79P_{13} + H_7 W_T \tag{4-17}$$

$$P_2 = H_8 N \tag{4-18}$$

$$\frac{dN}{dt} = 88.1[H_9 W_T - H_{10} N] \tag{4-19}$$

where $H_1 = .076 \sqrt{T_{15}^{\circ}}$

$$H_2 = \frac{P_{11}^{\circ}/T_{11}^{\circ}}{\sqrt{P_{11}^{\circ}(P_{11}^{\circ} - P_{13}^{\circ})/T_{11}^{\circ}}}$$

$$H_3 = .0182 \sqrt{P_{11}^{\circ}(P_{11}^{\circ} - P_{13}^{\circ})/T_{11}^{\circ}}$$

$$H_4 = 1.0 + 33.3/\sqrt{T_{15}^{\circ}}$$

$$H_5 = 1.5\sqrt{(P_2^{\circ} + P_{11}^{\circ}/2T_7^{\circ}(P_2^{\circ} - P_{11}^{\circ})}$$

$$H_6 = .0268\ \theta_{55}^{\circ}\sqrt{(P_2^{\circ} + P_{11}^{\circ})/2T_7^{\circ}(P_2^{\circ} + P_{11}^{\circ})}$$

$$H_7 = .354\sqrt{T_{11}^{\circ}}$$

$$H_8 = [3.43 \times 10^{-6}\ N^{\circ} - .2967 \times 10^{3}\ W_{11}^{\circ} + P_1^{\circ}/N^{\circ}]$$

$$H_9 = 1.02 \times 10^{4}\ T_{11}^{\circ}/N^{\circ}[1.0 - (P_{13}^{\circ}/P_{11}^{\circ})^{.25}]$$

$$H_{10} = [.96 \times 10^{-6}\ N^{\circ} + .238 \times 10^{-3}\ W_{11}^{\circ}]$$

These equations can be manipulated into the following form:

$$\frac{dN}{dt} = 88.1[\rho_6 N + \rho_7 \Delta\theta_{Bcv}] \qquad (4\text{-}20)$$

$$P_{15} = [\rho_4 N + \rho_5 \Delta\theta_{Bcv}] \qquad (4\text{-}21)$$

where $\rho_1 = (H_5+H_6)H_8/[1.0+H_7(H_2+H_5+H_6)]$

$$\rho_2 = H_4[-.79H_5-.79H_6+.71H_2]/[1.0+H_7(H_2+H_5+H_6)]$$

$$\rho_3 = H_2/[1.0+H_7(H_2+H_5+H_6)]$$

$$\rho_4 = H_1(1.0+H_2H_7)\rho_1/[1.0+.21H_1H_2H_4-\rho_2H_1(1.0+H_2H_7)]$$

$$\rho_5 = H_1[H_3-\rho_3(1.0+H_2H_7)]/[1.0+.21H_1H_2H_4-\rho_2(1.0+H_2H_7)H_1]$$

$$\rho_6 = [H_9(\rho_1+\rho_2\rho_4)-H_{10}]$$

$$\rho_7 = [H_9(\rho_2\rho_5-\rho_3)]$$

A block diagram of the linearized model of the pressure loop control model is shown in Figure 4-2. The structure of this block diagram is very unusual. It is first order; however, the input feeds directly to the system output. If the equation for ρ_6 is examined, it is seen that the system has a positive feedback term, $H_9(\rho_1 + \rho_2\rho_4)$, as well as a negative feedback term, H_{10}. These two quantities are approximately the same magnitude over the entire range of operation. This causes the system pole to be near the origin. Finally, the system output is not one of the system states.

In order to put the system in standard form, two things are done. First a series compensator is added to the model so that the input does not feed directly to the output. This changes the system equations to

$$\Delta\dot{\theta}_{Bcv} = -2.5\Delta\theta_{Bcv} + 2.5U_p \qquad (4\text{-}22)$$

$$\dot{N} = 88.1[\rho_7\Delta\theta_{Bcv} + \rho_6 N] \qquad (4\text{-}23)$$

$$P_{15} = \rho_4 N + \rho_5\Delta\theta_{Bcv} \qquad (4\text{-}24)$$

Then in order to have the system output, P_{15}, be one of the states of the control model, a linear

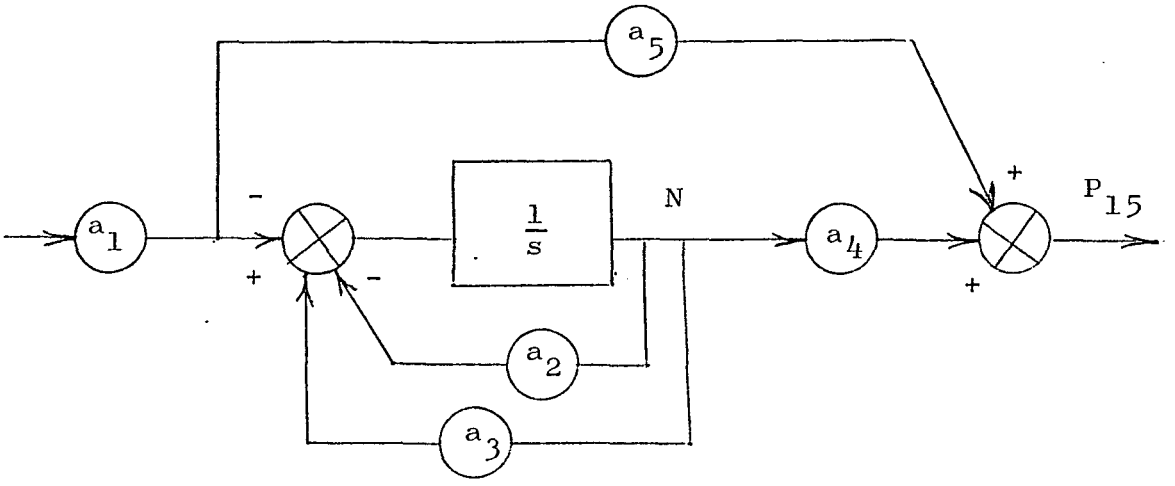

Figure 4-2. Linear Block Diagram of Flow Subsystem

transformation of variables is performed. This transformation yields the following system description

$$\begin{bmatrix} \dot{\Delta\theta}_{Bcv} \\ \dot{P}_{15} \end{bmatrix} = \begin{bmatrix} -2.5 & 0 \\ -2.5\rho_5 + \rho_4\rho_7 - \rho_5\rho_6 & \rho_6 \end{bmatrix} \begin{bmatrix} \Delta\theta_{Bcv} \\ P_{15} \end{bmatrix} + \begin{bmatrix} 2.5 \\ 2.5\rho_5 \end{bmatrix} U_p \tag{4-25}$$

The linear pressure control model and transfer function with coefficients evaluated at full power and low power are shown below

Full Power

$$\begin{bmatrix} \dot{\Delta\theta}_{Bcv} \\ \dot{P}_{15} \end{bmatrix} = \begin{bmatrix} -2.5 & 0 \\ -14.5 & 0 \end{bmatrix} \begin{bmatrix} \Delta\theta_{Bcv} \\ P_{15} \end{bmatrix} + \begin{bmatrix} 2.5 \\ 3.76 \end{bmatrix} U_p$$

$$\frac{P_{15}}{U_p} = \frac{3.7(S - 7.1)}{S(S + 2.5)}$$

Low Power

$$\begin{bmatrix} \dot{\Delta\theta}_{Bcv} \\ \dot{P}_{15} \end{bmatrix} = \begin{bmatrix} -2.5 & 0 \\ -7.15 & 0 \end{bmatrix} \begin{bmatrix} \Delta\theta_{Bcv} \\ P_{15} \end{bmatrix} + \begin{bmatrix} 2.5 \\ 2.72 \end{bmatrix} U_p$$

$$\frac{P_{15}}{U_p} = \frac{2.7(S - 4.1)}{S(S + 2.5)}$$

On examination of the transfer functions for the pressure loop control model, it is apparent that the dynamics and gain of the system change significantly with system state. The change is not as significant as for the temperature control loop, even though the describing equations are much more nonlinear.

4.3 Selection of Desired Transfer Function and Update Intervals

Based on these linear models and the decision to carry out the initial control experiments in the high power region of operations, the desired transfer functions chosen are:

$$\frac{T_{15}}{T_{15_D}} = \frac{(S+.0276)(S+.235)(S+1.65)(S+2.1)(S+4.3)(K_1)}{(S+.0276)(S+.235)(S+1.65)(S+1.2)(S+1.5)(S+1.8)}$$

$$\frac{P_{15}}{P_{15_D}} = \frac{(S-7.1)(K_2)}{(S+1.0)(S+1.5)}$$

The constants K_1 and K_2 are chosen so that

$$\frac{T_{15}}{T_{15_D}}\Big|_{S=0} = 1 \quad \text{and} \quad \frac{P_{15}}{P_{15_D}}\Big|_{S=0} = 1.$$

Each of these transfer functions is chosen to provide an overdamped response with a time constant similar to that of the uncontrolled system and zero steady state error to step inputs.

The selection of system and control update intervals is made, as in the previous examples, on the requirements that the linear models be accurate and that errors generated by making the control signals discrete rather than continuous are small. The system update interval is chosen based on having no coefficient of the control model vary more than ten per cent between updates. It is known that the rate-of-change of temperature demand does not exceed 150° R/second and that the rate-of-change of pressure demand does not exceed 50 PSI/second. These are physical constraints. Calculation of the approximate rate-of-change of the coefficients of the temperature and pressure loop control models based on these maximum rate-of-change demands, indicates that a system update interval of approximately .5 second is adequate. The desired transfer functions chosen for the temperature and pressure control loops have dominant time constants of approximately 1.0 second. A control update interval of .02 second insures that errors generated by the discrete nature of the control signal are small.

4.4 Computer Program to Control SNM

The basic flow chart for a program to implement SDSVF is developed in Chapter 2, shown in Figure 2-1. The timing of the system update and control update is initially controlled in the following manner. A clock is available

which generates a positive pulse every ΔT seconds. Each time a positive pulse occurs, the control is updated and a counter incremented. The counter is checked against a reference, and if the reference is exceeded, a system update is initiated. Figure 4-3 shows a timing diagram and a flow chart of this logic sequence, where the system update reference is five control updates. This causes a system update every $5\Delta T$ seconds for a control update interval of ΔT seconds.

The task of writing the control program involves writing a program to implement the flow chart shown in Figure 4-3. The computer language used is a modified version of FORTRAN which contains statements which permit input from and output to the COMCOR 1500 Interface, which in turn communicates with the COMCOR 5000 Analog Computers. The flow charts for the system update and control update portions of the program are shown in Figure 2-1. System update involves measuring the system state, defining the linear models, and calculating feedback coefficients. The only programming required to measure the system state is to request input from the appropriate channels of the interface. The equations to define the linear models are given in Equations (4-10) and (4-25). The programming required to calculate the feedback coefficients and forward gain is given in Section 2.3b of Chapter 2. Control update involves measuring system state, calculating control, and

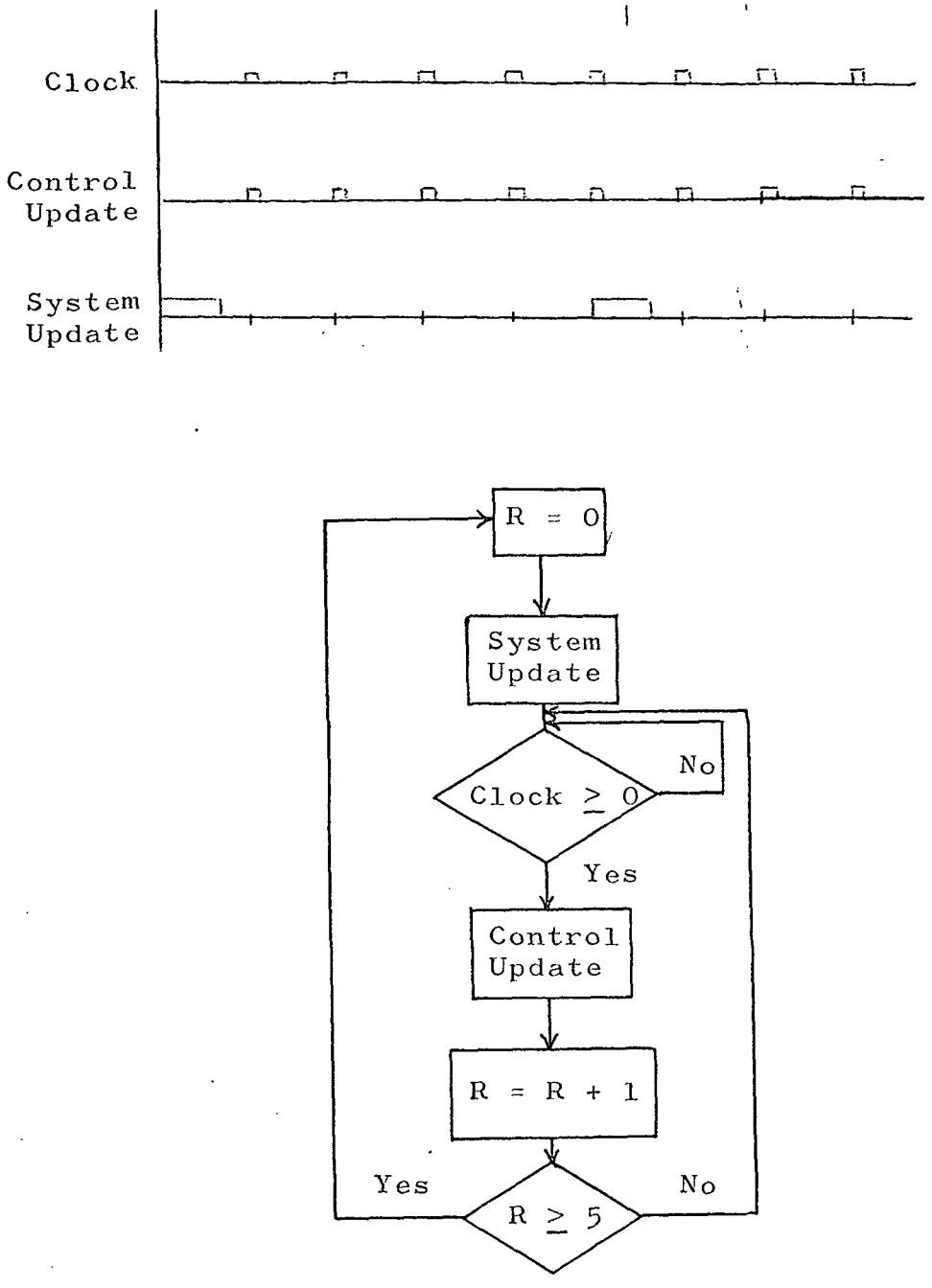

Figure 4-3. Timing Diagram of Control and System Updates and Block Diagram of Program to Implement Timing

transmitting control to the system. The programming required is completely straightforward. The state is measured using available FORTRAN commands to communicate with the analog computer through the interface. Transmitting the values of control to the analog computer is accomplished in the same manner. Calculating control requires only implementing the equation

$$u = K[r - \underset{\sim}{k}^T \underset{\sim}{x}] \tag{4-26}$$

for each control loop where

r is the desired output, K the forward gain,

$\underset{\sim}{k}^T$ the feedback coefficient vector and

$\underset{\sim}{x}$ the state vector.

Once the subroutines are written for the system and control updates, it is discovered that a system update requires approximately .07 second. Thus if the program is written as shown in the flow chart of Figure 4-3, whenever a system update is initiated, no control update will occur for .07 second. This is significantly longer than the desired control update interval of .02 second. To avoid this long delay, a slight modification to the program is made. A control update is called for approximately halfway through the system update. This implies a control update interval longer than .02 second, but not enough longer to affect system performance.

4.5 Control Experiments on the Simplified Nonlinear Model

Figure 4-4 is a schematic diagram showing the hardware involved in the SNM control experiments and the information exchanged. The purpose of these experiments is to demonstrate that SDSVF can be used to control a complex analog model (SNM) in real-time using a digital computer and to gain experience to aid in controlling CAM. The desired transfer functions in Section 4.3 are specified as

$$\frac{T_{15}}{T_{15_D}} = \frac{(S+.0276)(S+.235)(S+1.65)(S+2.1)(S+4.3)(K_1)}{(S+.0276)(S+.235)(S+1.65)(S+.12)(S+1.5)(S+1.8)}$$

$$\frac{P_{15}}{P_{15_D}} = \frac{(S-7.1)(K_2)}{(S+1.0)(S+1.5)}$$

The control update interval is .02 second. Figures 4-5, 4-6, 4-7, and 4-8 show the system response to step demands of 25 PSI and 250° R with model update intervals of .25, .50, 1.0, and 2.0 seconds. The operating point is T_{15} = 4250° R and P_{15} = 300 PSI. The actual response of a linear system having the desired transfer function is indicated in each case. The two responses are very similar for short update intervals but, as anticipated, when the update interval is increased, the actual response deviates more and more from the desired response. It is apparent from the responses that there is coupling between the loops. A

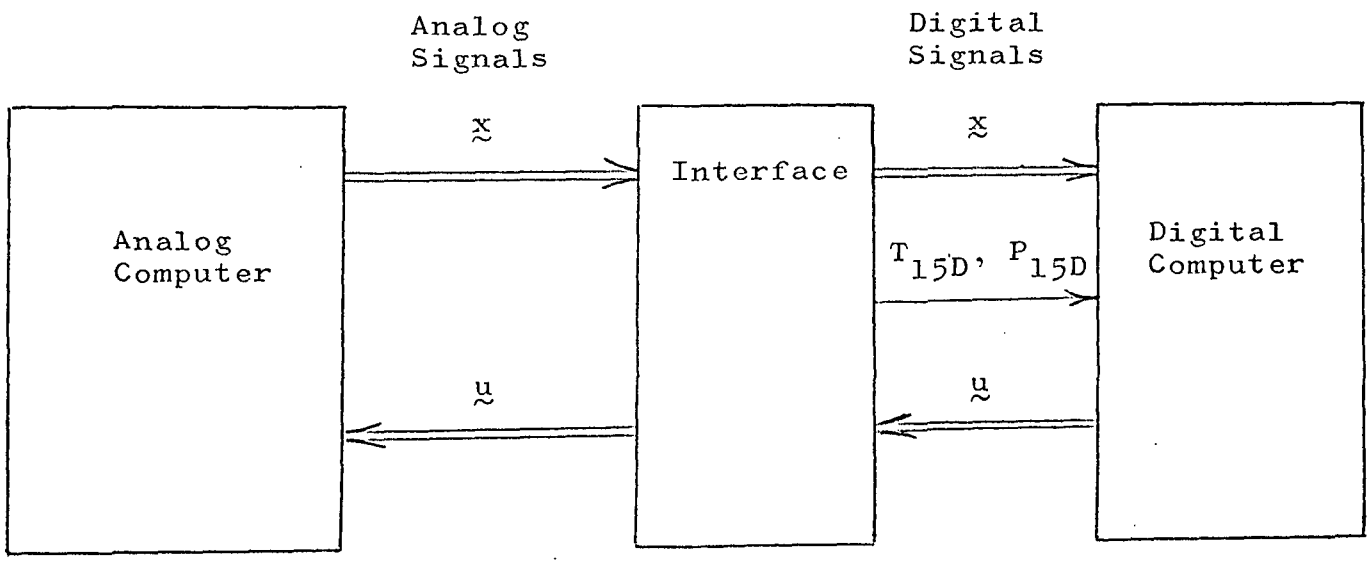

Figure 4-4. Hardware Involved in Initial Control Experiments on the SNM

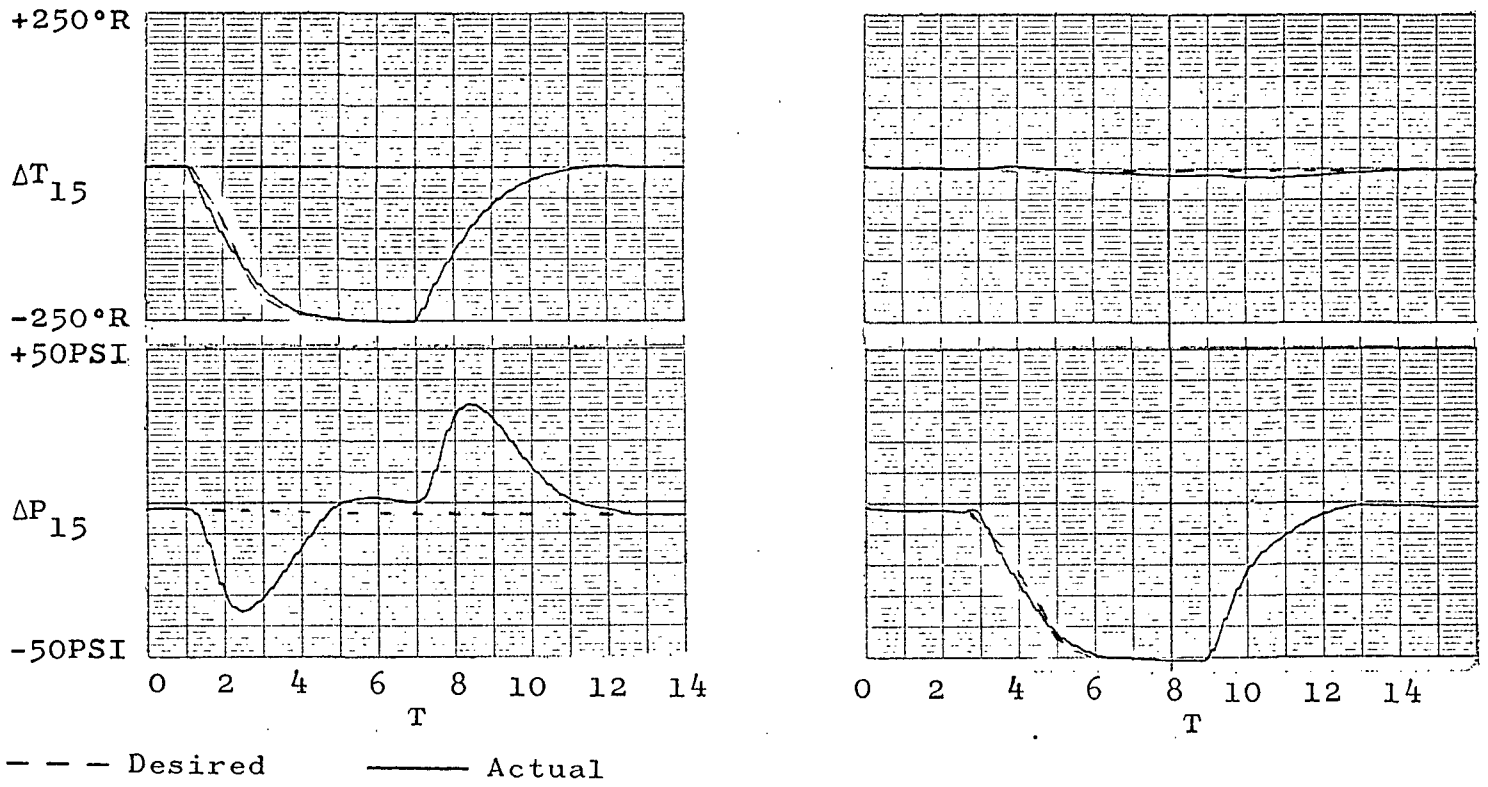

Figure 4-5. Response of System to Step Inputs (T_{15} = 4250°R, P_{15} = 300 PSI, Update = .25)

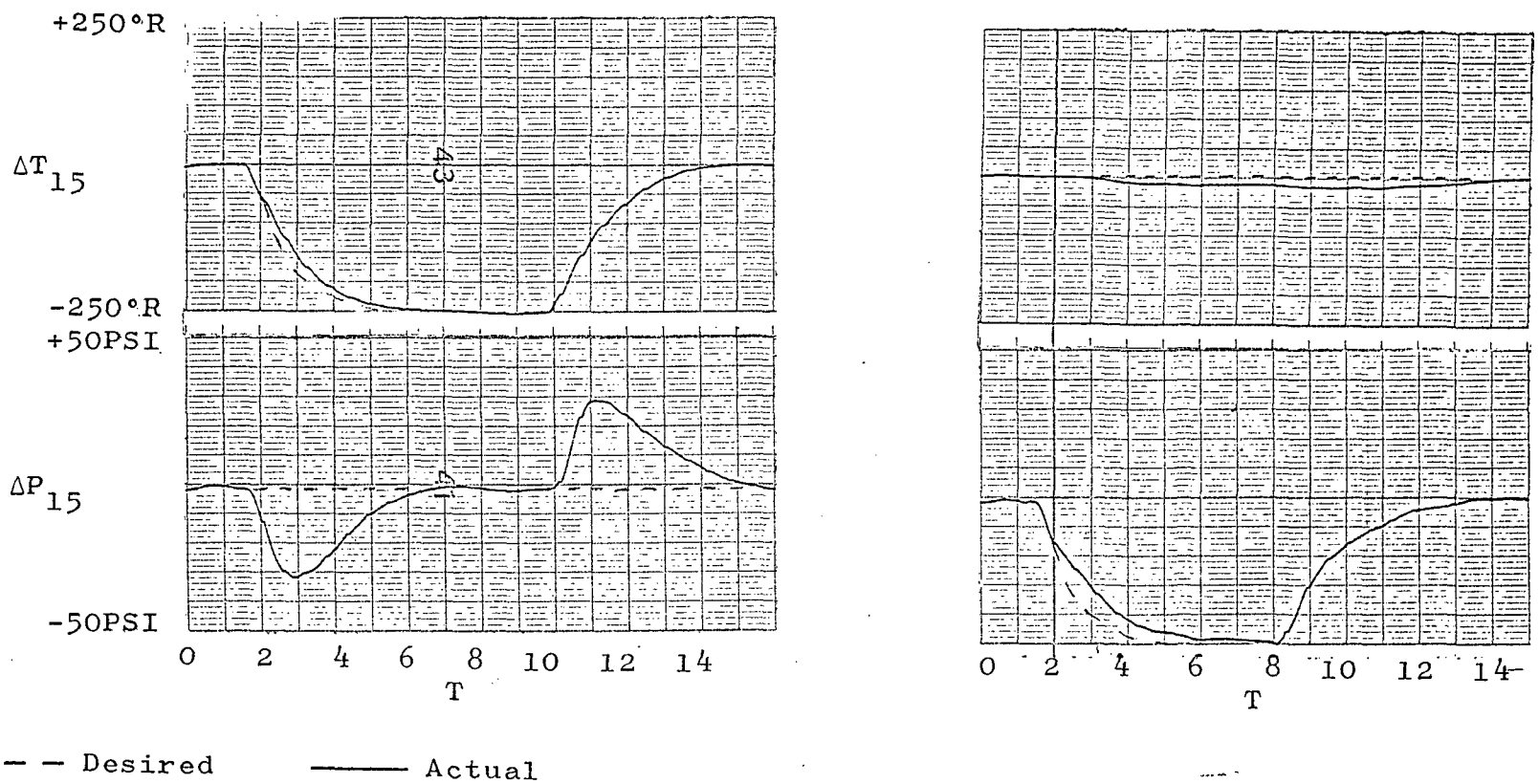

Figure 4-6. Response of System to Step Inputs (T_{15} = 4250°R, P_{15} = 300 PSI, Update = .5)

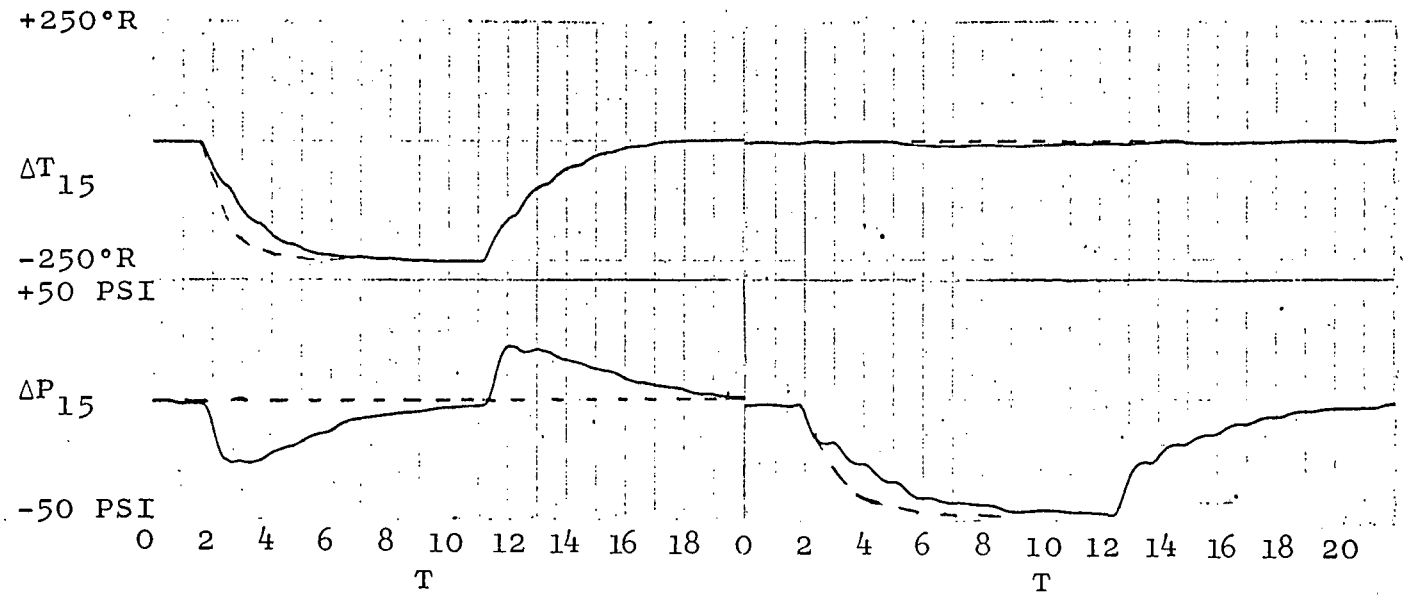

Figure 4-7. Response of System to Step Inputs (T_{15} = 4250°R, P_{15} = 300 PSI, Update = 1.0)

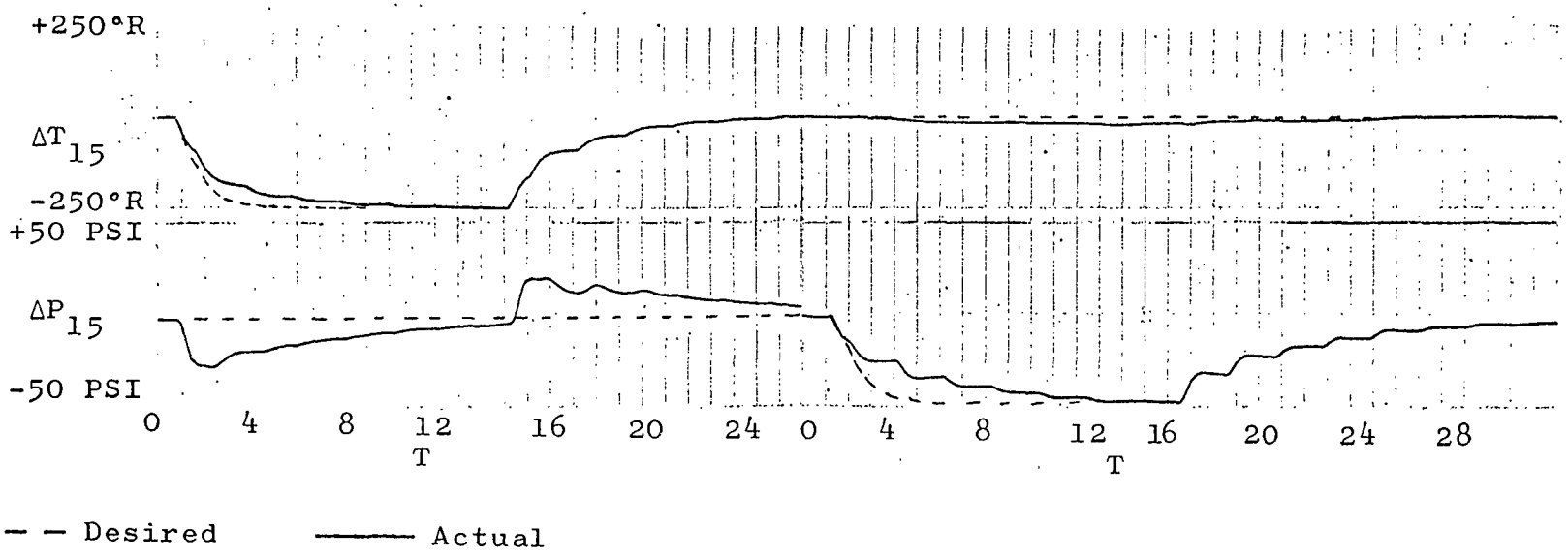

Figure 4-8. Response of System to Step Inputs (T_{15} = 4250°R, P_{15} = 300 PSI, Update = 2.0)

step change in the pressure causes transient errors in the temperature loops and vice versa.

Experiments conducted to determine the effect of varying the control update interval indicate no significant change when the interval is increased by a factor of three. It is possible to decrease the coupling between the two control loops by increasing the bandwidth of the desired transfer functions. However, the bandwidth cannot be increased significantly because the large feedback gains required made the system very sensitive to measurement errors.

4.6 Control Experiments with Reduced Order Models

The control experiments in Section 4-5 show that it is possible to control the SNM using SDSVF based on the control models defined in Section 4-2. The temperature loop control model defined in Section 4-2 is sixth order. However, the frequency responses of the SNM in Figure 3-10 indicate that a lower order model may be adequate. This is an attractive possibility since a reduction in the order of the control model results in a significant decrease in the system update computation time.

It has been common engineering practice (Meghreblian and Holmes 1960) when designing control systems for nuclear reactors to approximate the three delayed neutron groups with a single equivalent group.

Referring to Section 4-2, the equations for the precursor groups are

$$\frac{dCI_1}{dt} = 181S - .0276\ CI_1 \tag{4-5}$$

$$\frac{dCI_2}{dt} = 369S - .235\ CI_2 \tag{4-6}$$

$$\frac{dCI_3}{dt} = 110S - 1.65\ CI_3 \tag{4-7}$$

The single equivalent precursor group has the form

$$\frac{dCI}{dt} = -\lambda CI + \beta S \tag{4-27}$$

where $\lambda = \dfrac{\beta}{\Sigma \dfrac{\beta_i}{\lambda_i}} = .081 \qquad \beta = \Sigma\, \beta_i = 660$

Using this approximation reduces the temperature loop control model to fourth order. The only modifications to the control scheme are that the control model equations are changed and the desired transfer function is changed to

$$\frac{T_{15}}{T_{15_D}} = \frac{(S+.081)(S+2.1)(S+4.3)(K_1)}{(S+.081)(S+1.2)(S+1.5)(S+1.8)}$$

Since the equivalent precursor is not a state of the SNM, it must be estimated. This is accomplished by measuring nuclear power (S) and using that to drive an analog circuit which implements Equation (4-27).

Figures 4-9 and 4-10 show the response of the system to step inputs of 250° R and 25 PSI when the fourth order temperature control model is used. The model update times are .50 and 1.0 seconds respectively and the operating point is T_{15} = 4250° R, P_{15} = 300 PSI. There is no significant deterioration of the system response when compared to Figures 4-6 and 4-7.

The temperature control model is now fourth order; however, the frequency response data indicate that an even further simplification of the control model is possible. From Figure 4-1, it is seen that the portion of the model that describes the heating of the propellant contains two feed forward paths. This produces two zeroes in the transfer function. This portion of the block diagram has three poles for a pole zero excess of one. This suggests that it may be possible to approximate the three temperature differential equations by a single differential equation. The three temperature differential equations from the SNM are

$$\frac{dT_{15}}{dt} = .005[3.88|W_n|(T_2 - T_{15}) + 3300S] \qquad (3\text{-}46)$$

$$\frac{dT_2}{dt} = .005[3.94|W_n|(T_1 - T_2) + 6260S] \qquad (3\text{-}47)$$

$$\frac{dT_1}{dt} = -.0039[2.82|W_n|T_1 + 4260S] \qquad (3\text{-}48)$$

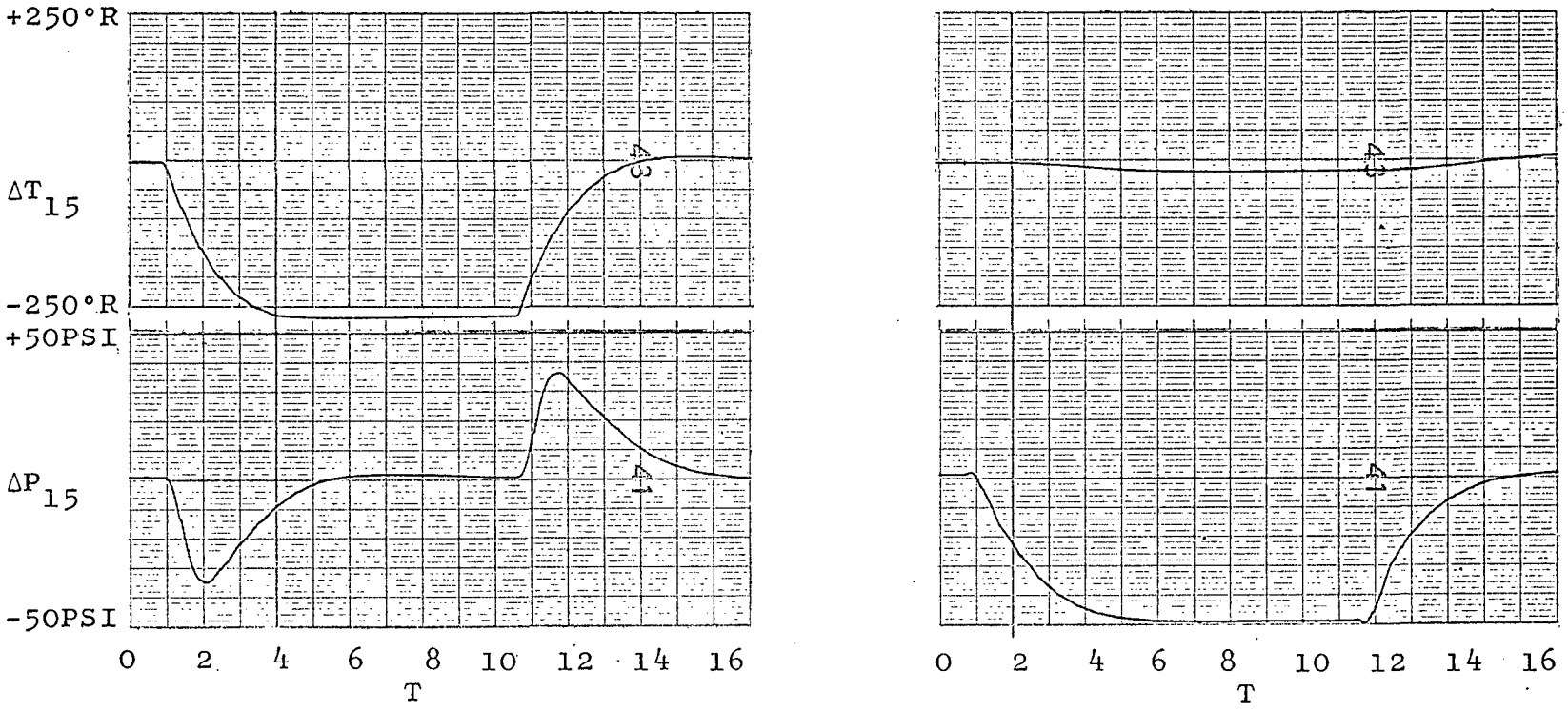

Figure 4-9. Response of System to Step Inputs with a Fourth Order Temperature Loop Control Model (T_{15} = 4250°R, P_{15} = 300 PSI, Update = .5)

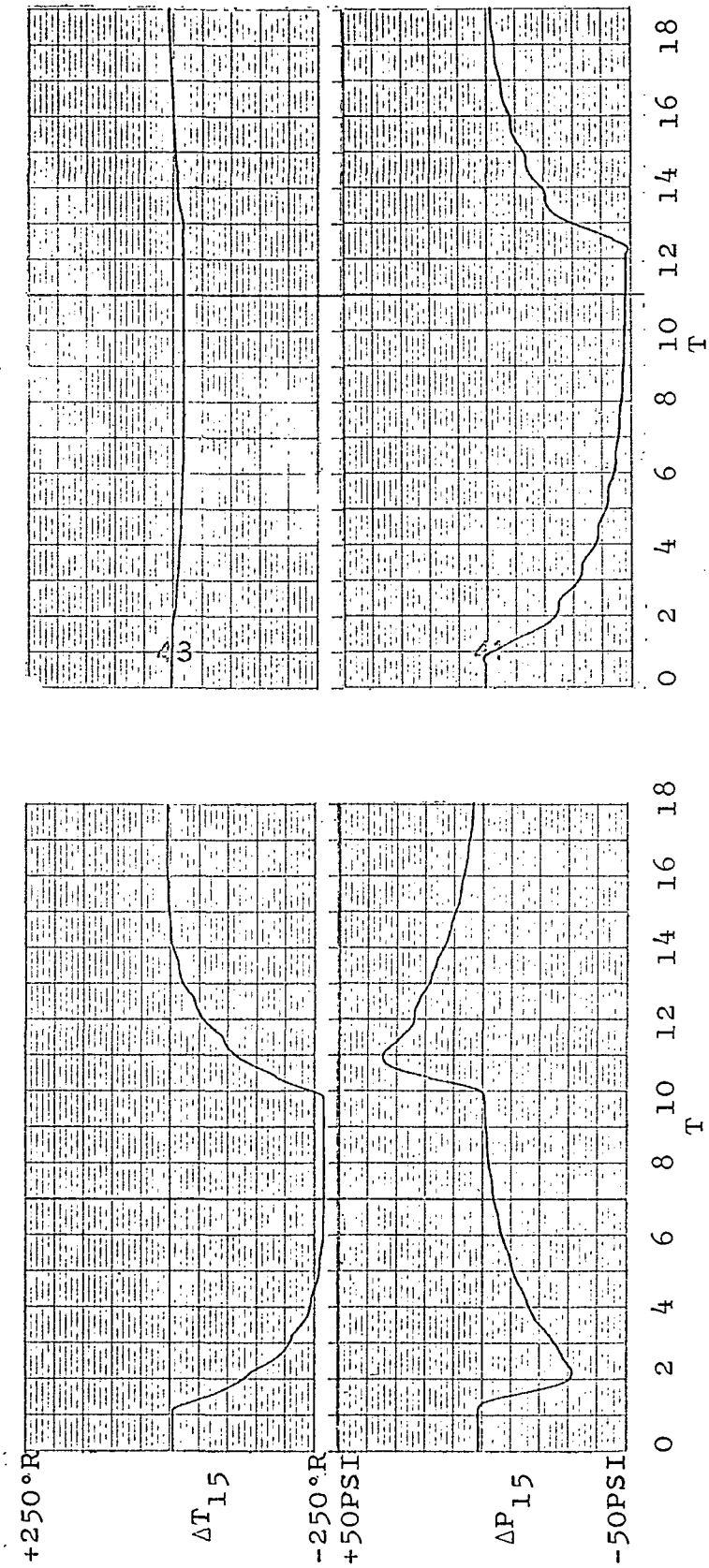

Figure 4-10. Response of System to Step Inputs with a Fourth Order Temperature Loop Control Model (T_{15} = 4250°R, P_{15} = 300 PSI, Update = 1.0)

The form chosen for the single approximate differential equation is

$$\frac{dT_{15}}{dt} = -k_1 \left|W_n\right| T_{15} + k_2 S \qquad (4\text{-}28)$$

The coefficients k_1 and k_2 are determined by minimizing the mean squared error between the response of T_{15} resulting from a step change in nuclear power, S, as predicted by Equations (3-46), (3-47), and (3-48), and that predicted by Equation (4-28) with W_n held constant. The resulting equation is

$$\frac{dT_{15}}{dt} = -.0075 \left|W_n\right| T_{15} + 29.4S \qquad (4\text{-}29)$$

This simplification results in a temperature loop control model that is second order. Figures 4-11 and 4-12 show the response of the system to step inputs of 250° R and 25 PSI. The model update intervals are .50 and 1.0 seconds. The operating point is $T_{15} = 4250^{\circ}$ R, $P_{15} = 300$ PSI. The desired transfer function is

$$\frac{T_{15}}{T_{15_D}} = \frac{(S + .081)(K_1)}{(S + .081)(S + 1.7)}$$

Comparing these responses to those shown in Figures 4-6 and 4-7 indicates again that system performance has not been degraded.

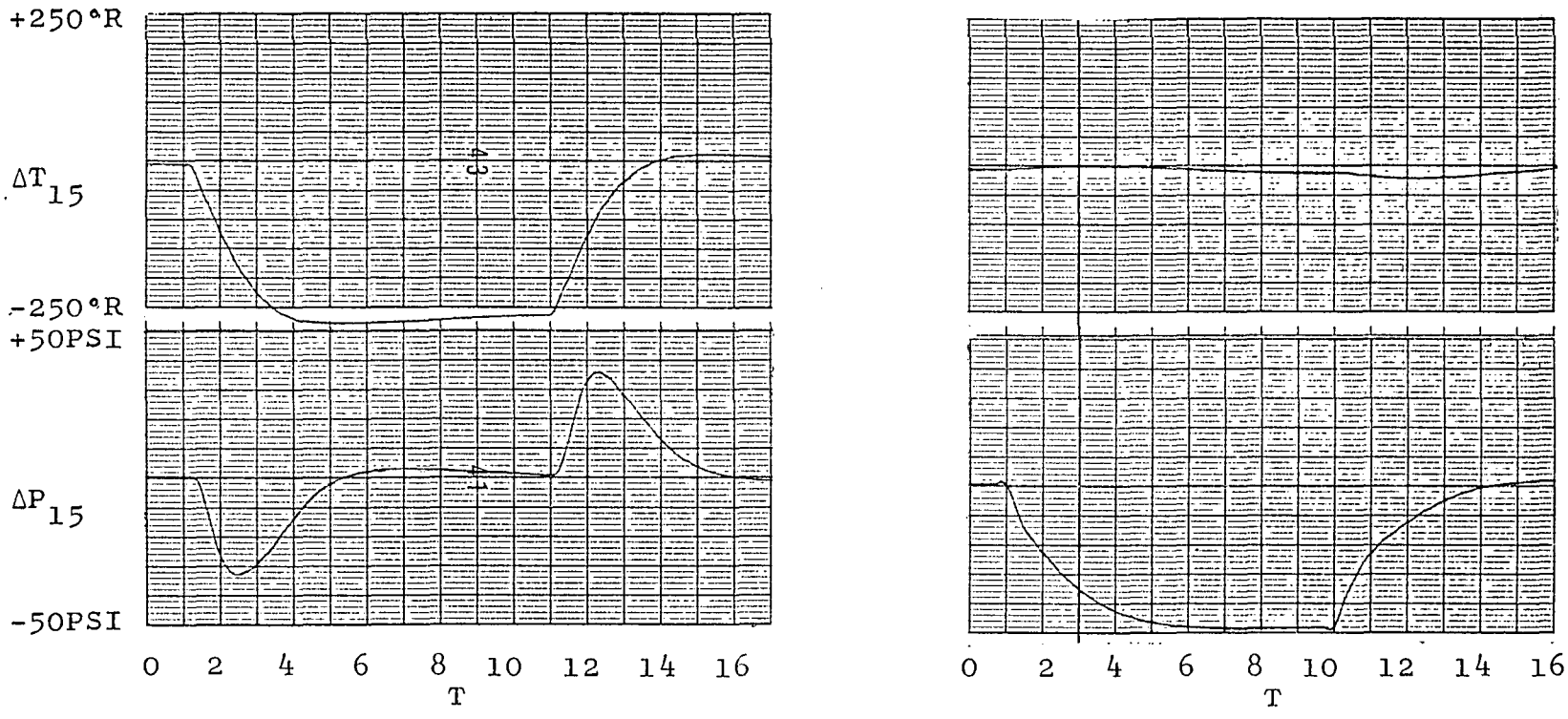

Figure 4-11. Response of System to Step Inputs with a Second Order Temperature Loop Control Model (T_{15} = 4250°R, P_{15} = 300 PSI, Update = .5)

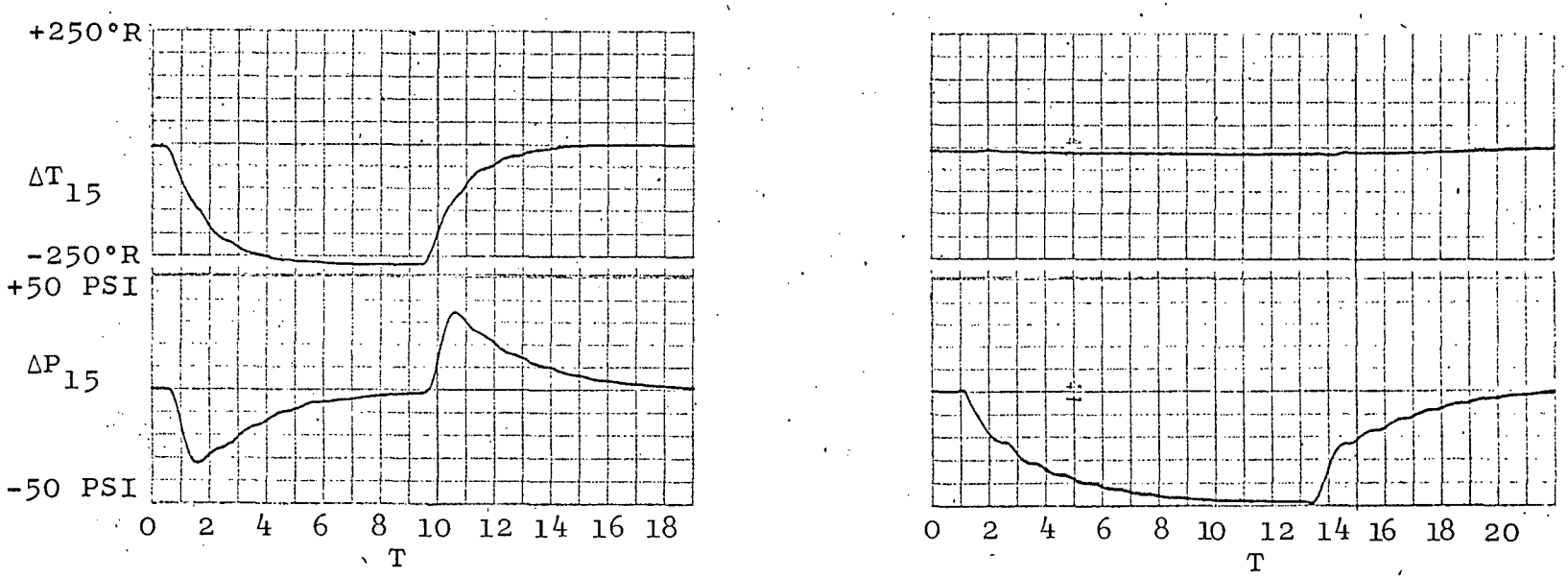

Figure 4-12. Response of System to Step Inputs with a Second Order Temperature Loop Control Model (T_{15} = 4250°R, P_{15} = 300 PSI, Update = 1.0)

The previous control experiments show that the control system provides adequate control for step changes in temperature and pressure demand. However, the types of inputs to which the NERVA control system is expected to respond are ramp demands. It is common practice in linear control system design to improve the response of a system to ramp inputs by adding a series compensator with a pole and a zero to the system (Truxal 1955). If the zero is chosen so that the sum of the reciprocals of the pole and zero locations is zero, then the system error to ramp inputs will be zero. This method of compensation is used in both the pressure and temperature control loops. The desired transfer functions for the temperature and pressure control loops are

$$\frac{T_{15}}{T_{15_D}} = \frac{(S + .081)(S + 1.45)(K_1)}{(S + .081)(S + 1.4)(S + 3.0)}$$

$$\frac{P_{15}}{P_{15_D}} = \frac{(S - 7.1)(S + 1.65)(K_2)}{(S + 1.2)(S + 1.7)(S + 2.6)}$$

Figures 4-13 and 4-14 show the block diagrams of the simplified and compensated temperature and pressure control models. Figures 4-15 and 4-16 show the responses of the system to ramp demands in pressure of 25 and 50 PSI while the temperature demand is held constant. The system update time is .25 second. These responses indicate that it is

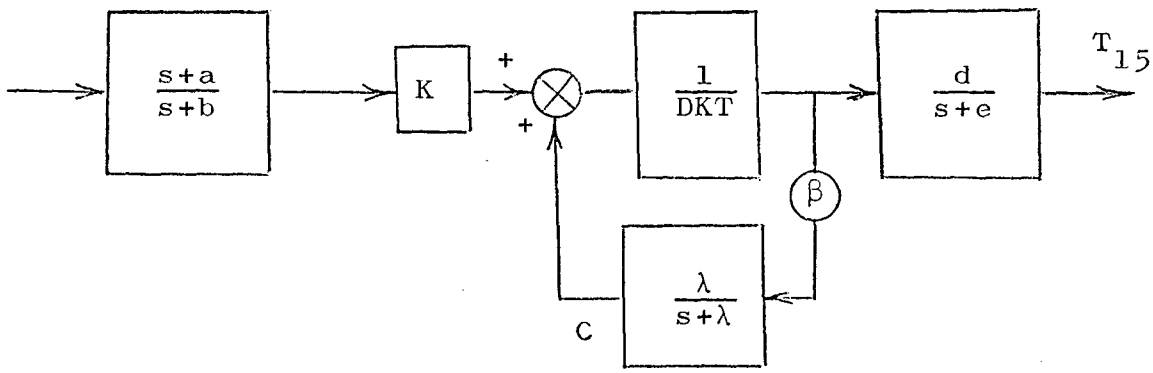

Figure 4-13. Block Diagram of Compensated Temperature Loop

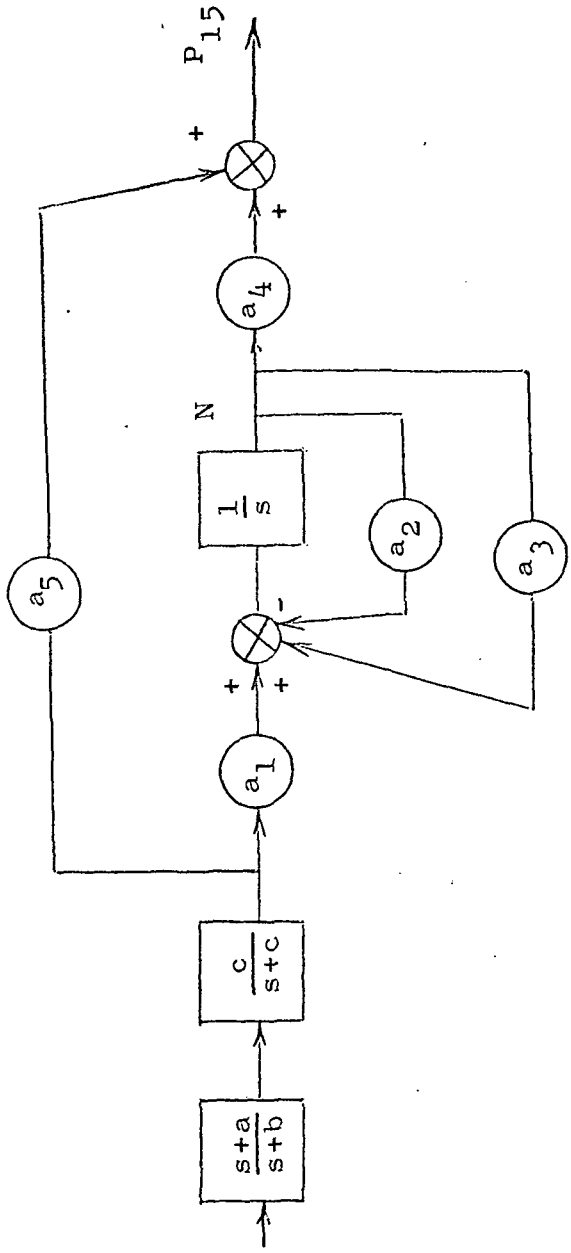

Figure 4-14. Block Diagram of Compensated Pressure Loop

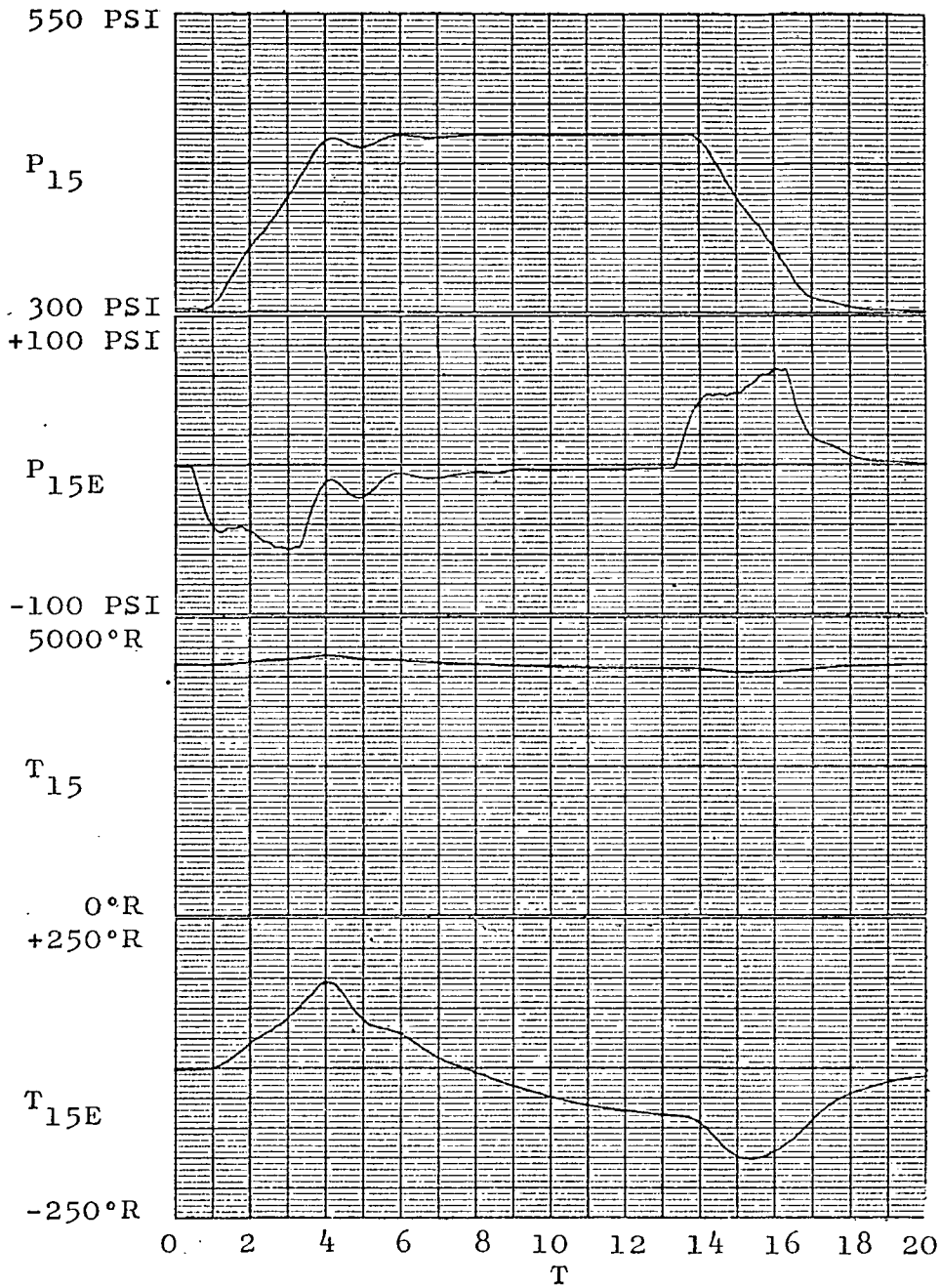

Figure 4-15. Response of System to Ramp Pressure Demand of 50 PSI/sec

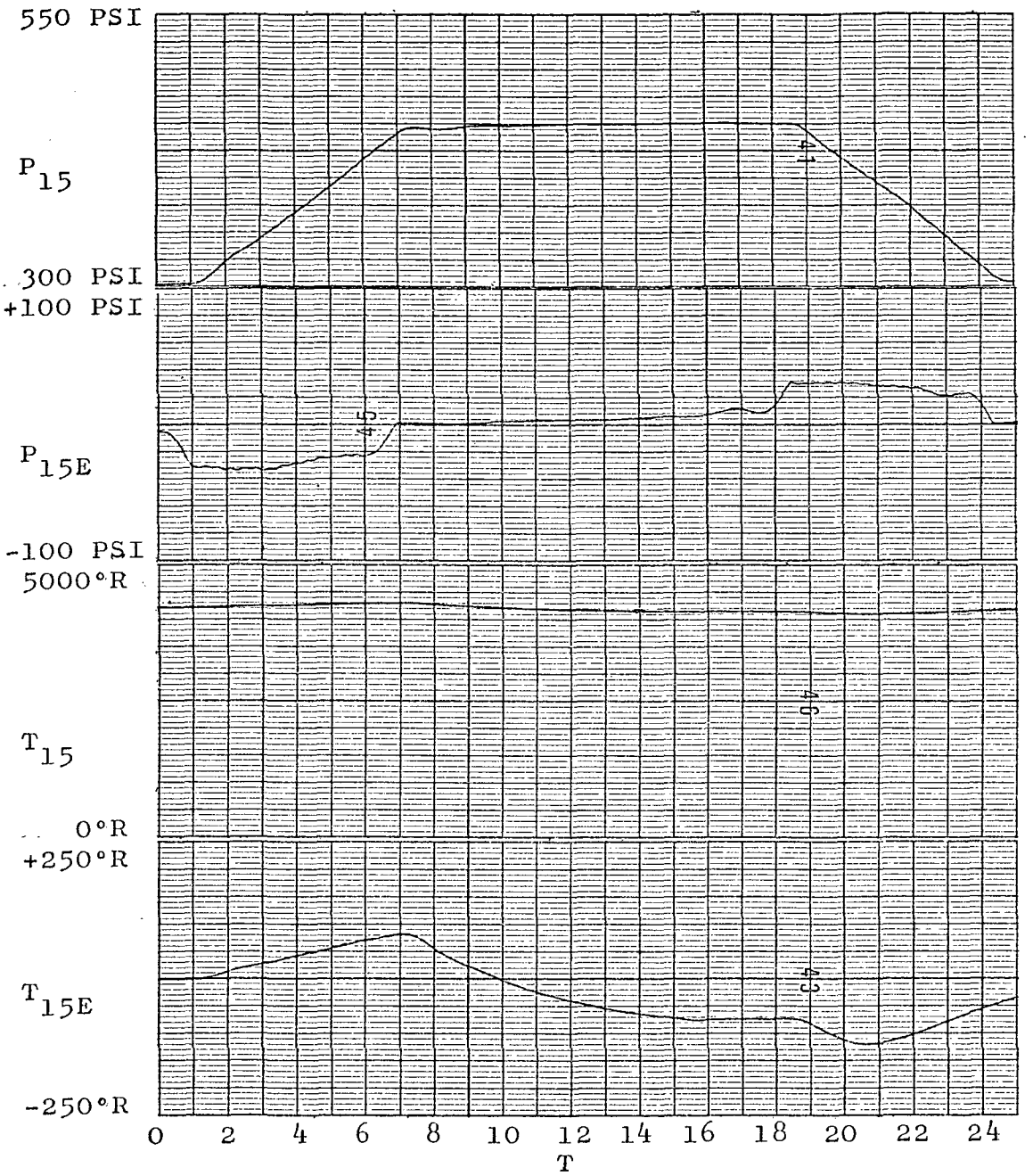

Figure 4-16. Response of System to Ramp Pressure Demand of 25 PSI/sec

possible to use series compensation to obtain good response to ramp input demands.

4.7 Summary of Chapter

The experiments conducted in this chapter show that SDSVF is capable of providing on-line digital control of a complex, high order, nonlinear system. It is further demonstrated that a simplified control model can be used without degrading system performance and that normal linear design techniques can be used to provide good system response to ramp inputs.

In the next chapter the control scheme tested on the Simplified Nonlinear Model is applied to the Common Analog Model.

CHAPTER 5

ON-LINE DIGITAL COMPUTER CONTROL OF THE COMMON ANALOG MODEL USING STATE DEPENDENT STATE VARIABLE FEEDBACK

5.1 Introduction and Outline of the Chapter

In Chapter 4 the concept of SDSVF is used to develop an on-line digital computer control system for the SNM. The final control system design is based on two third order single input-single output linear control models, one for the temperature control loop and one for the pressure control loop. The models both include added compensators to improve the system response to ramp demand inputs. The use of SDSVF to control the Common Analog Model of the NERVA Engine System is investigated in this chapter.

The SNM is developed in Chapter 3 in order to provide a control model on which to base the design of a control system for the CAM. Therefore the control analysis performed in Chapter 4 on the SNM is exactly that required to design a control system for CAM. This means that the control system developed for the SNM can and in fact must be used to control CAM. The success of this approach is dependent on two assumptions:

1. The linear control models based on the SNM are reasonable representations of CAM.
2. The SDSVF method of control is reasonably insensitive to model errors.

The initial portion of Chapter 5 describes the changes required in order to adapt the SNM control program to control CAM. These changes are not fundamental in nature but are necessary because the digital computer must be time-shared with the CAM Simulation. Also, the CAM is to be controlled over a larger region of operation than was the SNM. The description of the changes in the control program is followed by a series of experiments which demonstrate that the control system does provide adequate control of the CAM Simulation over a wide operating range to both ramp and step input demands. Following these experiments, the sensitivity of the SDSVF method of control to errors in the control model is checked. The control method is shown to be insensitive to control model errors by varying the dominant time constants of the CAM by $\pm$ 25 per cent and executing normal start-up and shut-down maneuvers.

5.2 Modifications to the Control Program

The CAM and the SNM are both models of the NERVA Nuclear Rocket Engine. The SNM has been developed by starting with the CAM equations and eliminating those

portions of the model which are not important from a control system design point of view. Therefore, conceptually there is no difference in controlling CAM and controlling the SNM. The only change required in the control system is that rather than measure the state of the SNM, the state of CAM is measured and the control that is calculated is applied to the CAM control inputs rather than the SNM inputs.

Practically, however, two slight modifications to the control program are required. In the control experiments described in Chapter 4, the digital computer is involved only in the calculations required to implement the SDSVF method of control. When the CAM Simulation is controlled, the digital computer is an integral part of the CAM Simulation and is available only on a time-shared basis for computations required to implement SDSVF control. The computations required of the SIGMA 5 Digital Computer as part of the CAM Simulation require slightly more than one-half of the total computing time. This places a definite lower limit on the system update interval. The computation time required for system update in the time-sharing mode is determined by running the system update portion of the control program while the CAM Simulation is operating and measuring the elapsed time from the beginning of the system update until the end of the update. The required system update computation time measured in this

fashion is approximately .15 second. This is more than twice as long as the computation time required in the case where the digital computer is not time-shared, which is .07 second. The computation time is, however, less than the system update interval of .35 second, selected for the CAM control experiments based on the experiments in Chapter 4. The control update interval for the CAM control experiments is the same as for the SNM, .02 second. The method of timing the control update and system update is shown in Figure 5-1.

The other change in the control program is necessary because the CAM Simulation is to be controlled over a wider range of operation than was the SNM. This wider range of operation results in significant changes in the dynamics of the CAM. To attempt to assign a single desired transfer function over the entire range of operation results in large feedback gains and therefore increased sensitivity to measurement errors and noise. To avoid this problem, the desired transfer functions are made a function of the system state. First the open loop transfer functions of the system are examined at various operating points. Then, closed loop desired transfer functions are chosen that do not require large feedback gains. On this basis it is apparent that only the dominant pole of each of the desired transfer functions must be a function of state. The relationships chosen are to make the dominant

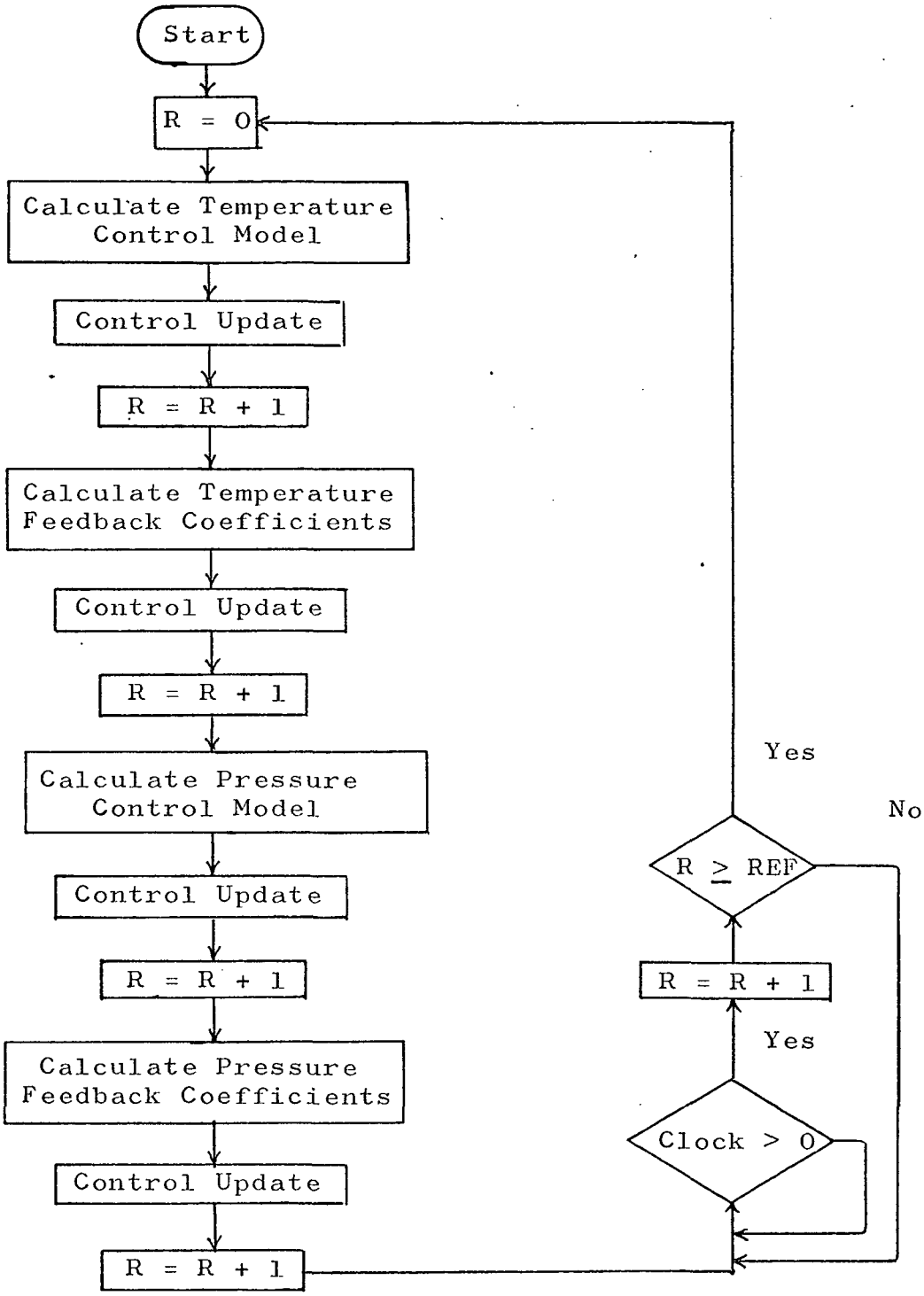

Figure 5-1. Flow Chart of CAM Control Program

pole in the temperature loop proportional to W_n and the dominant pole in the pressure loop proportional to P_{15}. The equations to determine the locations of the two poles are shown below:

$$a_T = -[.025\ W_n - .15] \tag{5-1}$$

$$a_p = -[.003\ P_{15} - .15] \tag{5-2}$$

With these modifications to the SNM control program, it is possible to perform experiments on the CAM Simulation.

5.3 Control Experiments on the Common Analog Model

The design objective for the CAM control system is to provide adequate control of CAM to step and ramp input demands over a wide operating range. Adequate in this case implies no excessive overshoots to sudden changes in input demand, small errors during a transient, small steady-state errors, and minimization of effects of changes in one control loop on the other. The extent to which the SDSVF control system satisfies these objectives is determined by performing control experiments on the CAM Simulation.

The control system is first tested to determine its response to step input demands. The significant characteristics of the control system are the desired transfer

functions, the system update interval, and the control update interval which are given below:

1. Desired transfer function

$$\frac{T_{15}}{T_{15_D}} = \frac{(S + .081)(S + 1.45)(K_1)}{(S + .081)(S + 1.4)(S + 3.0)}$$

$$\frac{P_{15}}{P_{15_D}} = \frac{(S - 7.1)(S + 1.65)(K_2)}{(S + 1.2)(S + 1.7)(S + 2.6)}$$

2. System update interval

   temperature loop = .35 second

   pressure loop = .35 second

3. Control update interval

   temperature loop = .02 second

   pressure loop = .02 second

Figure 5-2 shows the system response to step input demands of 125° R and 25 PSI, at the operating point T_{15} = 4250° R and P_{15} = 300 PSI. At this operating point both the temperature and pressure loop controllers work well. There is less than 10 per cent overshoot to a step change in input, the response does not oscillate excessively, and the coupling between loops is not significant. Figures 5-3 and 5-4 show the system response to step inputs at the operating points T_{15} = 4250° R, P_{15} = 450 PSI and T_{15} = 2000° R, P_{15} = 200 PSI. These responses are similar to those in Figure 4-2. The response in Figure 5-3 indicates

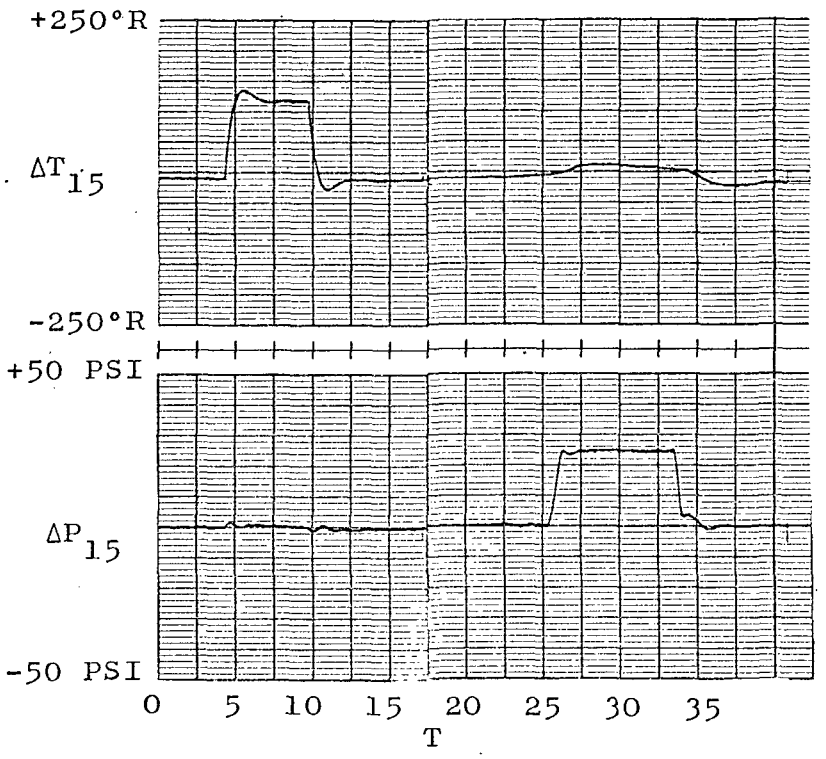

Figure 5-2. Response of CAM to Step Inputs (T_{15} = 4250°R, P_{15} = 300 PSI)

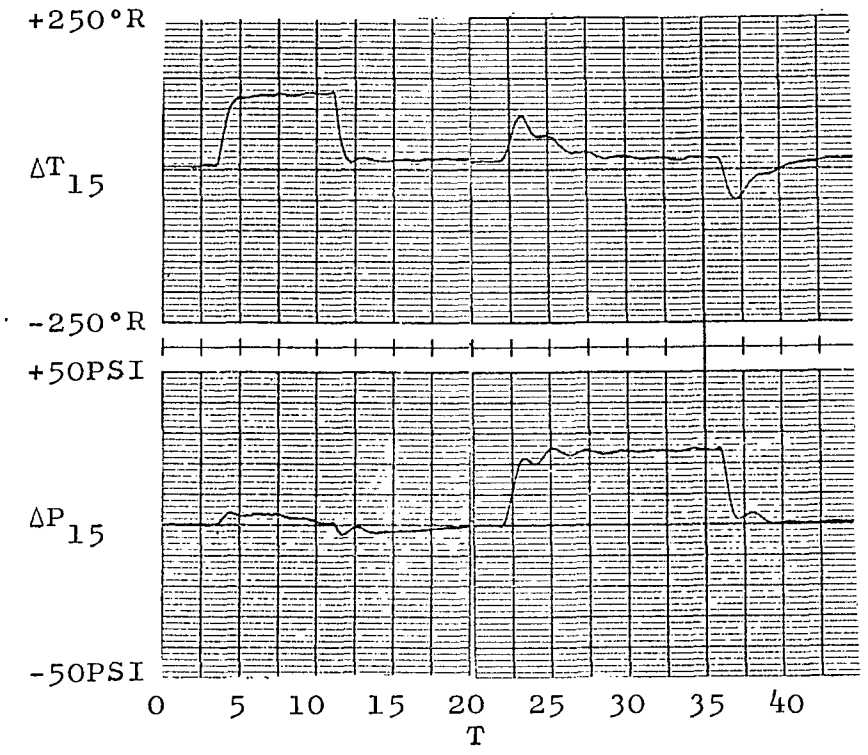

Figure 5-3. Response of CAM to Step Inputs (T_{15} = 4250°R, P_{15} = 450 PSI)

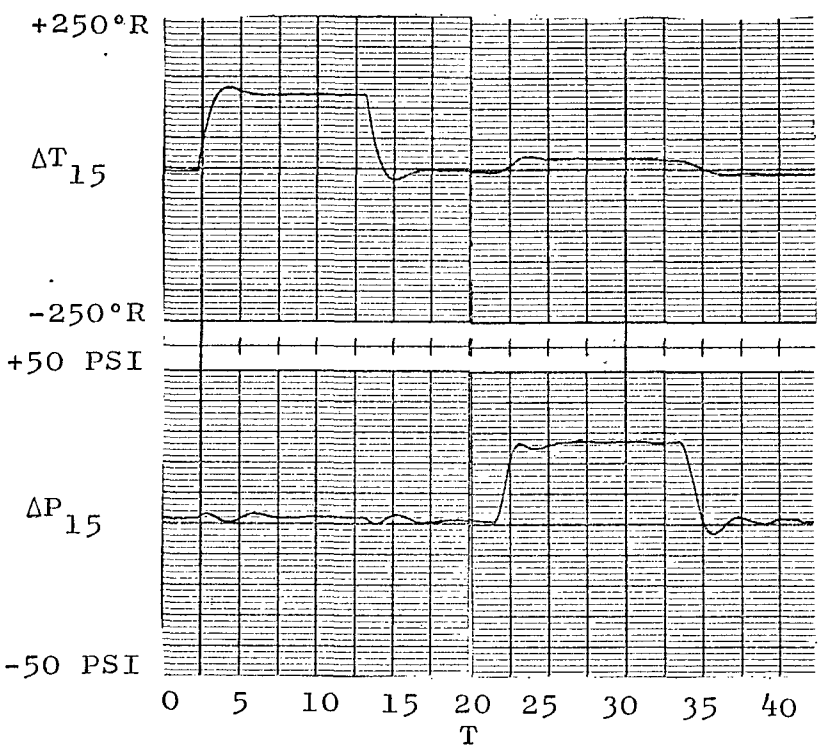

Figure 5-4. Response of CAM to Step Inputs (T_{15} = 2000°R, P_{15} = 200 PSI)

increased coupling between the two control loops, particularly the effect on the temperature of a sudden change in pressure. These responses show that the control system provides a quick smooth response to step inputs over a wide range of operating conditions. The decoupling of the two control loops is excellent for the lower power operating points, although a step change of 25 PSI in the pressure loop results in an error of approximately 75° R in the temperature control loop at the high power operating point. This error is quickly eliminated by the action of the temperature loop control system.

The control system for the NERVA engine will receive its most stringent test when the NERVA engine is either required to start-up or shut-down and at the same time maintain high efficiency. During a normal high efficiency start-up, the temperature demand is ramped at 150° R per second up to 4250° R then held constant, while the pressure demand is ramped at 5 PSI per second up to approximately 300 PSI and then ramped at 50 PSI per second up to 450 PSI. Figures 5-5 and 5-6 show the response of the CAM Simulation with SDSVF control to this type of input demand. The system response is very similar to the input demands. The errors between the demanded temperature and the actual temperature and the demanded pressure and the actual pressure are also shown in Figures 5-5 and 5-6. The temperature error is less than 50° R for the majority

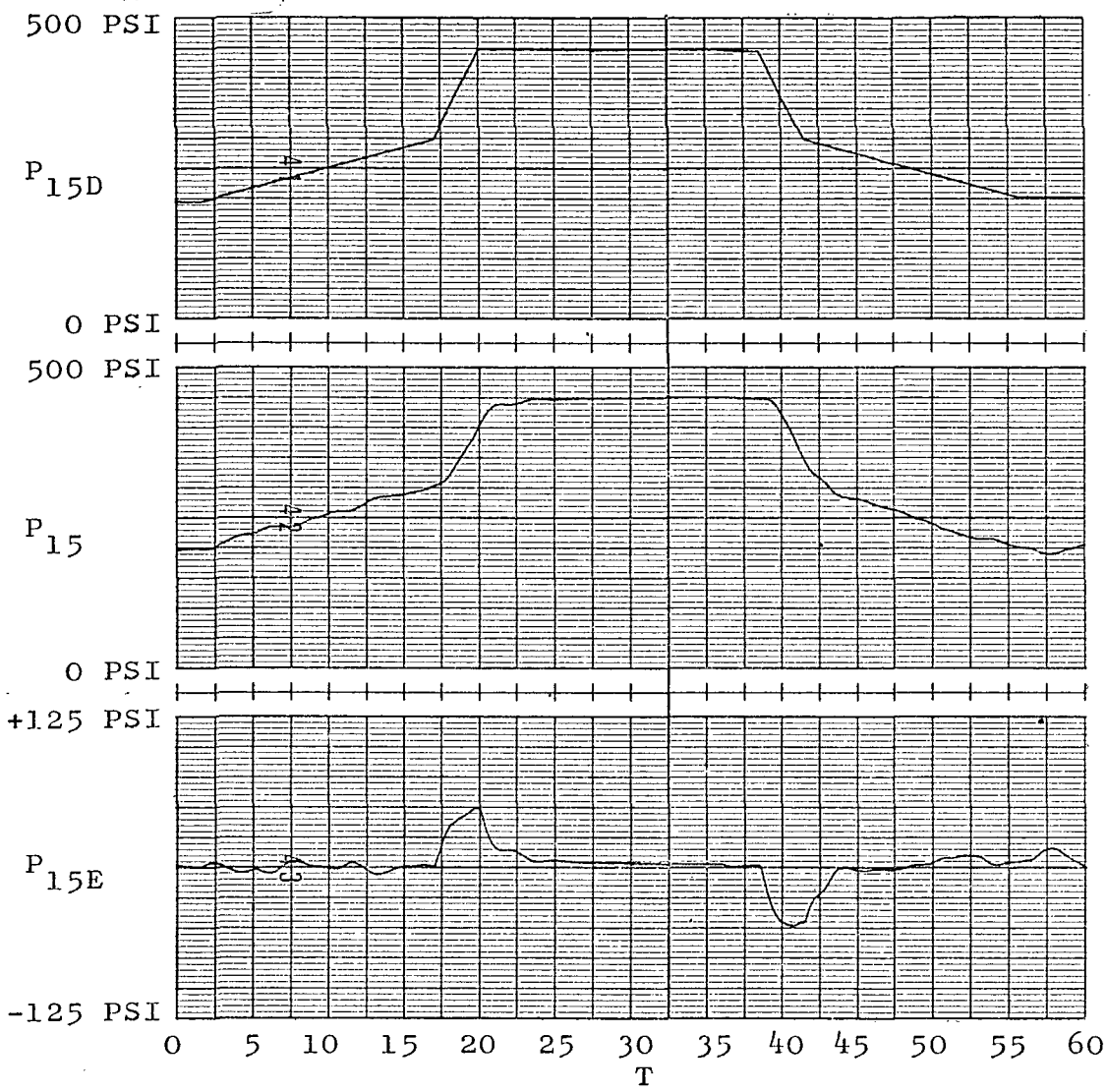

Figure 5-5. Response of Pressure Loop During Normal Start-up and Shut-down

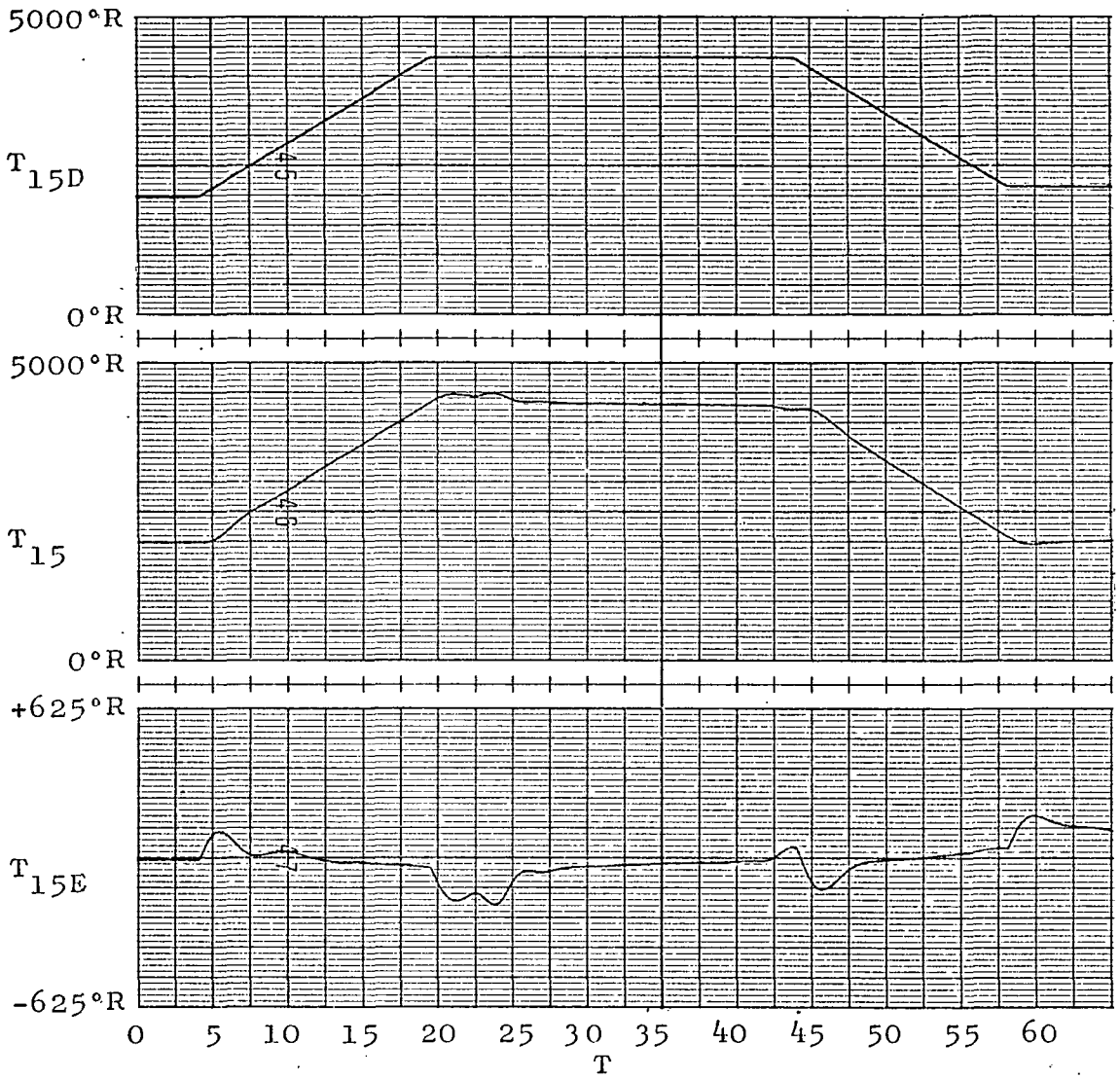

Figure 5-6. Response of Temperature Loop During Normal Start-up and Shut-down

of the ramped portion of the response but overshoots the desired final temperature by approximately 175° R. The pressure error is negligible during the 5 PSI per second portion of the response but increases to approximately 40 PSI during the 50 PSI per second portion of the response. Figures 5-7 and 5-8 show the system response to two other start-up demands. Figure 5-7 shows the response for a half speed start-up. Figure 5-8 shows the response when the normal temperature demand is input but the pressure is held constant and then ramped at 50 PSI per second to full power. The errors for the half speed start-up are less than those for a full speed start-up and the errors from the start-up shown in Figure 5-8 are approximately the same. These responses demonstrate that SDSVF control does provide adequate start-up and shut-down responses.

5.4 Sensitivity Experiments on the Common Analog Model

The experiments in Section 5.3 show that the SDSVF control system does provide adequate control over a wide range of operating conditions. The ability of SDSVF to perform well for the actual NERVA engine also depends on the sensitivity of the control method to errors in the control models, since the CAM cannot possibly be an exact representation of NERVA. The fact that the linear control models used to design the control system for CAM are based on the SNM, which is only an approximate model of CAM,

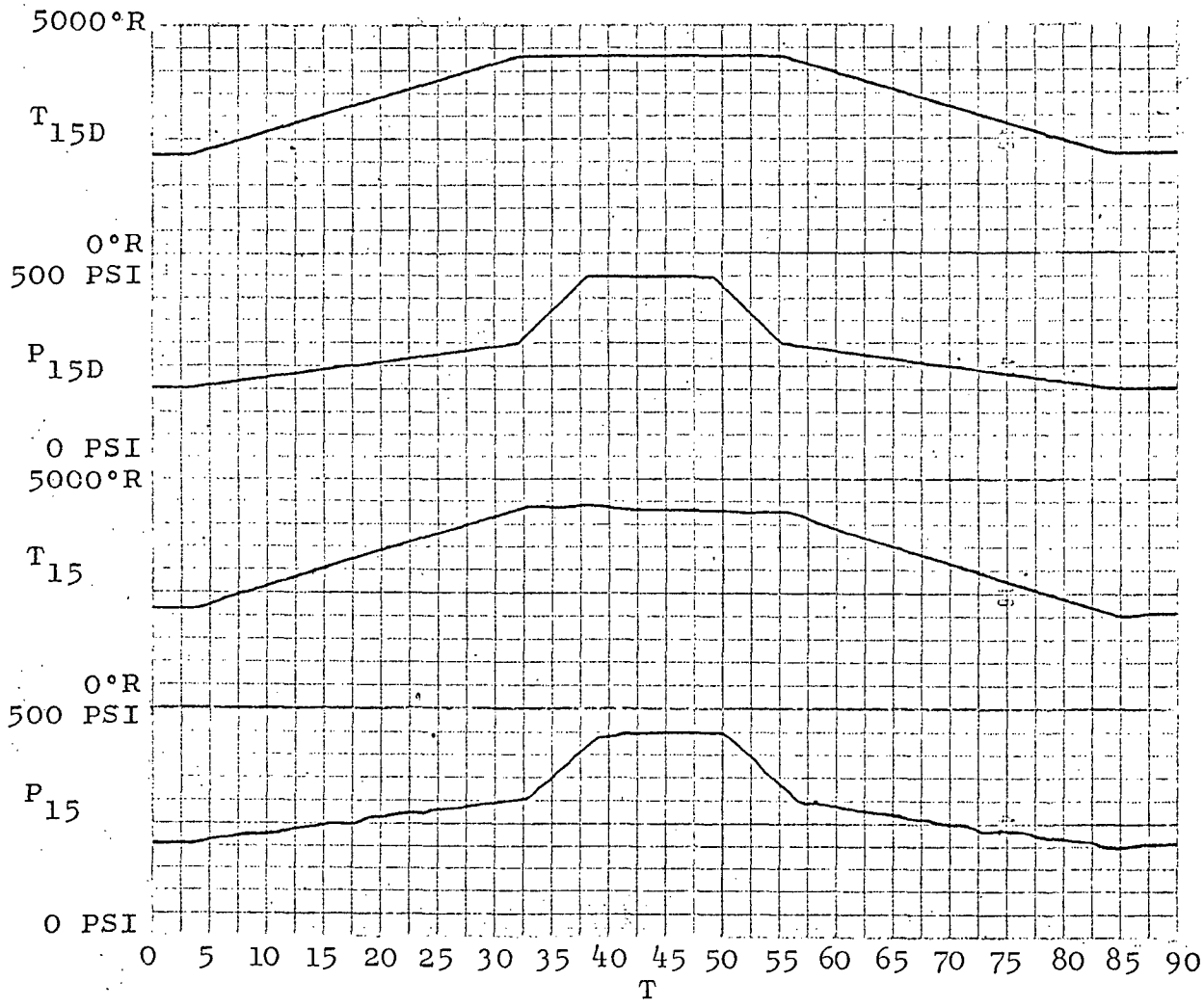

Figure 5-7. Response of CAM During a Half-Speed Start-up and Shut-down

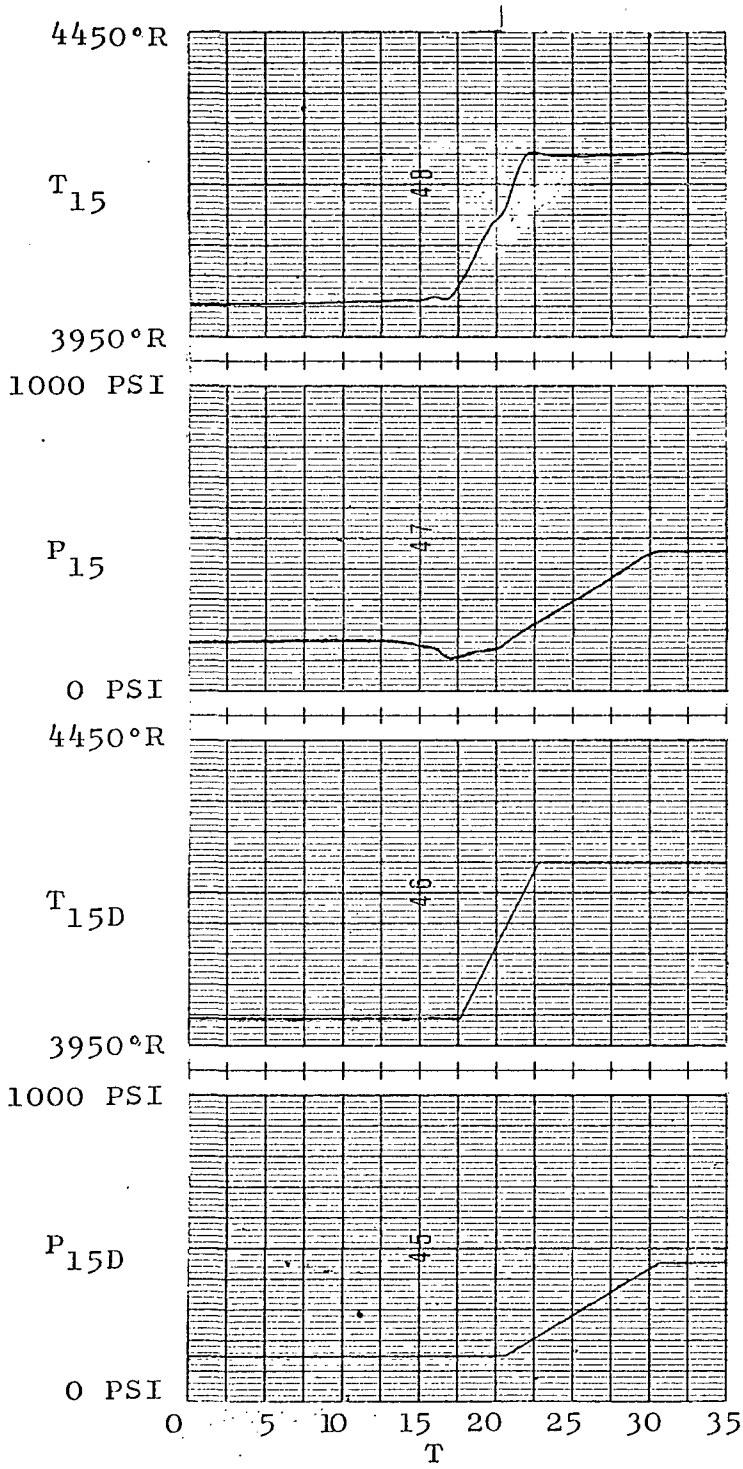

Figure 5-8. Response of CAM off Nominal Trajectory

indicates that SDSVF is not extremely sensitive to control model errors. The sensitivity of the control method is further tested by varying the dominant time constants of the CAM Simulation and executing normal start-up and shut-down maneuvers with the same control system used previously.

The first change made in the CAM is to vary the time constants of the heat transfer portion of the nuclear reactor. Figures 5-9 and 5-10 show start-up and shut-down with the heat transfer time constant varied by plus 50 per cent. In Figures 5-11 and 5-12, the time constant is varied by minus 50 per cent. The errors between demanded and actual outputs are also shown in Figures 5-9, 5-10, 5-11, and 5-12. Comparison of Figures 5-9, 5-10, 5-11, and 5-12 to Figures 5-5 and 5-6 indicates that the responses are very similar. Comparison of the errors shows as expected an increase in both the pressure and temperature control loop errors. The maximum temperature error in Figure 5-9 is approximately 270° R and the maximum pressure error in Figure 5-10 is approximately 50 PSI; this compares to 175° R and 40 PSI from Figures 5-5 and 5-6. The temperature and pressure errors in Figures 5-11 and 5-12 are approximately 280° R and 50 PSI.

To test the sensitivity of the control system to errors in the pressure loop control model, the time constant of the turbine/turbopump assembly is varied first by plus 25 per cent and then by minus 25 per cent.

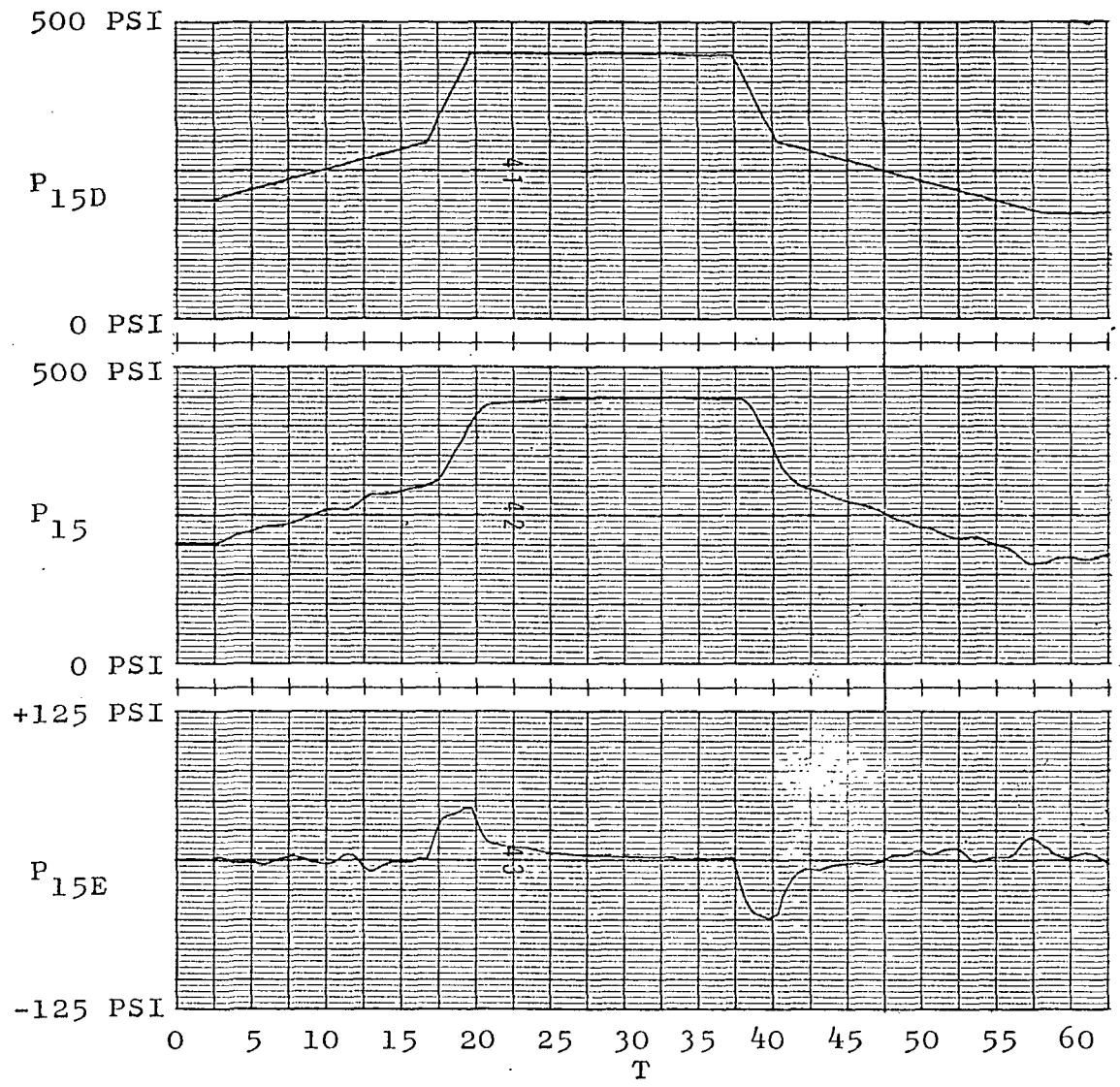

Figure 5-9. Normal Start-up and Shut-down Response of P_{15} with +50 Per Cent Error in Temperature Loop Control Model Time Constant

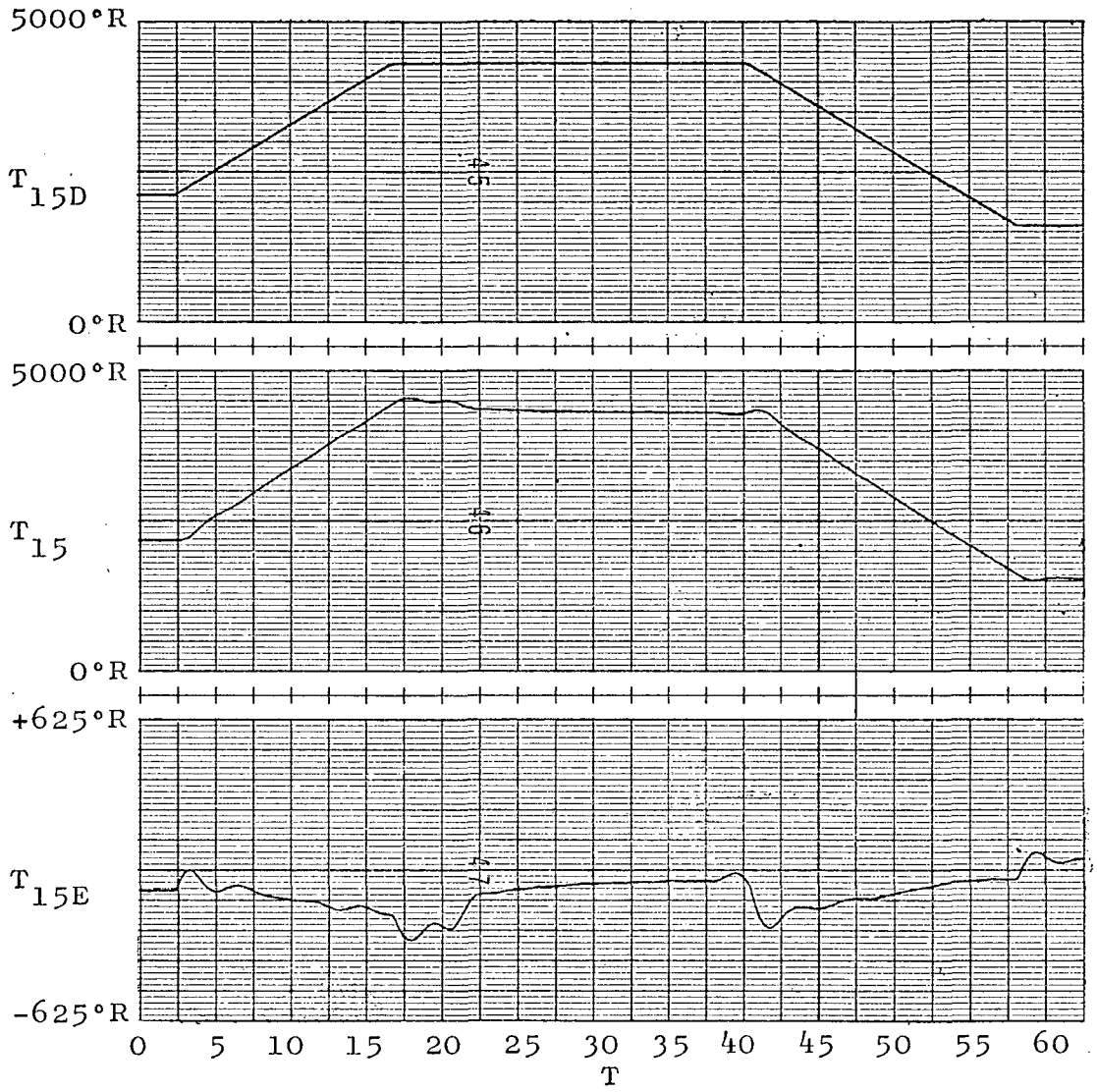

Figure 5-10. Normal Start-up and Shut-down Response of T_{15} with +50 Per Cent Error in Temperature Loop Control Model Time Constant

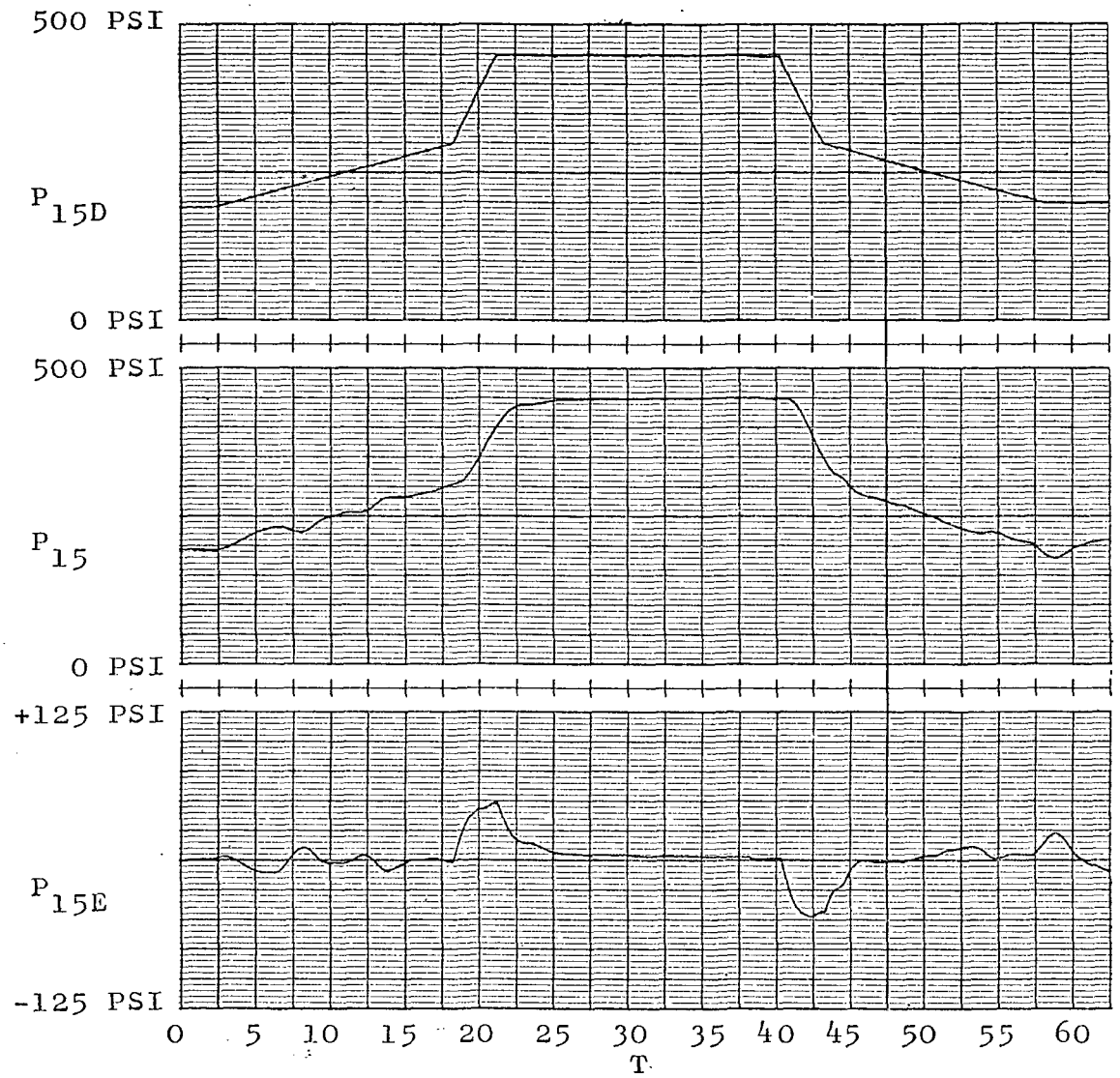

Figure 5-11. Response of P_{15} During a Normal Start-up and Shut-down with -50 Per Cent Error in the Temperature Loop Control Model Time Constant

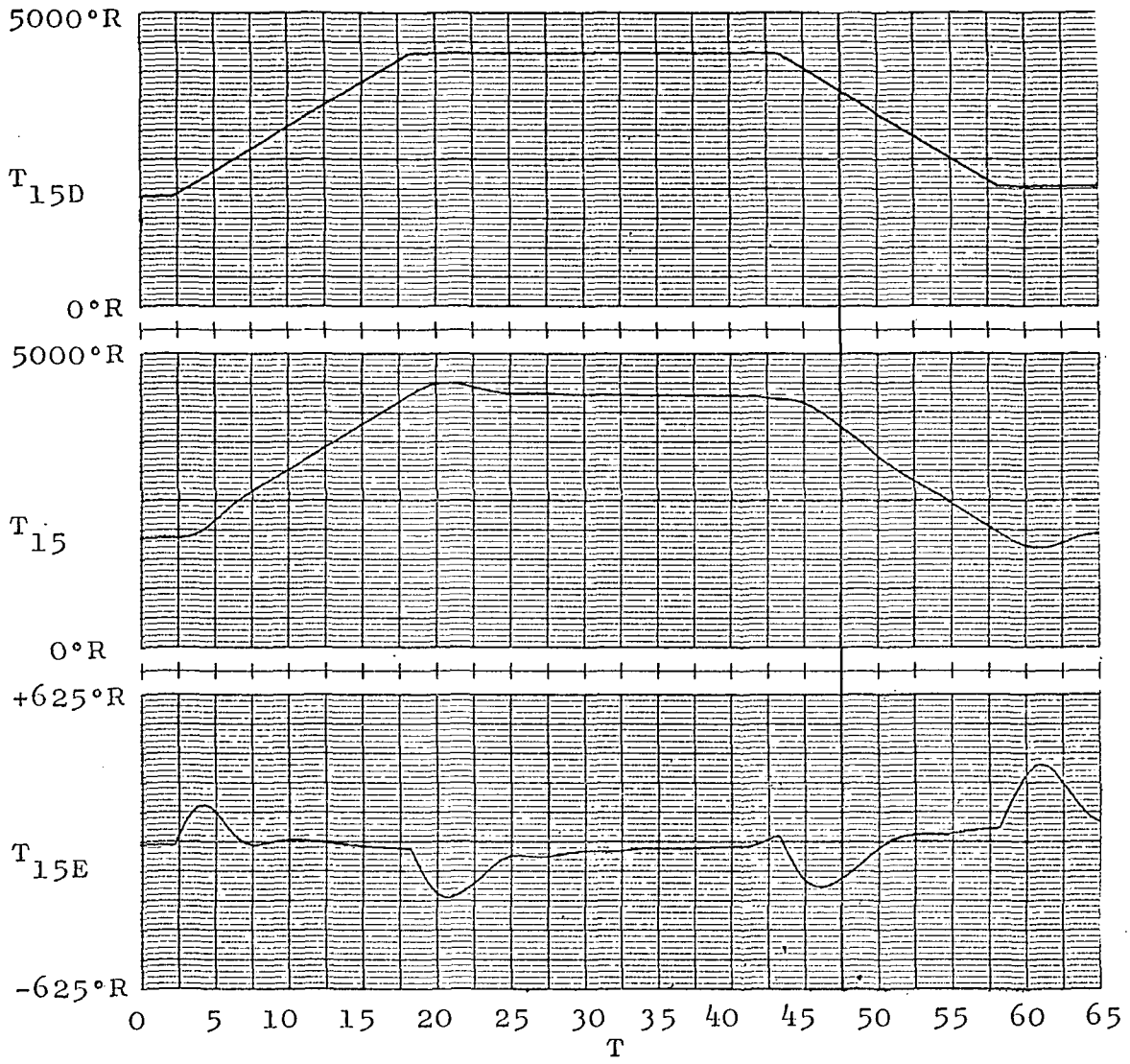

Figure 5-12. Response of T_{15} During a Normal Start-up and Shut-down with -50 Per Cent Error in Temperature Loop Control Model Time Constant

Figures 5-13, 5-14, 5-15, and 5-16 show the start-up and shut-down responses for these conditions. The control loop errors are also shown in these figures. The maximum temperature and pressure errors in Figures 5-13 and 5-14 are approximately 175° R and 60 PSI, respectively. The maximum errors in Figures 5-15 and 5-16 are approximately 200° R and 50 PSI, respectively. These are not significantly larger than the errors in Figures 5-5 and 5-6 of 175° R and 40 PSI.

The responses shown in Figures 5-9 through 5-16 indicate that the SDSVF control system provides adequate performance with significant errors in the control model. As expected, the errors increase as the model errors become larger but the control system does provide adequate performance with these control model errors.

5.5 Summary of the Chapter

The control system designed in Chapter 4 for the SNM is used, with only minor changes, to control the CAM Simulation. The control system provides adequate response to both step and ramp input demands over a wide region of operation. The control system is shown to be relatively insensitive to control model errors by varying dominant system time constants of both major control loops by at least plus and minus 25 per cent with no significant deterioration in the system response.

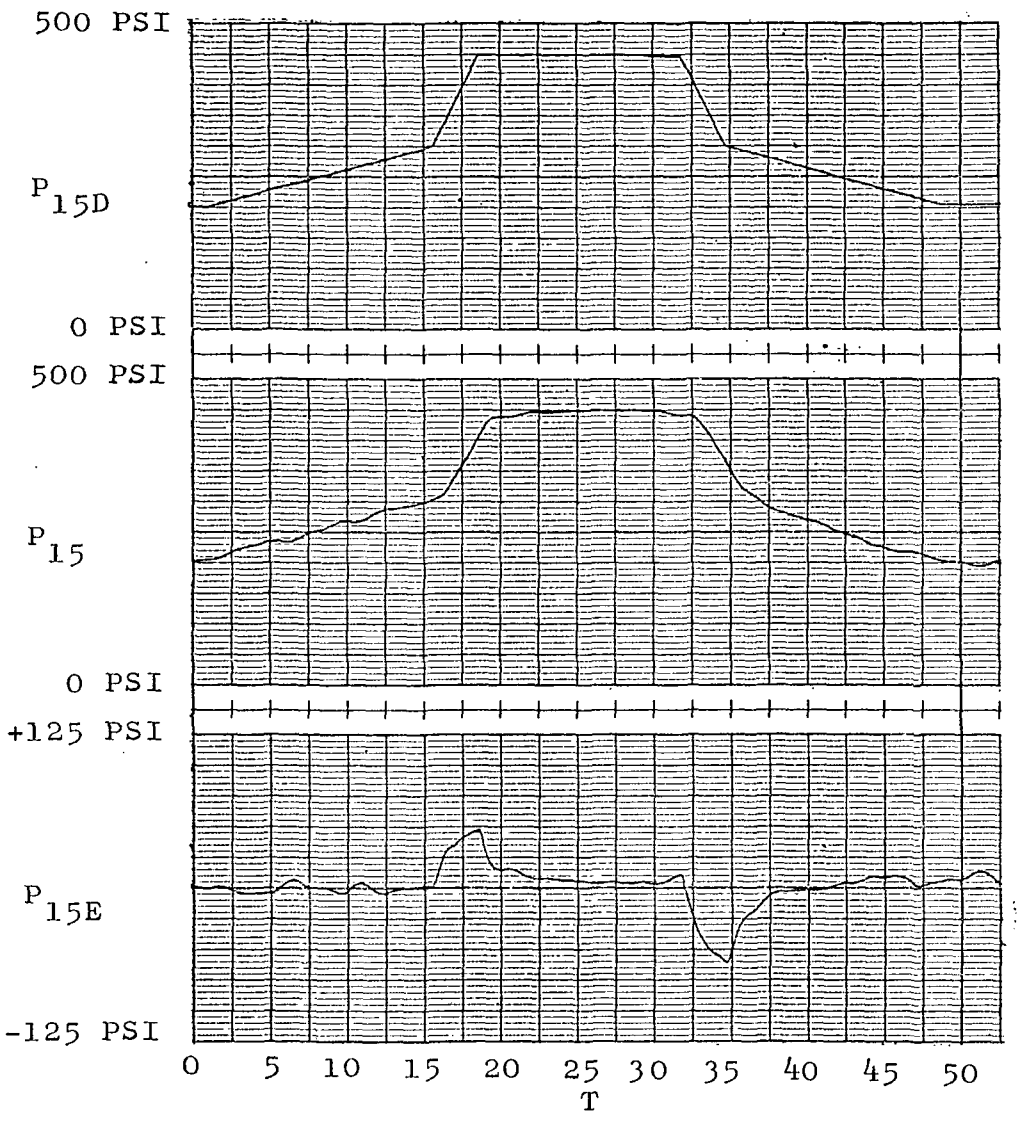

Figure 5-13. Response of P_{15} During a Normal Start-up and Shut-down with a +25 Per Cent Error in Temperature Loop Control Model Time Constant

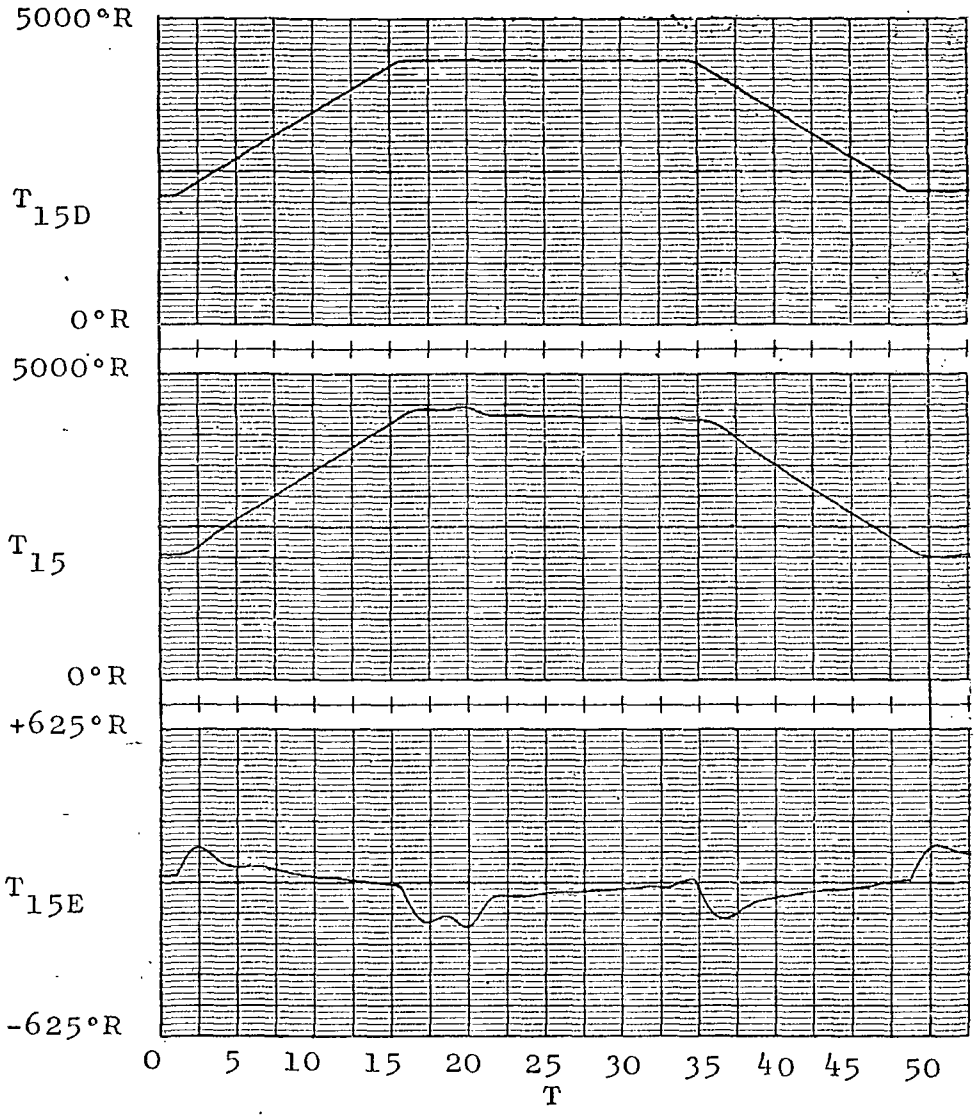

Figure 5-14. Response of T_{15} During a Normal Start-up and Shut-down with +25 Per Cent Error in Pressure Loop Control Model Time Constant

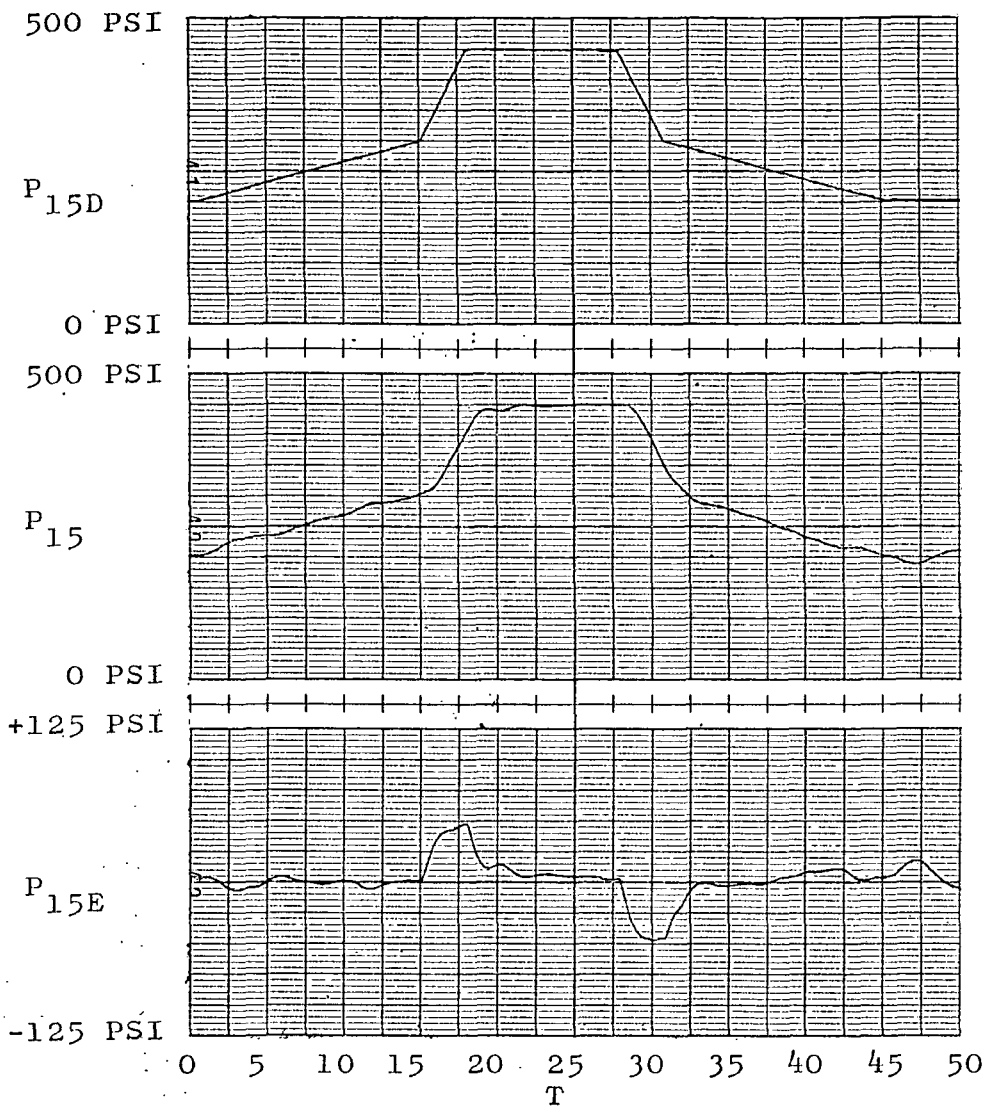

Figure 5-15. Response of P_{15} During a Normal Start-up and Shut-down with a -25 Per Cent Error in Pressure Loop Control Model Time Constant

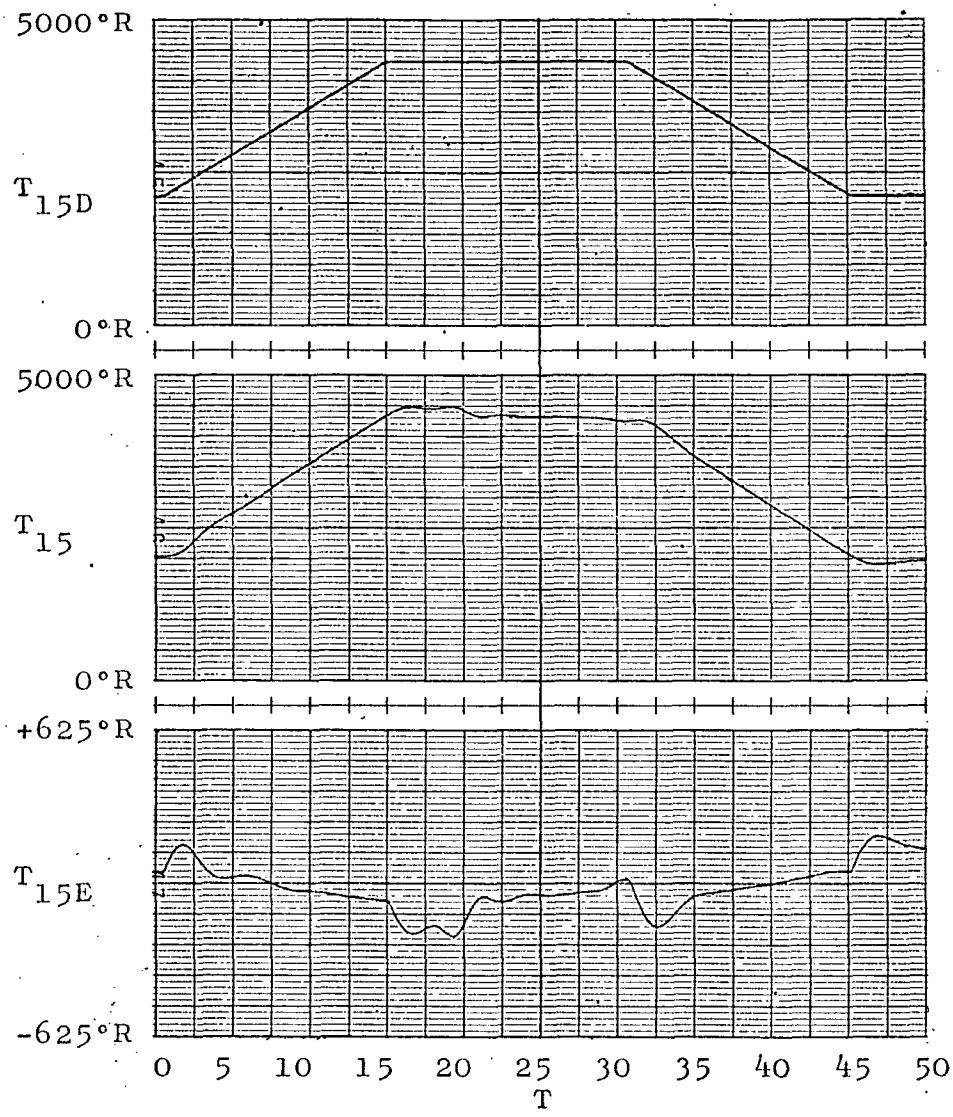

Figure 5-16. Response of T_{15} During a Normal Start-up and Shut-down with a -25 Per Cent Error in the Pressure Loop Control Model Time Constant

These experiments indicate that the SDSVF method of control can be used to design an on-line digital computer control system for the NERVA engine.

CHAPTER 6

SUMMARY AND CONCLUSIONS

6.1 Summary

This study is concerned with the design of an on-line digital computer control system for the NERVA nuclear rocket engine. The actual NERVA engine has not yet been constructed; however, there is available an accurate and detailed mathematical model of the NERVA engine. This model is called the *Common Analog Model* and a hybrid simulation of the model is available. Examination of this model reveals that the NERVA engine is a high-order non-linear, and tightly coupled multiple input-multiple output system.

Theoretically, the solution to the optimal control problem for a large class of nonlinear systems is available from Pontryagin's Maximum Principle or Bellman's Dynamic Programming. Practically, however, both of these methods have serious drawbacks which severely limit their usefulness when dealing with high-order nonlinear systems such as NERVA. This study uses the method of State Dependent State Variable Feedback control as a practical method for controlling complex, high-order nonlinear systems. SDSVF avoids the problems inherent in the Maximum Principle and

Dynamic Programming by specifying the optimal closed loop system in terms of a desired transfer function rather than in terms of a performance index to be maximized or minimized. The use of the concept of a desired transfer function is made possible in the nonlinear case by using an on-line digital computer to define state dependent linear control models, each valid in some small region of state space. The on-line computer also computes feedback gains required to realize the desired closed loop transfer function. Thus the control method requires periodic sampling of the system state, calculation of linear models, and computation of feedback coefficients.

A linearization technique is developed and a method of computing the required feedback coefficients based on the work of Schultz and Melsa (1969) is chosen. It is shown that the procedures involved in both the linearization and feedback gain calculation are easily programmed. The most time consuming computation is the inversion of a matrix of the same order as the control model. This computation is required in calculating the feedback gains. The control method is then demonstrated and the effect of the interval between model and feedback gain update is illustrated.

SDSVF is then applied to the problem of controlling the CAM. The control method cannot be applied to the CAM equations directly because of the extremely high order of

the system. Therefore the Simplified Nonlinear Model of NERVA is developed to be used in control system design. Following the development of the SNM, a SDSVF control system is developed and tested on the SNM. The control system provides adequate control of the SNM and is then used to control the CAM Simulation. The control and sensitivity experiments performed on the CAM Simulation, using a SDSVF control system, indicate that it is possible to design an on-line digital computer control system for the NERVA engine.

The contributions of this study are the development of the SNM of the NERVA engine and the introduction of the concept of SDSVF control. The validity of the model and the usefulness of the control concept are demonstrated by designing an on-line digital computer control system for the CAM Simulation using SDSVF control with the SNM used as the control model.

6.2 Conclusions

The State Dependent State Variable Feedback method of control utilizes concepts from both modern control theory and classical control theory to provide an alternate method of control system design and analysis for nonlinear and/or time-varying systems. The many approximations involved in applying SDSVF to a specific problem make it difficult to draw general conclusions about the usefulness

of the method. The results of this study do, however, provide a basis for some general statements. If the model of the system is accurate, if it is possible to perform the system update calculations frequently enough to insure accuracy of the linear control models, and the states of the system can be accurately measured, then it is possible to obtain a desired response as specified by a desired transfer function to any degree of accuracy. When these conditions cannot be satisfied the actual response of the system differs from the desired response. The only way to determine the effect of not satisfying one of these conditions is by simulation. Based on the experiments performed in this study, the effect of using an update interval that is too long is to make the system response sluggish. No stability problems were encountered until the update interval was increased by a factor of four. The control method appears to be reasonably insensitive to errors in the dynamics of the control model, but errors in the static gain result in steady-state errors in the output. The problem of inaccurate measurement of the system state was not examined in this study.

The major advantage of SDSVF appears to be that it permits the use of the powerful analysis and design tools of linear control theory to solve nonlinear and/or time-varying control problems. This is a significant advantage in view of the lack of practical design methods for

nonlinear and/or time-varying control systems. The major disadvantages of the method are the requirements for

1. An on-line digital computer.
2. An accurate mathematical model.
3. Measurement or estimation of the system state.
4. A desired response defined in terms of a linear transfer function.

The requirement for use of a digital computer restricts the control method to problems that justify the expense. However, the current trend in the computer field toward lower cost and higher performance will reduce or eliminate this problem. The second and third disadvantages listed are common to any control method using state variable feedback. The requirement that desired system performance be specified in terms of a linear transfer function limits the method somewhat, but there exist many problems for which this is in fact the preferred method.

It appears that SDSVF does not inherently involve any serious disadvantages when compared to other control methods. The decision to use the method revolves primarily around the question of whether or not the performance that can be obtained using SDSVF justifies the expense and effort involved in modeling the system, making the required measurements, and using a digital computer.

6.3 Recommendations

The SDSVF method of control is developed in this study and applied to a complex high-order nonlinear control problem. The results of this study indicate the method has significant potential. Additional studies in which the method is applied to the problem of controlling complex high-order nonlinear and/or time varying systems are needed in order to determine if unexpected problems arise and to determine the sensitivity of the method to control model and state measurement errors.

Methods of reducing the method's dependence on accurate static gain in the control model warrant further study. One possible method that should be investigated is the use of SDSVF to condition the plant, then use of series compensation to achieve zero steady-state error.

APPENDIX A

DESCRIBING EQUATIONS OF THE COMMON ANALOG MODEL

A.1 Introduction

The equations describing the Common Analog Model of the NERVA Nuclear Rocket Engine are contained in this appendix. Portions of the model equations are classified and have been deleted. The nomenclature and units used in the CAM equations are given. Figure A.1 is a simplified flow schematic of the NERVA engine.

A.2 Nomenclature of Common Analog Model Equations

Variables	Definition	Units
CI_j	= Precursor concentration in j^{th} group	
Co	= Isentropic spouting velocity	ft/sec
Dk	= Reactivity	$
E	= Fluid enthalpy	BTU/lb
ET	= Turbine efficiency	
f	= Function	
F_θ, DKFD	= Reflector reactivity factor	
H	= Enthalpy of solid material	BTU/lb
K	= Flow resistance	
M, TRQ	= Torque	lb-ft
M_r, XMRE	= Reflector density factor	

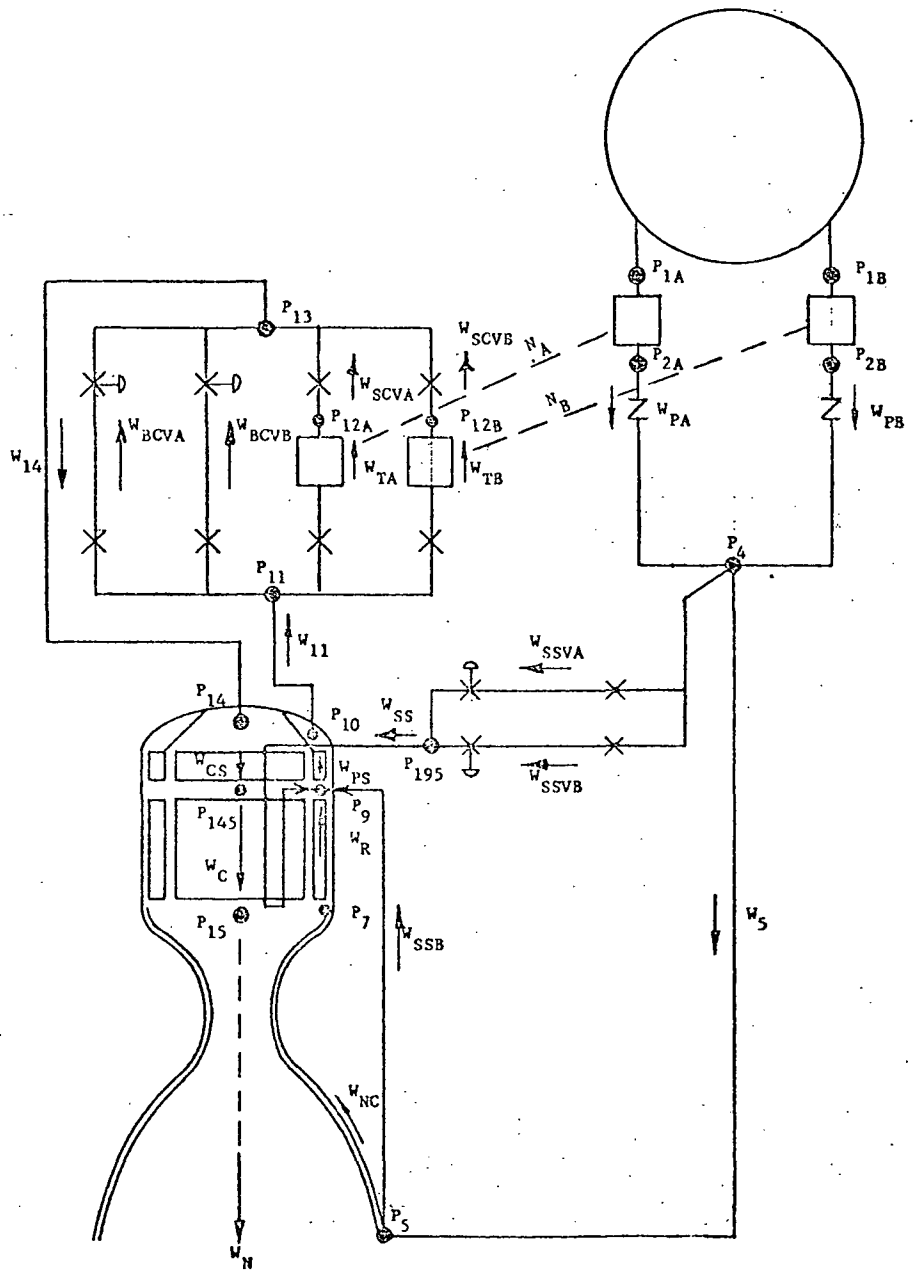

Figure A-1. Flow Schematic of NERVA Engine

Variables	Definition	Units
N,RPM	= Speed	rpm
P	= Pressure	psia
Q_j	= Decay heat power in j^{th} group	%
R	= Density	lb/ft^3
s	= Laplace operator	
S	= Thermal power in fueled sections	%
SOPY	= Turbine inlet enthropy	
S_N	= Nuclear power	%
S_{NQ}	= Thermal power in unfueled sections	%
t	= Time	sec
T	= Fluid temperature	°R
u	= Mean peripheral blade speed	ft/sec
W	= Mass flowrate	lb/sec
θ,TH	= Angular position	deg
φ,PH	= Material temperature	°R
ΔE_S,DLES	= Isentropic enthalpy drop	BTU/lb

Subscripts Indicating Location on Flow Diagram

1	= Pump inlet
2	= Pump discharge
4	= Junction of pump discharge lines
5	= Nozzle inlet
7	= Reflector inlet plenum
9	= Reflector exit plenum
10	= Peripheral shield exit plenum

11 = Bypass and turbine inlet

12 = Turbine exit

13 = Bypass and series valve exit

14 = Shield entrance plenum

145 = Core inlet plenum

15 = Nozzle chamber

19 = Junction of pump discharge lines

195 = Support structure control valve discharge

20 = Stem inlet

22 = Support system discharge

23 = Support bypass discharge

Qualifying Subscripts

A,B = Parallel components

BCV = Bypass control valve

C = Reactor core, average

c = Corrosion

C_i = Reactor core, i^{th} section

ch = Core hydrogen

cs = Central shield

ct = Core thermal (reactivity)

d = Drum

D = Demand

e = Exit

E = Error

f = Feedback

i = Radial inside

J = Jacket

M = Measured

N = Nozzle

NC = Nozzle coolant

O = Radial outside

P = Pyrographite

P = Pump

ps = Peripheral shield

R = Reflector

SCV = Series control valve

SG = Structural graphite

SK = Skirt

SKC = Skirt coolant

SS = Support system

SSB = Support system bypass

ssd = Support system downcomer

SSj = Support system, j^{th} section

ssu = Support system upcomer

ssv = Support system control valve

t = Total

T = Turbine

T2 = Stem

T3 = Liner

A.3 Common Analog Model Equations

Pump Equations

1. $P_{1A,B} = 30,\ T_{1B} = 40$

2. $P_{2A,B} = P_{1A,B} + N^2_{A,B}\ f_1\ (\frac{W_{PA,B}}{N_{A,B}})$

3. $T_{4B} = T_{1B} + .015\ (P_{2B} - P_{1B})$

4. $M_{PA,B} = N^2_{A,B}\ f_2\ (\frac{W_{PA,B}}{N_{A,B}})$

5. $\frac{dN_{A,B}}{dt} = 88.1\ (M_{TA,B} - M_{PA,B})$

Pump Discharge Line Equations

1. $\frac{dW_{PA,B}}{dt} = 127.5(P_{2A,B} - P_4) - .7833\ W_{PA,B}|W_{PA,B}|$

$W_{PA,B} \geq 0$

2. $\frac{dP_4}{dt} = \frac{1810 + 1.4P_4}{1.23}\ (W_{PA} + W_{PB} - W_5 - W_{SSVA} - W_{SSVB})$

3. $T_{19} = T_{4B}$

4. $P_{19} = P_4$

Support System Connection to Nozzle Torus Equations

1. $\frac{dW_5}{dt} = 34.2\ (P_4 - P_5) - .1091\ W_5|W_5|$

2. $$\frac{dP_5}{dt} = \frac{1810 + 1.4P_5}{4.441} (W_5 - W_{NC} - W_{SSB})$$

3. $$T_5 = T_{4B}$$

Reflector Inlet Plenum Equations

1. $$\frac{d}{dt} R_7 = .368 (W_{nc} - W_r)$$

2. $$\frac{d}{dt} T_7 = \frac{.368}{R_7} (W_{nc}T_{nc} - W_rT_7)$$

3. $$P_7 = T_7 f_1 (R_7) - f_2 (R_7)$$

4. $$T_7 min = 52. + .043 P_7 \quad P_7 < 210 \text{ psia}$$

Reflector Exit Plenum Equations

1. $$\frac{dR_9}{dt} = .188 (W_r + W_{ss} + W_{ssb} - W_{ps})$$

2. $$P_9 = \frac{5.32 R_9T_9}{(1. - .186 R_9} - 214. R_9^2$$

3. $$\frac{dT_9}{dt} = \frac{.188}{R_9} (W_rT_{re} + W_{ss}T_{22} + W_{ssb}T_{23} - W_{ps}T_9)$$

Turbine/Simulator and Bypass Equations

1. $$W_{11} = 17.79 \sqrt{R_{10}(P_{10}-P_{11})}$$

2. $$\frac{dR_{11}}{dt} = .166 (W_{11} - W_{BCVA} - W_{BCVB} - W_{TA} - W_{TB})$$

3. $T_{11} = T_{10}$

4. $P_{11} = 5.32 R_{11} T_{11}$

5. $W_{TA,B} = 8.294 \frac{P_{11}}{\sqrt{T_{11}}} f\left(\frac{P_{11}}{P_{12A,B}}\right)$

6. $E_{11} = 3.145 T_{11} - 95.9 \qquad T_{11} \leq 221$

$= 3.831 T_{11} - 247.5 \qquad T_{11} > 221$

7. $SOPY = f(E_{11}, P_{11})$

8. $\Delta E_{SA,B} = E_{11} - f(SOPY, P_{12A,B})$

9. $C_{OA,B} = 224 \sqrt{\Delta E_{SA,B}}$

10. $\left(\frac{U}{C_O}\right)_{A,B} = .0404 \frac{N_{A,B}}{C_{OA,B}}$

11. $ET_{A,B} = f\left(\frac{U}{C_O}\right)_{A,B}$

12. $M_{TA,B} = 7430 \frac{W_{TA,B}}{N_{A,B}} ET_{A,B} * \Delta E_{SA,B}$

13. $E_{12A,B} = E_{11} - ET_{A,B} * \Delta E_{SA,B}$

14. $\frac{dR_{12A,B}}{dt} = 1.85 (W_{TA,B} - W_{SCVA,B})$

15. $T_{12A,B} = .318E_{12A,B} + 30.5 \qquad E_{12A,B} \leq 600$

$= .261E_{12A,B} + 64.6 \qquad E_{12A,B} > 600$

16. $P_{12A,B} = 5.32R_{12A,B}T_{12A,B}$

17. $W_{SCVA,B} = .1151\ \theta_{SCVA,B}\sqrt{R_{12A,B}(P_{12A,B} - P_{13})}$

18. $W_{BCVA,B} = .0210\ \theta_{BCVA,B}\sqrt{R_{11}(P_{11} - P_{13})}$

19. $\frac{dT_{13}}{dt} = \frac{.129}{R_{13}}\left[W_{SCVA}T_{12A} + W_{SCVB}T_{12B} + (W_{BCVA} + W_{BCVB})T_{11} - W_{14}T_{13}\right]$

20. $\frac{dR_{13}}{dt} = .129(W_{SCVA} + W_{SCVB} + W_{BCVA} + W_{BCVB} - W_{14})$

21. $P_{13} = 5.32R_{13}T_{13}$

22. $W_{14} = 21.6\sqrt{R_{13}(P_{13} - P_{14})}$

Peripheral Shield Exit Plenum Equations

1. $\frac{d}{dt} R_{10} = .119\ (W_{ps} - W_{11})$

2. $\frac{d}{dt} T_{10} = \frac{.119}{R_{10}}\ (W_{ps}T_{pse} - W_{11}T_{10})$

3. $$P_{10} = \frac{(5.32\ R_{10}T_{10})}{(1.0 - .186R_{10})} - 214.\ R_{10}^{2}$$

Central Shield Entrance Plenum Equations

1. $$\frac{d}{dt} R_{14} = .107\ (W_{14} - W_{cs})$$

2. $$\frac{d}{dt} T_{14} = \frac{.107}{R_{14}} (W_{14}T_{13} - W_{cs}T_{14})$$

3. $$P_{14} = \frac{5.32\ R_{14}T_{14}}{(1. - .186\ R_{14})} - 214.\ R_{14}^{2}$$

Central Shield and Core Support Plate Exit Plenum Equations

1. $$\frac{dR_{14.5}}{dt} = .173\ (W_{cs} - W_{c})$$

2. $$\frac{dT_{14.5}}{dt} = \frac{.173}{R_{14.5}} (W_{cs}T_{cse} - W_{c}T_{14.5})$$

3. $$P_{14.5} = 5.32\ R_{14.5}T_{14.5}$$

Thrust Chamber Equations

1. $$\frac{dR_{15}}{dt} = .0630\ (W_{c} - W_{N})$$

2. $$P_{15} = 5.32\ R_{15}T_{15}$$

3. $$W_N = 13.33 \frac{P_{15}}{\sqrt{T_{15}}}$$

4. $$\frac{dT_{15M}}{dt} = \frac{W_N^{.5}}{2.85} \quad (T_{15} - T_{15M})$$

Support System Inlet and Bypass Equations

1. $$\theta_{ssva,b} = \text{independent variable}$$

2. $$K_{ssva,b} = f(\theta_{ssva,b})$$

3. $$W_{ssva,b} = 16.5 \left(\frac{|P_{19}-P_{19.5}|}{K_{ssva,b}+62.7} \right)^{.5} \left[\frac{(P_{19}-P_{19.5})}{|P_{19}-P_{19.5}|} \right]$$

4. $$W_{ss} = .899 \left(R_{ss} |P_{19.5}-P_9| \right)^{.5} \frac{(P_{19.5}-P_9)}{|P_{19.5}-P_9|}$$

5. $$\frac{d}{dt} P_{19.5} = 580. \ (W_{ssva} + W_{ssvb} - W_{ss})$$

6. $$W_{ssb} = .201 \ |P_5-P_9|^{.5} \left[\frac{(P_5-P_9)}{|P_5-P_9|} \right]$$

Support System Equations

1. $$\frac{dR_{ss2e}}{dl} = 100 \left[W_{ss} - 1.00 \sqrt{R_{ss} |P_{ss2e}-P_9|} \frac{(P_{ss2e}-P_9)}{|P_{ss2e}-P_9|} \right]$$

2. $$P_{ssle} = \frac{5.32R_{ssle}\,(65-35_e^{-1.7R_{ssle}})}{(1 - 0.186R_{ssle})} - f\,(R_N)$$

$$- h\,(R_N) \cdot h\,(T_N)$$

For $T_{ssle} \leq (65. - 35.\ e^{-1.7R_{ssle}})$

3. $$P_{ssle} = \frac{5.32R_{ssle}T_{ssle}}{(1 - 0.186R_{ssle})} - f\,(R_N)$$

For $T_{ssle} > (65. - 35.\ e^{-1.7R_{ssle}})$

4. $$f\,(R_N) = f\,(R_{ssle})$$

5. $$h\,(R_N) = h\,(R_{ssle})$$

6. $$h\,(T_N) = h\,(T_{ssle})$$

7. $$P_{ss2} = \frac{5.32 * R_{ss2} * T_{ss2}}{1. - .186 * R_{ss2}} - f\,(R_N)$$

3. $$f\,(R_N) = f\,(R_{ss2})$$

9. $$\frac{dR_{ss2}}{dt} = 100\left[W_{ss} - 1.25\sqrt{R_{ss2}|P_{ss2}-P_9|}\,\frac{(P_{ss2}-P_9)}{|P_{ss2}-P_9|}\right]$$

10. $$P_{ss2e} = \frac{5.32R_{ss2e}T_{ss2e}}{(1 - 0.186R_{ss2e})} - f\,(R_N)$$

11. $$f\,(R_N) = f\,(R_{ss2e})$$

12. $$\frac{dR_{ssle}}{dt} = 100\left[W_{ss} - 0.958\sqrt{R_{ss}|P_{ssle}-P_9|}\,\frac{(P_{ssle}-P_9)}{|P_{ssle}-P_9|}\right]$$

13. $$T_{20} = T_{19} + \left[\frac{0.743}{.00296|W_{ss}| + .043}\right]\frac{S}{W_c}$$

14. $$T_{ss1} = T_{20} + \left[\frac{0.0696}{1 + 0.416|W_{ss}|}\right](T_{ss4} - T_{ss1})$$

15. $$T_{ssle} = 2.\ T_{ss1} - T_{20}$$

16. $$P_{ss3} = P_{ss2e} - \left(\frac{W_{ss}}{1.81}\right)^2\left(\frac{1}{R_{ss2e}}\right)$$

17. $$R_{ss3} = \frac{P_{ss3}}{5.32T_{ss3}}$$

Kinetics Equations

1. $$\frac{dS_N}{dt} = (0.0276\ Cl_1 + 0.235\ Cl_2 + 1.65\ Cl_3) - 660.38\ (1. - DKT)S_N$$

2. $$\frac{d}{dt}\ Cl_1 = 180.99\ S_N - 0.0276\ Cl_1$$

3. $$\frac{d}{dt}\ Cl_2 = 369.08\ S_N - 0.235\ Cl_2$$

4. $$\frac{d}{dt}\ Cl_3 = 110.31\ S_N - 1.65\ Cl_3$$

5. $$\frac{d}{dt}\ Q_1 = 0.000117\ S_N - 0.00322\ Q_1$$

6. $\frac{d}{dt} Q_2 = 0.000757\ S_N - 0.05525\ Q_2$

7. $\frac{d}{dt} Q_3 = 0.003734\ S_N - 0.2707\ Q_3$

8. $S_{NQ} = 6.672\ (Q_1+Q_2+Q_3) + 0.6301\ S_N$

9. $S = S_N + Q_1 + Q_2 + Q_3$

Reactivity Equations

1. $Dk_r = 0.26M_r\ [1.-.0623M_r] + .00762\ [\Phi_r-524.]\ [1.0+.442M_r\ (1.0-.0466M_r)] - 4.43F_\theta$

2. $F_\theta = .00501M_r\ (1.-.312M_r) + .000134\ (\Phi_r-524.)\ [1.0+.398M_r\ (1.-.0543M_r)]$

3. $Dk_{ch} = 15.0\ [0.138R_{14.5} + 0.841R_{15}]$

4. $Dk_{ssd} = 0.553\ [-0.414R_{ss1e} + 11.99R_{ss2} - 11.21R_{ss2e}]$

5. $Dk_{ct} = -.77 \times 10^{-3}\ (\Phi_c - 540)$

6. $M_r = \frac{2.53}{2.0}\ [R_7 + R_{re}]$

7. $Dk_{ssu} = 1.16\ R_{ss3}$

8. $Dk_d = 4.50\ \mathrm{Sin}^2\ (\theta_{DM}/2.) - 1.85$

9. $Dk_f = Dk_r + Dk_{ch} + Dk_{ct} + Dk_{ssu} + Dk_{ssd}$

10. $Dk_c = -1.00$

11. $Dk_t = Dk_f + Dk_c + (1 + F_\theta)\, Dk_d$

APPENDIX B

DESCRIPTION OF THE AEROJET NUCLEAR SYSTEMS COMPANY'S HYBRID COMPUTER FACILITY

B.1 Introduction

This appendix describes briefly the equipment available in the Aerojet Nuclear Systems Company's hybrid computer facility. The Common Analog Model was implemented on this equipment. All hybrid control experiments described in this study were performed using the Aerojet hybrid computer facility.

B.2 Laboratory Facilities

The ANSC hybrid computer laboratory provides large scale analog and hybrid simulation capability. The equipment consists of six analog computers, a digital computer, a hybrid interface, and associated peripheral equipment.

Five large analog computers provide for large scale analog or hybrid simulation. Three of these are solid-state COMCOR CI-5000's, and two are EAI 231R-V computers. The five consoles are capable of being slaved together in groups of from 2 to 5 consoles or run separately, with or without the digital computer. The three COMCOR computers communicate with the digital computer through the hybrid

interface while the two EAI computers communicate directly through the COMCOR computers. There is a total of 198 integrators, 334 summers, 222 multipliers, and 54 variable diode function generators available on the five consoles. Of the 880 coefficient potentiometers, 480 can be automatically set from the digital computer and an additional 280 can be automatically set with the EAI Automatic Digital Input/Output System (ADIOS). All above mentioned components can be automatically read out using either the digital computer or the ADIOS. Each of the five consoles provides extensive general purpose logic capability. Both analog and logic trunking are set up between all consoles. All consoles feature high speed repetitive operation.

For smaller problems a COMCOR CI-150 solid state analog computer, with 75 amplifiers, is available.

Extensive analog recording and display capability is available. A recorder track provides for centralized patching to and remote control of up to twelve 8-channel Brush recorders. Two X-Y recorders are also available. Three Weston-Boonshaft and Fuchs DA-410 Frequency Response Analyzers and an ESIAC Root Locus Plotter, Model 10, are available for controls analysis. The ESIAC enables rapid plotting of Bode and root locus plots from transfer functions as well as curve fitting transfer functions to experimental frequency response data. The DA410 is used for obtaining frequency response data from the computer

model. A Sangamo Model 4700 FM magnetic tape system provides for record and playback of up to 14 channels of analog information.

The XDS Sigma 5 digital computer provides for hybrid simulation. This computer is a third generation machine with a core of 32,768 - 32 bit words and a cycle time of 850 nanoseconds. Its peripheral equipment includes a 750,000 word rapid access magnetic disk, a seven channel - 556 bit per inch magnetic tape unit, a 400 card per minute card reader, a 300 line per minute printer and an electric typewriter with paper tape input/output capability.

Digital computer programs have been developed to aid in rapid setup and checkout of hybrid or analog problems in the ANSC lab. The steady state checkout program checks all model equations at any desired operating point and indicates the location of any steady state errors that may be present. This program is run at least once each day and takes less than 10 minutes to check a large scale four console hybrid program.

APPENDIX C

CONTROL PROGRAMS FOR THE SIMPLIFIED NONLINEAR MODEL AND THE COMMON ANALOG MODEL

The two programs shown in this appendix are typical of those used in the control experiments described in this study. The first program was used in initial experiments in controlling the SNM. Control is based on a sixth order temperature loop control model and a second order pressure loop control model. The second program was used in the final control experiments on the CAM. Control in this case is based on third order control models for both control loops.

Main Program for SNM Control

```
      DIMENSION Q(6)
      DIMENSION A(6,6),B(6),P(6,6),PIN(6,6),D(7),YT(6),
     1   YP(2)
      DIMENSION PT(5),R(6),PG(10),PP(10),PPP(2,2),PPPIN
     1   (2,2)
      DIMENSION DEST(11),DESTP(11),C(6),E(7),BP(5),AP(5,5),
     1   DP(4)
      COMMON CONT.CONP,CONTO,CNOPO
      COMMON PD,TD,SP,ST
      COMMON GT(10),GP(5),T,J,1COUNT
      LOGICAL ISL1,ISL2,ISL3,ISL4
      READ 500,NT,NP
      PRINT 550,NT
C
C          CALCULATE DESIRED TRANSFER FUNCTION
      CALL RADCR(27,THBC,.01,0)
      THBCO-THBC
      CALL EQN(NT,DEST)
      CALL EQN(NP,DESTP)
C
C       SET UP COMMUNICATION TO CONSOLE Z
      CALLCON('Z')
      CALL MODE('C')
C         INITIALIZE PARAMETERS
      CONT=0.
      GT(1)=0.
      GT(2)=0.
      GT(3)=0.
      GT(4)=0.
      GT(5)=0.
      GT(6)=0.
      GT(7)=0.
      GT(8)=0.
      BTI9R=0[
      GT(10)=0.
      GP(3) = 0.0
      GP(4) = 0.0
      GP(5) = 0.0
      C(1)=.945
      C(2)=.047
      C(3)=-.001
      C(4)=0.
      C(5)=0.
      C(6)=0.
      1COUNT=0
      T=0.
      I=0.
      J=1
      DT=.005
```

```
      A(5,5)=86.72*Z1-.235
      A(5,6)=608.85*Z1
      A(3,2)=0.0
      A(4,1)=0.0
      A(4,2)=0.0
      A(4,3)=0.0
      A(5,1)=0.0
      A(5,2)=0.0
      A(5,3)=0.0
      A(6,1)=0.0
      A(6,2)=0.0
      A(6,3)=0.0
 3333 MM=1
      M=-1
1     CALLRSL(ISL1,26)
      IF(ISL1) GO TO 100
      GO TO 1
100    CONTINUE
      IF(M.GT.0)GO TO 102
      CALL RADCR(37,T11,-.002,22,P15,.002,35,SN,-.01,34,
          DKTT,1-,0)
      CALL RADCR(33,PC3,.0002,32,PC2,.0002,31,PC1,.0002,0)
      T15=.945*PC3+.047*PC2+(-.001*PC1)
      WN=13.33*P15/SQRT(T15)
      PT(1)=3.98*WN
      PT(2)=3.94*WN
      PT(3)=2.21*WN
      DKTU=DKTT
   30   PI(4)=(1.-DKTO)*660.
      PT(5)=660.*SN
550    FORMAT(10X,I3)
C
C       CALCULATE A
      A(1,1)=-.005*PT(1)
      A(1,2)=.00515*PT(1)
      A(1,3)=-.0001175*PT(1)
      Z1=1./PT(4)
      A(1,4)=.4572*Z1
      A(1,5)=3.892*Z1
      A(1,6)=27.33*Z1
      A(2,2)=-.005*PT(2)
      A(2,3)=.00392*PT(2)
      A(2,4)=.8635*Z1
      A(2,5)=7.35*Z1
      A(2,6)=51.62*Z1
      A(3,3)=_.005*PT(3)
      A(3,4)=.5886*Z1
      A(3,5)=5.01*Z1
      A(3,6)=35.19*Z1
      A(4,4)=5.0*Z1-.0276
      A(4,5)=42.535*Z1
      A(4,6)=298.65*Z1
      A(5,4)=10.18*Z1
```

```
      A(2,1)=0.0
      A(3,1)=0.0
      A(6,4)=3.036*Z1
      A(6,5)=25.85*Z1
      A(6,6)=181.5*Z1-1.65
C
C       CALCULATE B
      B(1)=16.55*PT(5)*Z1
      B(2)=31.3*PT(5)*Z1
      B(3)=21.3*PT(5)*Z1
      B(4)=181.*PT(5)*Z1
      B(5)=369.*PT(5)*Z1
      B(6)=110.*PT(5)*Z1
C
C       CALCULATE CHAREQ EQN
      AA1=-(A(4,4)+A(5,5)+A(6,6))
      AA2=A(4,4)*A(5,5)+A(6,6)*(A(4,4)+A(5,5))
     1-A(6,5)*A(5,6)-A(5,4)*A(4,5)-A(6,4)*A(4,6)
      AA3=A(6,5)*A(5,6)*A(4,4)+A(5,4)*A(4,5)*A(6,6)
     1-A(5,4)*A(6,5)*A(4,6)-A(6,4)*A(4,5)*A(5,6)
     2+A(6,4)*A(4,6)*A(5,5)-A(4,4)*A(5,5)*A(6,6)
      BB1=-(A(3,3)+A(2,2)+A(1,1))
      BB2=A(1,1)*A(2,2)+A(3,3)*(A(1,1)+A(2,2))
      BB3=-A(1,1)*A(2,2)*A(3,3)
      D(7)=1.
      D(6)=AA1+BB1
      D(5)=AA2+AA1*BB1+BB2
      D(4)=AA3+AA2*BB1+AA1*BB2+BB3
      D(3)=BB1*AA3+AA2*BB2+AA1*BB3
      D(2)=AA3*BB2+AA2*BB3
      D(1)=AA3*BB3
C       CALCULATE P
      DO 20 II=1,NT
20    P(II,NT)=B(II)
      DO 22 JJ=2,NT
      J1=NT-JJ+1
      K=J1+1
      DO 22 II=1,NT
      P(II,J1)=D(K)*B(II)
      DO 22 L=1,NT
      P(II,J1)=P(II,J1)+A(II,L)*P(L,K)
   22 CONTINUE
C
C         CALCULATE P INVERSE
C
      CALL SIMEQ(P,C,NT,PIN,Q)
C
C       CALCULATE K
      CC1=0.
      DO 23 JJ=1,NT
23    CC1=P(JJ,1)*C(JJ)+CC1
```

```
      GAINT=DEST(1)/CC1
     GGT=1./GAINT
C
C       CALCULATE PHASE VARIABLE FEEDBACKS
      DO 24 II=1,NT
24    R(II)=(DEST(II)-D(II))*GGT
C
C       CALCULATE PHYSICAL VARIABLE FEEDBACKS
      DO 25 II=1,NT
      GT(II)=0.
      DO 25 JJ=1,NT
25    GT(II)=GT(II)+PIN(JJ,II)*R(JJ)
      PRINT 601,GAINT
      PRINT 601,GT
      IF(MM.EQ.0)GO TO 101
      MM=0
102    CONTINUE
      CALL RADCR(33,PC3,.0002,32,PC2,.0002,31,PC1,.0002,
     135,SN,-.01,25,T7,-.002,26,WT,.01,27,THBC,.01,24,RPM,
          -.00002,
     237,T11,-.002,22,P15,.002,0)
      W11=WN
      THSS=11.
      T15=.945*PC3+.047*PC2+(-.001*PC1)
      P13=P15*(1.+33.3/SQRT(T15))
      P11=.354*WT*SQRT(T11)+.79*P13
      P2=.000003434*RPM*RPM-.000296*W11*RPM+30.
      X1=SQRT(T15)
      X2=P11/T7
      X2=SQRT(X2)
      X3=P11-P13
      X3=SQRT(X3)
      X4=(P2+P11)/(2.*T7)
      X4=SQRT(X4)
      X5=P2-P11
      X5=SQRT(X5)
      X6=SQRT(T11)
      X7=P13/P11
      X7=SQRT(X7)
      X7=SQRT(X7)
C
C       CALCULATE AP  &  BP
31     PG(1)=.076*X1
      CALL RADCR(27,THBBB,.01,0)
      PG(2)=.0182*THBBB*X2/X3
      PG(3)=.0182*X2*X3
      PG(4)=(1.+33.3/X1)
      PG(5)=2.*X4/X5
```

```
      PG(6)=.0134*THSS*PG(5)
      PG(7)=.354*X6
      PG(8)=.000003436*RPM-.0002967*WN+30./RPM
      PG(9)=10200.*T11/RPM
      PG(9)=PG(9)*(1.-X7)
      PG(10)=.00000096*RPM+.0002385*WN
       PP(10)=1./(1.+PG(7)*(PG(2)+PG(5)+PG(6)))
      PP(1)=(PG(5)+PG(6))*PG(8)*PP(10)
      PP(2)=(-.79*(PG(5)+PG(6))+.21*PG(2))*PP(10)*PG(4)
      PP(3)=PG(3)*PP(10)
      PP(10)=1./(1.+.21*PG(1)*PG(2)*PG(4)-PP(2)*PG(1)
     1*(1.+PG(2)*PG(7)))
      PP(4)=PG(1)*(1.+PG(2)*PG(7))*PP(1)*PP(10)
      PP(5)=(PG(1)*(PG(3)-PP(3))*(1.+PG(7)*PG(2)))*PP(10)
      PP(7)=PG(9)*(PP(2)*PP(5)-PP(3))
      PP(6)=88.1*PP(6)
      PP(7)=88.1*PP(7)
      AP(1,1)=-2.25
      AP(1,2)=0.
      AP(2,1)=-2.25*PP(5)+PP(4)*PP(7)-PP(5)*PP(6)
      AP(2,2)=PP(6)
      BP(1)=2.25
      BP(2)=2.25*PP(5)
C
C       CALCULATE CHAREQ EQN
      DP(3)=1.
      DP(2)=2.25-PP(6)
      DP(1)=2.25*PP(6)
C
C       CALCULARE P  &  P INVERSE
      PPP(1,2)=BP(1)
      PPP(2,2)=BP(2)
      PPP(1,1)=AP(1,1)*PPP(1,2)+AP(1,2)*PPP(2,2)+DP(2)*BP(1)
      PPP(2,1)=AP(2,1)*PPP(1,2)+AP(2,2)*PPP(2,2)+DP(2)*BP(2)
      DD=PPP(1,1)*PPP(2,2)-PPP(2,1)*PPP(1,2)
      PPPIN(1,1)=PPP(2,2)/DD
      PPPIN(1,2)=-PPP(1,2)/DD
      PPPIN(2,1)=-PPP(2,1)/DD
      PPPIN(2,2)=PPP(1,1)/DD
C
C       CALCULARE GAIN  &  FEEDBACKS
      GAINP=DESTP(1)/PPP(2,1)
      ZZ=1./GAINP
      GP111=(DESTP(1)-DP(1))*ZZ
      GP222=(DESTP(2)-DP(2))*ZZ
      GP(1)=GP111*PPPIN(1,1)+GP222*PPPIN(2,1)
      GP(2)=GP111*PPPIN(1,2)+GP222*PPPIN(2,2)
      PRINT 601,GAINP
      PRINT 601,GP
      IF(ICOUNT.GT.0)GO TO 101
```

```
      CALL MODE('C')
101    IF(I.GT.0)GO TO 3
3      CONTINUE
      CALL RSL(ISL2,27)
      IF(ISL2)GO TO 4
      STOP
4     CALL RSL(ISL3,28)
      IF(ISL3)GO TO 3
      CALL RADCR(33,PC3,.0002,32,PC2,.0002,31,PC1,.0002,
          21,CI3,
     1.0001,20,CI2,.000004,30,CII,.000001,36,TD,.0002,0)
      CALL RADCR(22,P15,.002,27,THBC,.01,23,PD,.002,0)
      CONP=GAINP*(PD   -GP(1)*(THBC-THBBB)-GP(2)*P15)
      CONP=CONP+THBBB-THBCO
      CONT=GAINT*(TD    -GT(1)*PC3-GT(2)*PC2-GT(3)*PC1-
          GT(4)*CI1-
     1GT(5)*CI2-GT(6)*CI3)
      T15=.945*PC3+.047*PC2+(-.001*PC1)
      CONT=CONT/10.
      CONP=-CONP
      CALL WDACR(05,CONP,.01,21,CONT,1.,0)
      ICOUNT =ICOUNT +1
      IF(ICOUNT,LT.100)GO TO 222
      CALL MODE('H')
      ICOUNT=0
      GO TO 3333
222   GO TO 3
500   FORMAT(2I2)
501   FORMAT(4F10.0)
600   FORMAT(1H1)
601    FORMAT(5X,6F15.5)
602    FORMAT(///)
      END
```

Main Program for CAM Control

```
      LOGICAL ISL1,ISL2,ISL3,ISL4
      DIMENSION C(10),CP(10),A(110,10),B(10),DEST(11),
     1    DESTP(11)
      DIMENSION P(10,10),PIN(10,10),Q(10),GT(10),PG(10)
     1    DIMENSION GP(10),PP(10),D(11)
      DIMENSION AP(10,10),BP(10),DP(11),PPP(10,10),PPPIN
     1    (10,10)
      COMMONGAINT,GAINP,THBBB,THBCO,GT,GP
      COMMON KN
      COMMON X110
      COMMON X10,00
      COMMON OTO,Y10
C
C     INITIALIZE PARAMETERS
C
      DO 75 I=1 ,10
      GO(I)=0.
75    GT(I)=0.
      KK=0
      READ 500,NT,NP
      PRINT 550,NT,NP
500   FORMAT(2I2)
550   FORMAT(5X,214)
      CALL RADCR(27,TBC,.01,31,X110,-.01,34,DKTT,.05,0)
      DKTTO=DKTT
      THBCO=THBC
      C(1)=1.0
      C(2)=0.
      C(3)=0.
      CP(1)=0.
      CP(2)=1.
      CP(3)=0.
C
C     SET UP ANALOG COMPUTER
C
      CALL CON('Z')
      CALL MODE('C')
C
C     CALCULATE DESIRED TRANSFER FUNCTION TEMPERATURE
C         LOOP AND STATIC INPUTS
C
100    CONTINUE
      CALL RADCR(33,WN,.008,34,DKTT,.05,35,SN,-.005,24,
     1    DKDO,-.05,0)
      KM=KM+1
      IF(KM.LT.14)GO TO 47
      KM=0
      DDT=.025*WN-.15
```

```
      DEST(4)=1.
      DEST(3)=3.081+DDT
      DEST(2)=.243+DDT*3.081
      DEST(1)=.243*DDT
      DKDDO=.85*DKDO
      UTO=DKDO/(1.+B(3)/2.5)
      Y1O=+B(3)/2.5*UTO
C
C     CALCULATE TEMPERATURE CONTROL MODEL
C
47    CONTINUE
      DKTT=DKTT-DKTTO+DKDDO
      PT1=2.21*WN
      PT4=(1.-DKTT)*660.
      PT5=660.*SN
      A(1,1)=-.003239*PT1
      A(1,2)=31.3*.081/PT4
      A(2,1)=0.
      A(2,2)=53.46/PT4-.081
      B(1)=31.3*PT5/PT4
      B(2)=660.*PT5/PT4
      A(1,3)=B(1)
      A(2,3)=B(2)
      A(3,1)=0.
      A(3,2)=0.
      A(3,3)=-2.5
      B(3)=-1.25
      D(3)=1.
      D(2)=-A(1,1)-A(2,2)
      D(1)=A(1,1)*A(2,2)
      D(4)=D(3)
      D(3)=2.5*D(3)+D(2)
      D(2)=2.5*D(2)+D(1)
      D(1)=2.5*D(1)
C
C     UPDATE CONTROL
C
      CALL ROLL
C
C     UPDATE FEEDBACK GAINS
C
      CALL PMAT(A,B,D,P,NT)
      CALL SIMEQ(P,C,NT,PIN,Q)
      CALL GAIN(P,C,DEST,D,PIN,NT,GAINT,GT)
C
C     UPDATE CONTROL
C
      CALL ROLL
C
C     CALCULATE DESIRED TRANSFER FUNCTION PRESSURE LOOP
```

```
C
      CALL RADCR(32,T15,.0002,25,T7,-.001667,26,WT,-.005,
     1    27,THBC,.01
     1,14,RPM,-.000025,10,T11, .001667,22,PIT,-.001,21,
     1    W11,.005,0)
      P15=PIT
      IF(MK.LT.5)GO TO 789
      MK=0
      DDD=.0025
      DDP=DDD*P15-.15
      DESTP(4)=1.
      DESTP(3)=4.3+DDP
      DESTP(2)=4.42+DDP*4.3
      DESTP(1)=4.42*DDP
C
C     BEGIN CALCULATION OF PRESSURE CONTROL MODEL
C
789     MK=MK+1
      THSS=11.
      P13=P15*(1.+33.3/SQRT(T15))
      P11=.354*WT*SQRT(T11)+.79*P13
      P2=.000003434*RPM*RPM-.000296*W11*RPM+30.
      X20=X10
      X10=T15
      X30=(X20-X10)/X20
      T15=(1.+X30)*T15
      X1=SQRT(T15)
      X2=P11/T7
      X2=SWRT(X2)
      X3=P11-P13
      X3=SWRT(X3)
      X4=(P2+P11)/(2.*T7)
      X4=SWRT(X4)
      X5=P2-P11
      X5=SWRT(X5)
      X6=SWRT(T11)
      X7=P13/P11
      X7=SWRT(X7)
      X7=SWRT(X7)
      PG(1)=.076*X1
      CALL RADCR(27,THOOO,.01,0)
      THOO3=THOO2
      THOO2=THOO1
      THOO1=THOOO
      THOOO=(THOO3+THOO2+THOO1)*.333
      THBBB=THOOO
C
C     UPDATE CONTROL
C
      CALL ROLL
```

```
C
C      CONTINUE MODEL UPDATE
C
   PG(2)=.0400*THOOO*X2/X3
   PG(3)=.0400*X2*X3
   PG(4)=(1.+33.3/X1)
   PG(5)=2.*X4/X5
   PG(6)=.0134*THSS*PG(5)
   PG(7)=.354*X6
   PG(8)=.00000343*RPM-.0002967*WN+30./RPM
   PG(9)=10200.*T11/RPM
   PG(9)=PG(9)*(1.-X7)
   PG(10)=.00000096*RPM+.0002385*WN
   PP(10)=1./(1.+PG(7)*(PG(2)+PG(5)+PG(6)))
   PP(1)=(PG(5)+PG(6))*PG(8)*PP(10)
   PP(2)=(-.79*(PG(5)+PG(6))+.21*PG(2))*PP(10)*PG(4)
   PP(3)=PG(3)*PP(10)
   PP(10)=1./(1.+.21*PG(1)*PG(2)*PG(4)-PP(2)*PG(1)
  1*(1.+PG(2)*PG(7)))
   PP(4)=PG(1)*(1.+PG(2)*PG(7))*PP(1)*PP(10)
   PP(5)=(PG(1)*(PG(3)-PP(3))*(1.+PG(7)*PG(2)))*PP(10)
   PP(6)=PP(1)+PP(2)*PP(4)
   PP(6)=PG(9)*PP(6)
   PP(6)=PP(6)-PG(10)
   PP(6)=88.1*PP(6)
   PP(6)=0.
   PP(7)=PG(9)*(PP(2)*PP(5)-PP(3))
   PP(7)=88.1*PP(7)
   AP(1,1)=-2.25
   AP(1,2)=0.
   AP(2,1)=-2.25*PP(5)+PP(4)*PP(7)-PP(5)*PP(6)
   AP(2,2)=PP(6)
   BP(1)=2.25
   BP(2)=2.25*PP(5)
   AP(1,3)=BP(1)
   AP(2,3)=BP(2)
   AP(3,3)=-2.5
   AP(3,1)=0.
   AP(3,2)=0.
   BP(3)=-1.65
   DP(3)=1.
   DP(2)=2.25-PP(6)
   DP(1)=-2.25*PP(6)
   DP(4)=DP(3)
   DP(3)=2.5*DP(3)+DP(2)
   DP(2)=2.5*DP(2)+DP(1)
   DP(1)=2.5*DP(1)
C
C      UPDATE CONTROL
C
```

```
      CALL ROLL
C
C     UPDATE FEEDBACK GAINS
C
      CALL PM T(AP,BP,DP,PPP,NP)
      CALL SIMEQ(PPP,CP,NP,PPPIN,Q)
      CALL GAIN(PPP,CP,DESTP,DP,PPPIN,NP,GAINP,GP)
C
C     UPDATE CONTROL AND STATIC INPUT
C
      THRRR=THBBB-THBCO
      UU=2.958*THRRR
      X10=-1.959*THRRR+X110
      CALL ROLL
C
C     MAKE DECISION TO CONTINUE OR TERMINATE
C
 3    CALL RSL(ISL2,27)
      IF(ISL2)GO TO 4
      STOP
 4    IF(KK.EQ.1)GO TO 100
      KK=1
      GO TO 100
      END
```

Subroutine to Calculate Control Update

```
      SUBROUTINE ROLL
      DIMENSION GT(10),GP(10)
      COMMONGAINT,GAINP,THBBB,THBCO,GT,GP
      COMMON KN
      COMMON X110
      COMMON X10,00
      COMMON JTO,Y10
      CALL RADCR(32,T15,.0002,30,CI1,.000001,36,TD,.0002,22,
     1P15,-.001,27,THBC,.01,23,PD,.001,20,Y1,.05,31,X1,-.01,
          0)
      CONT=GAINT*(TD-GT(1)*T15-GT(2)*CI1-GT(3)*Y1-Y10))*.1
     1+UTO*.1
      CONT=1.5*CONT
      CONP=GAINP*(PD-GP(1)*(THBC-THBBB)-GP(2)*P15-GP(3)*
          (X1-X10))+00
      KN=KN+1
600   FORMAT(10X,5F15.4)
       BMP=-CONP
      CALL WDACR(05,CONP,.01,21,CONT,1.0,0)
      CONTINUE
      CONTINUE
      RETURN
      END
```

Subroutine to Calculate Feedback Gains

```
      SUBROUTINE GAIN(P,C,DEST,D,PIN,NT,GAINT,GT)
      DIMENSION P(10,10),C(10),DEST(11),R(10),D(11),GT(10),
          PIN(10,10)
      CC1=0.
      DO 23 JJ=1,NT
 23    CC1=P(JJ,1)*C(JJ)+CC1
      GAINT=DEST(1)/CC1
      GGT=1./GAINT
      DO 24 II=1,NT
24    R(II)=(DEST(II)-D(II))*GGT
      DO 25 II=1.NT
      GT(II)=0.
      DO 25 JJ=1,NT
  25  GT(II)=GT(II=+PIN(JJ,II)*R(JJ)
      RETURN
      END
```

Subroutine to Calculate Transformation Matrix

```
      SUBROUTINE PMAT(A,B,D,P,NT)
      DIMENSION P(10,10),B(10),D(11),A(10,10)
      DO 20 II=1,NT
20    P(II,NT)=B(II)
      DO 22 JJ=2,NT
      J1=NT-JJ+1
      K=J1+1
      DO 22 II=1,NT
      P(II,J1)=D(K)*B(II)
      DO 22 L=1,NT
      P(II,J1)=P(II,J1)+A(I1,L)*P(L,K)
22    CONTINUE
      RETURN
      END
```

REFERENCES

Bellman, Richard. Dynamic Programming. Princeton, N. J.: Princeton University Press, 1957.

Kalman, R. E. Mathematical description of linear dynamical systems. J.S.I.A.M. Control, Series A, Vol. 1, No. 2, 152-192, 1963.

Korn, G. A., and Korn, T. M. Mathematical Handbook for Scientists and Engineers. McGraw-Hill Book Company, 367, 1961.

Meghreblian, Robert V., and Holmes, David K. Reactor Analysis. New York: McGraw-Hill Book Company, 1960.

Melsa, J. L. A digital computer program for the analysis and design of state variable feedback systems. Engineering Experiment Station, Univ. of Arizona, 1967.

Minorski, N. Nonlinear Mechanics. Princeton, N. J.: Van Nostrand, 1963.

Mohler, R. R. Optimal nuclear rocket engine control. Proceedings of the Symposium on Nuclear Engineering, Univ. of Arizona, 137-163, 1965.

Perry, J. E., and Mohler, R. R. Nuclear rocket engine control. Nucleonics, April 1961, 80-84.

Pontryagin, L. S., Boltyanskii, V. G., Grankrelidze, R. V., and Mishchenko, E. F. The Mathematical Theory of Optimal Processes. New York: John Wiley and Sons, Inc., 1962.

Schroeder, R. W. NERVA--Entering a new phase. Astronautics and Aeronautics, May 1968, 42-53.

Schultz, D. G., and Melsa, J. L. State Functions and Linear Control Systems. New York: McGraw-Hill Book Company, 1967.

Schultz, D. G., and Melsa, J. L. Linear Control Systems. New York: McGraw-Hill Book Company, 1969.

Smith, H. P., Jr. Closed loop dynamics at nuclear rocket engines with bleed turbine drive. Nuclear Science and Engineering, 14, 1962, 371-379.

Smith, H. P., Jr., and Stenning, A. H. Open loop stability and response at nuclear rocket engines. Nuclear Science and Engineering, Vol. 11, 1961, 76-84.

Spence, R. W., and Durham, F. P. The Los Alamos nuclear rocket program. Astronautics and Aeronautics, June 1965, 42-46.

Truxal, John G. Control System Synthesis. New York: McGraw-Hill Book Company, 1955.

Tuel, W. G., Jr. On the transformation to (phase-variable) canonical form. IEEE Transactions on Automatic Control, Vol. AC-11, No. 3, 608, July 1966.

Weaver, L. E., and Secker, P. A. Synthesis at optimal feedback control for nuclear rocket engine start-up. Proceedings of the Symposium on Nuclear Engineering, Univ. of Arizona, 164-181, 1965.

Wheatley, E. A., and Mohler, R. R. A mathematical model to represent the basic dynamics of a nuclear rocket. Transactions of the American Nuclear Society, Vol. 3, No. 2, 386, 1960.